Forschungsgesellschaft für
Verbrennungskraftmaschinen und
Thermodynamik mbH

Final Report,

19 December 2013

Options to consider future advanced fuel-saving technologies in the CO_2 test procedure for HDV

By order of

ICCT

Report no. FVT -104/13/ Rex Em 06/13-6790 of 19.12.2013

ISO 9001

Inffeldgasse 19 A-8010 Graz
Tel.: +43/(0)316/873-30001 Fax: +43/(0)316/873-30002 office@fvt.at

Forschungsgesellschaft für Verbrennungskraftmaschinen und Thermodynamik mbH

Options to consider future advanced fuel-saving technologies in the CO_2 test procedure for HDV

Written by: D.I. Antonius Kies 19.12.2013

Dr. Martin Rexeis

D.I. Gérard Silberholz

D.I. Raphael Luz

Prof. Dr. Stefan Hausberger

Table of contents

Symbols and abbreviations

AFR	Air-fuel ratio
AMT	Automated manual transmission
COP	Conformity of production
DCT	Dual clutch transmission
EGR	Exhaust gas recirculation
FC	Fuel consumption [g/h], [g/km]
GTR	Global Technical Regulation
H	Enthalpy flow of exhaust gas [kW]
HDE	Heavy Duty Engine
HDH	Heavy Duty Hybrid
n_{in}	Torque converter input speed [min-1]
n_{out}	Torque converter output speed [min-1]
ORC	Organic Rankine Cycle
P	Power, mechanical or electrical
Pe	Engine power [kW]
PHEM	Passenger car and Heavy duty vehicle Emission Model
P_{wheel}	Driving power at wheels [kW]
SCR	Selective catalytic reduction
TEG	Thermoelectric generator
T_{in}	Torque converter input torque [Nm]
T_{out}	Torque converter output torque [Nm]
VECTO	Vehicle Energy consumption Calculation Tool
WHTC	World Harmonized Transient Cycle

1 Executive Summary

The currently foreseen test procedure for fuel consumption and CO_2 emissions from HDV in the European Union is based on component testing and simulation. A vehicle simulation tool (Vehicle Energy consumption Calculation Tool, VECTO) is under development, in which total fuel consumption is simulated based on vehicle longitudinal dynamics from the input data on the vehicle and engine characteristics. VECTO is a backward simulation tool which has been adapted with several features of forward simulation for calculating the energy demand, the fuel consumption and the resulting CO_2 emissions from HDV for specified velocity patterns. “Backward” simulation means that the power demand at the wheels is calculated from the velocity and the acceleration defined in the test cycle and from the driving resistances and the vehicle inertia. From the wheel, VECTO calculates backwards to the engine adding the power demand from drivetrain losses and from auxiliary consumers. The result is the engine operating point in terms of speed, torque and fuel consumption in 1 Hz over the cycle. Features of VECTO usually not implemented in backwards calculating models are, for example, a driver model to perform realistic full-load acceleration, torque interruption at gear shifts and look-ahead braking. To depict a realistic driving style for all possible combinations of mission profiles and HDV configurations, a simulation approach based on target speed cycles is applied in the HDV CO_2 certification. These target speed cycles are adapted by the VECTO driver model for vehicle-specific influences like full-load acceleration behavior and coasting and braking characteristics. This approach was found to be a good compromise between the ability to accurately simulate fuel consumption for all kinds of HDV types and the much lower model complexity of the backward approach compared to forward-looking simulation models.

With this approach, many influencing factors on the fuel consumption and the resulting CO_2 emissions can already be considered with vehicle-specific or generic data:

- Aerodynamic drag
- Rolling resistance
- Transmission ratios and resulting engine speed and torque
- Losses in the transmission system
- Vehicle weight
- Rotational inertias
- Load capacity
- Engine fuel efficiency in steady state and transient conditions
- Additional power demand from auxiliaries

However, several fuel-saving technologies cannot yet be captured by the current status of the procedure. These technologies would need either an extension of the simulation tool and/or additional (component) test procedures. In this study, options for such extensions of the currently foreseen CO_2 certification procedure are identified. For some of the options, the fuel-saving potential of the related technologies was evaluated using VECTO together with the new model extensions.

The options identified for integrating advanced fuel-saving technologies into the current CO_2 certification approach are summarized below.

Advanced engine technology

The internal combustion engine is depicted in VECTO by a stationary fuel consumption map and correction factors for transient behavior derived on the measured fuel consumption in the hot World Harmonized Transient Cycle (WHTC). This current approach is able to cover all engine technologies which show a mechanical benefit during the engine testing procedure (e.g. advanced fuel injection systems, mechanical turbo-compounding or waste heat recovery systems in which the output is connected to the engine crankshaft). An extension of the current method will be required for including technologies which either generate electrical power (e.g. electric turbo-compound) or which consume additional electricity from the vehicle electrical system (e.g. electric water pump). One simple extension could be to measure the electrical power generated and/or consumed by the advanced engine system in the WHTC and to add or to subtract this energy in the VECTO simulations from the electrical power to be generated by the alternator.

Waste heat recovery (WHR) systems like organic Rankine cycles and thermoelectric generators offer a fuel-saving potential from 1 to 4 %, according to recent publications. These technologies are not covered by the recent CO_2 certification method. The fuel benefit of WHR systems which are integrated into the engine system (e.g. using the waste heat of the exhaust gas recirculation radiator or of the main coolant circuit) could be covered in the CO_2 certification by the approach described in the previous paragraph. If the WHR device is placed separately in the exhaust system, its power generation could be simulated in VECTO based on an additional WHR module. A proposal with the necessary input parameters and a measurement approach is described in the main text.

Auxiliary systems

Auxiliary systems are devices that provide energy for functions other than propulsion. Auxiliaries are either needed for proper operation of the engine (e.g. engine cooling fan) or of vehicle related systems (e.g. compressor for pressurized air system). For truck applications – where the auxiliary influence on overall fuel consumption was assessed to be of secondary importance – the current CO_2 certification approach uses generic (but technology-specific) values for mechanical power consumption of the auxiliary units. The use of component-specific data is not foreseen at this time in the first VECTO version for HDV certification. Nevertheless, a considerable fuel-saving potential is seen by using more efficient auxiliaries in combination with smart controllers. Smart control tries running auxiliaries preferably in motoring phases when the additional power demand does not result in additional fuel consumption (“brake energy recuperation”). To set incentives for using such technologies in HDV, it seems to be important that such technologies also result in lower fuel consumption values in the future certification procedure. A detailed simulation of auxiliaries and their controllers would, unfortunately, add a lot of complexity in the simulation and in the test procedures. Also, in the current study, no simple procedure was found for considering vehicle-specific auxiliary behavior. Thus, it seems to be more efficient to implement the procedure in the beginning with simple generic auxiliary models as described above. After the procedure is well established, regular updates to consider new technologies will be necessary in any case, which gives room to add more sophisticated methods. Certainly, the elaboration of these future options has to be done early enough. We hope the current work can be used as a solid basis, since different options for considering improved auxiliary technology have been investigated.

For buses, more detailed methods (models and component test procedures) are already under discussion for the first VECTO application, since the share of auxiliaries in the fuel consumption of buses is much higher than for trucks.

Engine cooling fan

A detailed model for the engine cooling fan needs extensive input data from several components and information on the applied control strategy. The use of such a model for a particular vehicle in the framework of the CO_2 certification would require that all these parameters be determined by a certified process. Thus, the incorporation of a detailed fan model in VECTO seems to be too complex. However, in this study, a simplified model is introduced, which can be used to establish "technology-specific" generic values for the fan power demand in VECTO. ACEA has already provided tables with such generic values for several fan technologies.

Air compressor / pressurized air system

A full model for the pressurized air system would offer the possibility to simulate the intermittent operation of the compressor but would need extensive input data in terms of reservoir volumes and control strategies. For the simulation of the official CO_2 values for trucks, the use of generic values for pressurized air consumption and generic technology-dependent compressor efficiencies might be sufficient. A model like the one developed in this study could be used for the elaboration of tables with generic data for the different truck classes and mission profiles. For buses, where the power consumption of the compressor has a significantly larger impact on overall fuel consumption, the use of a detailed simulation approach that also considers component-specific input data might be reasonable. Such methods are actually under development in a separate project on bus auxiliaries in the HDV CO_2 certification.

Alternator / electrical system

In the current approach, the power consumption from the electrical system is considered by standard tables for electrical power consumption of the vehicle and default alternator efficiency. The use of component-specific alternator efficiency maps in a later stage of the legislation is very likely. For the case that the HDV is equipped with a smart generator control, a simple generic model with the battery state of charge as the main control variable is proposed in this study.

Steering pump / steering system

In this study, the characteristics of steering systems in terms of power consumption have been analyzed in cooperation with component suppliers. The predominant parameter was found in the losses in steering system idling conditions. Based on this finding, a method for the simulation of steering systems in VECTO is drafted, which is based on a measured component flow resistance coefficient and generic power consumption during steering actuations. Whether the potential fuel savings depicted by this advanced simulation approach for optimized systems are worth the additional efforts in the certification procedure remains to be discussed with the industry. The contribution of the steering systems to overall fuel consumption is assessed to be smaller than 1%.

Hybrid propulsion systems

The fuel efficiency of hybrids depends to a large extent on the strategy applied for deciding when the vehicle is running only on the electric motor and when the motor is assisted by the internal combustion engine (ICE), where the ICE acts as a generator to produce electrical energy and how much the capacity of the battery can be used to ensure an acceptable lifetime. A proper simulation of a hybrid HDV thus needs to implement the manufacturer's control algorithms. Such a simulation tool was set up and validated in the HDH GTR to serve as a future tool for the certification of HDE pollutant emissions. The HDH model in the GTR is based on a Hardware In the Loop Simulation (HILS), where the controller is the hardware, while the vehicle, the engines and the energy storage devices are simulated. The HILS model is a forward calculating vehicle model and runs in real-time to enable communication with the hardware. These additional features compared to VECTO, make the HILS model much simpler in simulation of many features relevant for accurate results on fuel consumption (driver model, transmission losses, engine model...). It would be complex to combine the models, and both methods need to be applied first to gain experience on eventual demands for amendments. Furthermore, the market share of hybrid HDV is expected to be rather small in the next few years. Thus, a VECTO/HILS version may rather be a target for 2020 or later. Nevertheless, HDH also need an option for CO_2 certification which reflects the fuel savings from this technology. Several options have been discussed, and the most detailed one was tested in the current study.

a) The detailed approach plans to simulate the HDV first in VECTO to ensure that all influences relevant for following the target speed cycle are considered, similarly to conventional HDV. Then, the resulting speed trajectory is used to run the HILS model, where the vehicle hybrid controller is connected. The fuel consumption in [g/kWh] from this simulation can be used together with the specific cycle work computed by VECTO [kWh/km] to compute the specific fuel consumption of the HDH [g/km].

b) A generic hybrid model could be implemented in VECTO, which would use vehicle-specific data on the electric motor and battery but a generic hybrid controller strategy. The accuracy would certainly be lower than a). Differences in the fuel efficiency of HDHs with similar hardware may not be clearly visible from the simulation results.

c) Instead of a generic model, a look-up table may be sufficient, which lists the fuel saving against the same vehicle with a conventional engine as a function of a normalized battery capacity and the normalized power of the electric motor. Normalization could use, for example, vehicle weight or the "free kinetic energy" of the vehicle in a standard driving condition. Most likely, a generic model would be applied to fill the look-up table. One advantage could be that extensive model tests are not necessary, since only the results would be used in the certification but not the model itself.

Option a) was applied for the model of a 12t delivery parallel hybrid truck, which was compared with a conventional diesel truck with equal peak power. The simulation result is a consumption reduction of 3 % for the hybrid truck, which seems to be too low. The reason for this was the simplified driver model of the HILS simulator, which did not follow the speed trajectory sufficiently and which shall be improved in the future. Nevertheless, the approach is promising and shall be worked on further.

Drivetrain technologies

VECTO uses “loss maps” to calculate the mechanical losses in the gearbox and the differential(s). In this context, a detailed test procedure for measuring the torque losses has been elaborated by the industry. This method already enables an accurate consideration of the actual mechanical losses in the drivetrain. An advanced VECTO transmission model for the simulation of automatic transmissions with a hydraulic element, which are typically used in city buses, is under development.

In the current proposal, the VECTO simulations consider only generic gear shift strategies for manual and automated manual transmissions. A much more complex approach would be to allow OEMs to implement their own gear shift strategies either by using OEM-specific shift polygons or by connecting external components to the model, i.e. hardware-in-the-loop (HIL) or software in the loop (SIL). However, this may require the use of a forward-approach simulation model and also real-time operation of the simulation. Additionally, a validation of the relevant control hardware, either on the chassis dynamometer or on-road, would be required, as it has to be ensured that the OEM control strategy in the simulation matches with real world operation. This certainly is a quite complex approach, and it is suggested first to gain experience with the GTR-HDH-HILS approach before using HILS more widely in type approval. The main problem seems to be the need of a model validation for each application by some physical tests to ensure that the HILS provides realistic results. Validation may be simplified by family concepts, but no experience is available yet on how families would have to be defined.

Vehicle aerodynamics and rolling resistance

Aerodynamic measures to reduce the air drag and optimized tires with lower rolling resistance are already well covered by the recent proposal for the CO_2 certification procedure. A new test method based on constant speed tests has been developed for the accurate quantification of a vehicle’s air resistance. A measurement standard already exists for determining the tire rolling resistance. The VECTO simulations then make use of this input data.

Lightweighting

The main mechanisms which lead to the fuel benefits of vehicle lightweighting measures (reduced rolling resistance, reduced power demand during accelerations and uphill driving, and the possibility to operate the engine in lower speed ranges) are already covered by the current model structure of VECTO.

Driver support systems

Driver support systems are designed to assist the driver either by displaying certain information, e.g. gear shift recommendations, or by directly acting on the vehicle controls like cruise control systems. The current VECTO version has already been extended to be able to calculate the fuel benefit of several driver support systems, like for a speed or an acceleration limiter. Also, generic models for engine start/stop systems and an eco-roll function, which takes advantage of the vehicle’s kinetic energy during downhill driving by automatic declutching, are already part of the VECTO code. The use of these models in the certification is, however, restricted to generic system behavior using standard parameters e.g. for under- and overspeed of the eco-roll function. The consideration of OEM-specific system behavior would either require a standardized test procedure for VECTO model input parameters or

direct coupling of a future-forward version of VECTO with the related OEM algorithms (either via SILS or HILS).

In general, the study analyzed many options for considering advanced fuel-saving technologies which will presumably enter the market in the next few years or which are already on the market. Some options can be implemented in the first stage of HDV CO_2 certification. But many of the technologies use complex control strategies which can hardly be implemented accurately in VECTO without using HILS or SILS. Such a simulation approach, however, seems to be too complex for a first step of implementing a new test procedure. Nevertheless, the development of the most efficient way of taking such technologies into consideration already needs to be pushed now to have an operating system in 2020+. We hope that the current study supports this task.

2 Introduction

The currently foreseen test procedure for fuel consumption and CO_2 emissions from HDV in the European Union is based on component testing and simulation. A vehicle simulation tool (Vehicle Energy consumption Calculation Tool, VECTO) is under development, in which total fuel consumption is simulated based on vehicle longitudinal dynamics from the input data on the vehicle and engine characteristics. With this approach, many influencing factors on the fuel consumption and the resulting CO_2 emissions can already be considered with vehicle-specific or generic data:

- Aerodynamic drag
- Rolling resistance
- Transmission ratios and resulting engine speed and torque
- Losses in the transmission system
- Vehicle weight
- Rotational inertias
- Load capacity
- Engine fuel efficiency in steady state and transient conditions
- Additional power demand from auxiliaries

However, several technologies are identified, which cannot yet be captured by the current status of the procedure. These technologies would need either an extension of the simulation tool and/or additional (component) test procedures. In principle, any extension of the CO_2 test procedure which can cover any further fuel-saving technology can be considered worthwhile, as gaining a better CO_2 value in the certification is further motivation for OEMs to bring fuel-saving technologies to the market. Also, customers will benefit from the comparison of different makes and models if more features of the applied vehicle technology are reflected in the official CO_2 value. However, most modern fuel-saving technologies are very complex and often gain fuel-saving potential by optimising the interaction of several vehicle systems. The evaluation of such technologies in real world driving conditions in a robust and generally valid way is difficult, which is a main requirement of an official certification procedure. All approaches have to be a sound compromise between the complexity needed to be sensitive to as many fuel-saving measures as possible, the robustness required to prevent cheating, and the efforts required to perform and audit the test procedure.

The study shall:

1) Identify the technologies which cannot be evaluated by the current draft CO_2 test procedure for HDV in the EU
2) Elaborate options for component testing and/or simulation of the important technologies from 1)
3) Discuss options found in 2) with ICCT, European Commission, and industry

4) Apply options (if found) on generic data[1]
5) Application of some of the options using the VECTO tool

.

This study is part of the ongoing process for the development of a European HDV CO_2 certification procedure. At the time of the finalisation of this report, no actual proposal of the regulations has been published; therefore, no reference to an official document can be given here. A technical handbook on the methods elaborated so far is expected to be published by DG CLIMA in May 2014.

Also, ACEA (European Automobile Manufacturer's Association) elaborated a "White Book on CO_2 declaration procedure HDV", which contains detailed proposals on general methods, test procedures, and the CO_2 simulation tool. Publication of this document is under discussion but has not been carried out so far.

[1] No tests on prototypes are foreseen in this project due to high costs and the unpredictable availability of components. Tests can follow in a next phase, when the options elaborated here shall be included in the test procedure in cooperation with industry

3 VECTO - Vehicle Energy consumption Calculation Tool

As mentioned in chapter 1, the test procedure currently foreseen for fuel consumption and CO_2 emissions from HDV in the European Union is based on component testing and simulation. The total fuel consumption is simulated based on vehicle longitudinal dynamics from the input data on the vehicle and engine characteristics by an adapted “backward” simulation approach. For this purpose, the simulation tool VECTO (Vehicle Energy consumption Calculation Tool) has been developed. VECTO comprises the following main model elements:

- A user interface for editing input data, managing simulation runs and displaying simulation results
- A database with default data (vehicle configurations, driving cycles for mission profiles, default values to use if specific component data is not available) as specified in the HDV CO_2 regulation
- A core model which performs the simulation of fuel consumption and CO_2 emissions
- A post-processing module for generating standardized results and for performing a set of standard checks to validate the model results

A scheme of the VECTO tool is shown in Figure 1.

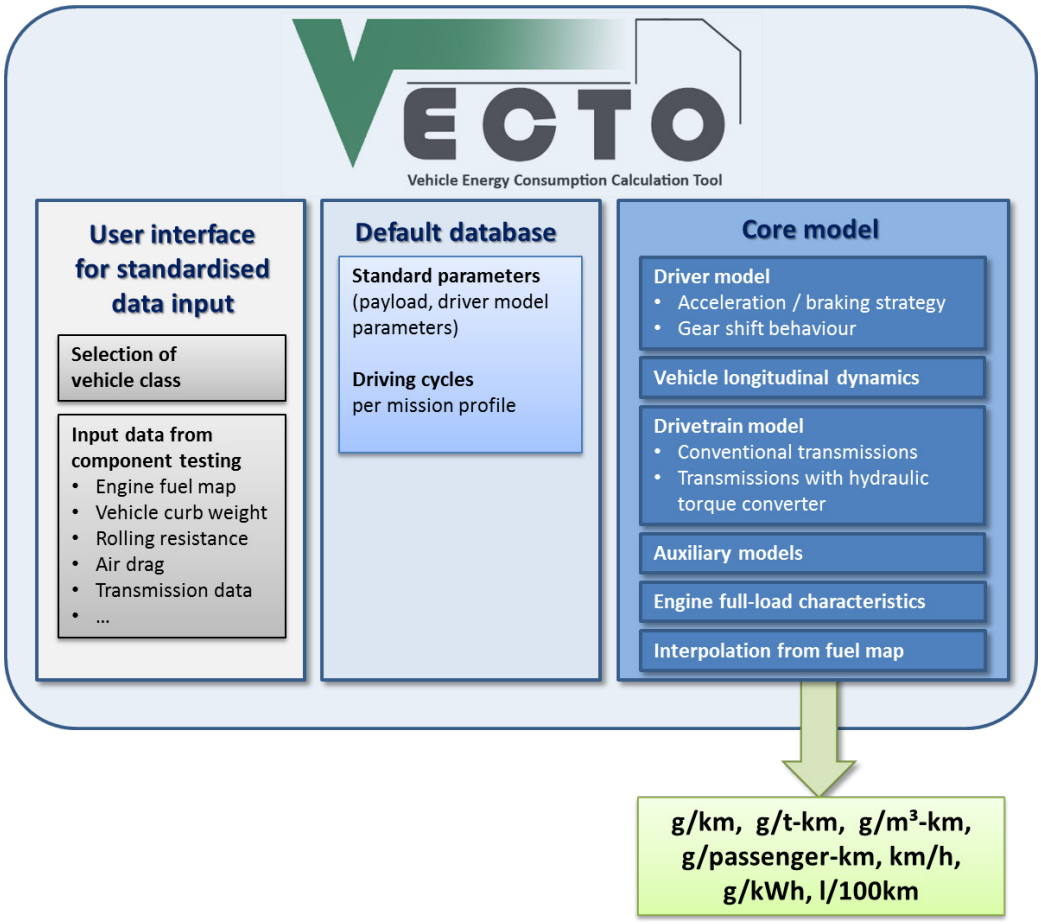

Figure 1: Scheme of the VECTO tool

The features of the main VECTO model elements are described below.

3.1 Graphical User Interface (GUI)

The VECTO GUI manages the editing of simulation runs, handles the import of input data and allows for the graphical display of input data and simulation results.

Figure 2 gives a screenshot of the VECTO main dialog.

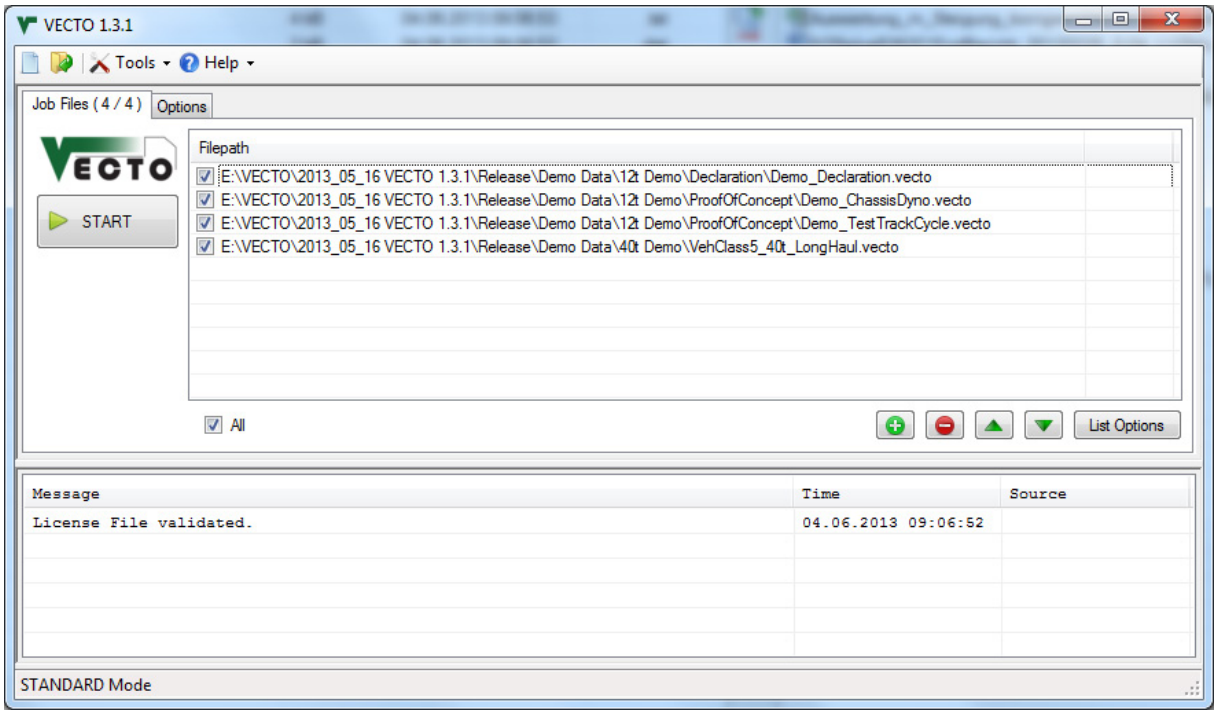

Figure 2: Screenshot of the VECTO main dialog

It is also possible to access the main program controls of VECTO via Command Line Arguments. This allows automation of calculation and evaluation using scripts.

3.2 Default database

The default database comprises all standard data as laid down in the HDV CO_2 legislation. These are:

- All standard parameters for the regulated HDV configurations (e.g., vehicle payload, driver model parameters),
- The driving cycles for the different mission profiles
- The tables with default parameters for all vehicle components, for which specific data are not available from component testing.

3.3 The core model

The core model comprises all simulation algorithms required for assessing the fuel consumption and CO_2 emissions according to the provisions in the HDV CO_2 legislation. The core model simulates HDV operation in a time-resolved scale. VECTO is based on backward simulation, i.e. the vehicle speed as defined in the target speed cycles is given as input for the

simulation of engine power and engine speed:[2] Vehicle speed, acceleration and road gradient determine the driving resistances and therefore the required power at the wheels. The engine power is calculated by adding the drivetrain losses and auxiliary power demand. If the vehicle is not able to follow the desired driving pattern in a certain time step, vehicle speed and acceleration are reduced stepwise until the power demand from the driving cycle can be covered by the full-load performance (determined mainly by the interaction of engine full-load power and gear shift behaviour etc.) of the HDV configuration.

In VECTO, a driver model was developed which allows for consideration of the main fuel-relevant characteristics of HDV real driving behaviour (for details see below). It also includes the gear shift model which is needed to calculate the engine speed.

The following sections provide a short description of the modules required within the core model.

3.3.1 Driver model

Driving behaviour has a major impact on fuel consumption and travel time. HDV driving behaviour is significantly influenced by the vehicle mass and the power-to-weight ratio of the HDV configuration. To depict a realistic driving style for all possible combinations of mission profiles and HDV configurations, a simulation approach based on target speed cycles is applied in the HDV CO_2 certification. These target speed cycles are defined as a function of driven distance by the following quantities:

- target vehicle speed,
- road gradient,
- and, for phases of standstill, vehicle stop time.

[2] This approach is contrary to the “forward” simulation approach, where a driver model actuates the vehicle control elements (throttle, brakes, etc.) to follow a driving cycle as well as possible, and vehicle speed and acceleration are calculated based on solving the differential equations of motion. The forward approach allows for more detailed modelling of each component and considers the dynamic system behaviour, but demands significantly more modelling effort and is generally less stable than backward modelling.

Figure 3 gives an example of a target speed cycle.

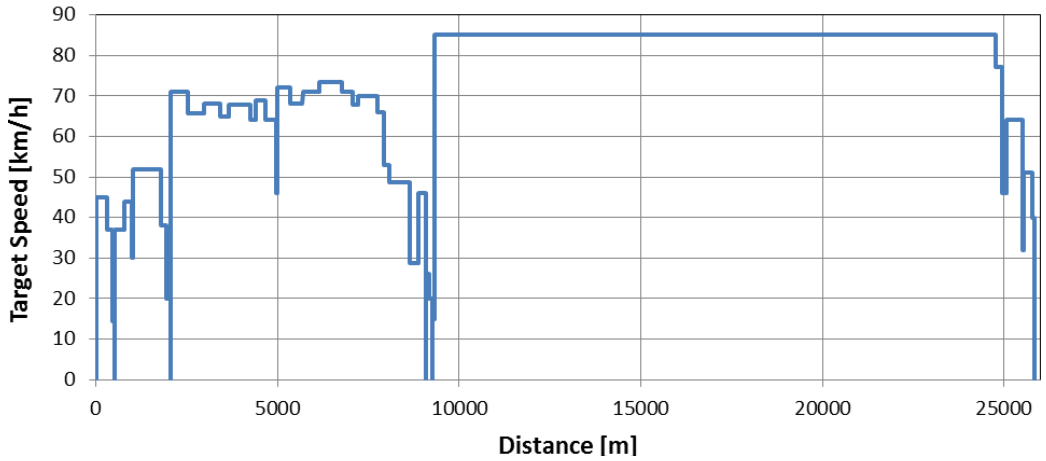

Figure 3: Example target speed cycle (Regional Delivery)

The target speed cycles are "artificial" as they only represent theoretical speed profiles for vehicles with unlimited acceleration and deceleration performance. Hence, a driver model is needed to calculate realistic trajectories based on the target speed, road gradient, and vehicle characteristics. The VECTO driver model adds the following elements of typical HDV driving behaviour to the driving pattern as defined by the target speed cycles:[3]

- The deceleration performance (phase of coast down followed by a deceleration defined as a function of vehicle speed)
- Overspeed function which allows the vehicle to exceed the target speed in downhill conditions to utilize the downhill momentum
- The gear shift strategy (different strategies for manual and automated (manual) gearboxes are covered)
- A limitation of full-load acceleration performance (e.g. for unloaded HDV where the driver does not use full engine power during accelerations)

The VECTO driver model is based on an algorithm which can be applied to all HDV categories. The driver model uses a set of generic parameters (e.g. desired acceleration as a function of vehicle speed, different parameter sets for the various HDV categories). In the VECTO driver model, the advanced control strategies “Eco-Roll”[4] and “Engine start/stop” are also implemented, which can be applied in the simulation if the vehicle is equipped with such functionality. Again, a generic (i.e. a generally valid) algorithm is used for each advanced control function. A set of OEM-specific parameters (e.g. maximum vehicle speed for engine

[3] The order of the list refers to the sequence in which the single functions are applied in the VECTO simulation.

[4]In the “Eco-Roll” mode, the engine is declutched from the drivetrain in downhill conditions to gain vehicle speed without engine braking until a certain overspeed is reached.

The engine start/stop system automatically shuts down the engine in standstill conditions to minimise idling fuel consumption.

stop) can be used in the model. In this regard, all specific parameters have to be declared by a verifiable process.

3.3.2 Vehicle longitudinal dynamics

The vehicle longitudinal dynamics module calculates the power demand to overcome the driving resistances (rolling resistance, air resistance, gradient resistance, and acceleration resistance). If the vehicle is not able to follow the desired driving pattern in a certain time step, vehicle speed and acceleration are reduced in the VECTO simulation until the power demand from the driving cycle can be covered by the full-load performance (determined mainly by the interaction of engine full-load power and gear shift behaviour etc.) of the HDV configuration. In the assessment of engine full-load, the dynamic engine characteristics (e.g. the limitations in dynamic torque build-up) are also depicted by a PT1 time lag approach.

3.3.3 Drivetrain model

The main tasks of this module are to calculate the torque transmission in the drivetrain (gearbox and differential) and the related torque losses. For gearboxes, the following two main technological concepts are covered in the model:

- Conventional transmission, which covers manual transmissions and automated manual transmissions
- Automatic gearboxes with hydrodynamic torque converters, which are mainly used in city bus applications.
- Retarder losses for primary or secondary retarders can be defined optionally

3.3.4 Auxiliary model

In the auxiliary model, the power consumption of the auxiliary units is calculated. The following types are considered at the moment:

- Engine cooling fan
- Alternator
- Air compressor
- Steering pump
- HVAC system (Heating, Ventilation and Air Conditioning system)

Depending on the approach chosen for considering these components in the HDV CO_2 certification procedure – which has not been fully decided yet – the implemented functions comprise different modelling levels, from the use of constant power demand values to more detailed generic functions for the different auxiliary components.

At a later stage, this module might be implemented using an interface for certified interaction with OEM-specific auxiliary control models.

3.3.5 Interpolation from the fuel map

Based on the calculated engine torque and engine speed, the fuel consumption in the current time step is interpolated from the engine fuel map. For this purpose, the "Delauney triangulation method" is used in VECTO. The interpolated value is then multiplied by the "WHTC correction factor" (see chapter 4.1.1), which is a constant value for a given engine for each mission profile.

The CO_2 emissions are then calculated on the basis of fuel consumption, applying the fuel-specific carbon mass fractions of the test fuel.[5]

3.4 Data post-processing

VECTO writes results for the main relevant model quantities (e.g. vehicle speed, engine speed, engine power etc.) in 1Hz time resolution, as well as cycle average results for fuel consumption, CO_2 emissions, and vehicle speed.

[5] Table 5 on page 78 shows an example of properties for different fuels.

4 Options for integrating different technologies

This chapter points out options for evaluating different fuel-saving technologies by the current draft CO_2 test procedure for HDV in the EU. The discussion focuses on the main technologies already on the market and those expected to enter the market in the near future. If the technology is not covered by the current draft CO_2 test procedure, options are outlined for covering the related benefit in fuel economy.

4.1 Advanced engine technology

Before discussing particular engine-related fuel-saving technologies, a brief description is given of the method for depicting engine-specific fuel efficiency in the EU CO_2 certification.

4.1.1 Current approach

The current method for incorporating engine technologies into the simulation tool is based on an engine test procedure consisting of:

1. A steady state fuel map covering approx. 80 different engine operation points.
2. Measured fuel consumption in the three WHTC[6] subcycles (urban, road, and motorway) after hot engine start.

Based on this data, in VECTO, for each time step of a simulated cycle, a baseline value for fuel consumption is interpolated from the steady state map according to the actual engine speed and torque. This baseline value is then multiplied by the "WHTC correction factor". This factor is a constant value for a given combination of engine and mission profile and is applied for the following reasons:

- To consider the effect of transient engine behaviour such as boost pressure build-up or of specific engine application strategies e.g. applied for heating of the aftertreatment system which is not covered by the steady state fuel consumption map.
- To assure the consistency of regulated emissions and fuel consumption between the WHTC test and the steady state fuel map.

The WHTC correction factor is calculated by VECTO in a pre-processing step by dividing the measured fuel consumption in the WHTC by the fuel consumption interpolated from the steady state map based on the 1Hz WHTC engine operation pattern. This is done separately for each WHTC subcycle (urban, road, and motorway), resulting in three subcycle-related

[6] The WHTC ("World Harmonized Transient Cycle") is a transient engine dynamometer cycle developed by the UN ECE GRPE group and defined in the Global Technical Regulation (GTR) No. 4. The WHTC is also part of the European EURO VI emission legislation.

WHTC correction factors.[7] The final WHTC correction factor is then calculated by weighting the three subcycle-related factors according to the mission profile.

This approach was validated by TUG for three of the mission profiles as drafted in the EU CO_2 certification procedure based on measurements on a EURO III engine and on a EURO VI prototype engine. The maximum deviations between measured and simulated fuel consumption were +0.4% for the EURO III engine and -1.2 % for the EURO VI engine.

4.1.2 Optimisation of engine efficiency

Technologies to improve the engine efficiency focus either on an optimisation of the combustion process, a reduction of the engine-internal parasitic and pumping losses, or on a recovery of the waste heat energy. The latter is discussed in section 4.2.

Measures that lead to an optimised combustion process include:

- Advanced fuel injection systems (e.g. increase of injection pressure, rate shaping)
- Advanced turbocharging systems (e.g. 2-stage turbo charging with intercooling)
- Variable valve control systems

A reduction of engine-internal parasitic losses can, for example, be achieved by demand-operated systems for water pumps and oil pumps. Technical solutions include systems which can be controlled mechanically (clutch systems) or that operate the pumps electrically.

In general, the current approach is able to cover all the engine technologies that are based on mechanical solutions and can be measured during the engine mapping process (e.g. mechanical turbo-compounding or a waste heat recovery system, in which the output is connected to the engine crankshaft). The related fuel benefit shows up in the steady state fuel map, and the effects of engine transients should – at least to some extent – also be covered by the WHTC correction factor approach.

An extension of the current method will be required for inclusion of technologies which either generate electrical power (e.g. electric turbo-compound) or which consume additional electricity from the vehicle electrical system (e.g. electric water pump).

A simple solution could be to measure the electrical power generated and consumed by the advanced engine system in the three subcycles of the WHTC.[8] These values could then be allocated to the mission profiles in the VECTO simulations, applying similar weighting factors as in the WHTC correction factor process. The resulting average values for electrical

[7] For the engine tests available so far, the WHTC factor was in a range of 1.05 (i.e. 5% higher fuel consumption measured in a WHTC subcycle than interpolated from the steady state map) to 0.99 (steady state map slightly overestimates WHTC subcycle).

[8] Only electrical power consumed by components not included in the generic values for electrical power consumption shall be measured.

power generated and consumed could then be considered by VECTO in the simulation of the power demand from the alternator.[9]

4.2 Waste heat recuperation

In this section, measures are presented for recovering part of the waste heat from the hot engine lost to the environment, and for every technique proposals are made for including them in VECTO. Depending on the operating point, 60 to 90 % of the fuel energy is lost as waste heat. In the main operation area, this loss is limited to 60 to 70 %. With the known air-fuel ratio from a stationary measurement of every engine operating point, the exhaust gas composition at ideal combustion was calculated (diesel + air à $CO_2 + H_2O + O_2 + N_2$). With the known exhaust gas temperature and table values for the specific enthalpy of the gases, the enthalpy flow at every operating point was determined, see *Equation **1*** on page 30.

The breakdown of the heat losses into waste heat from cylinder charge to engine block and exhaust enthalpy[10] for a standard 12 L diesel engine (Hausberger, 2009-12) for tractors is shown in Figure 4.

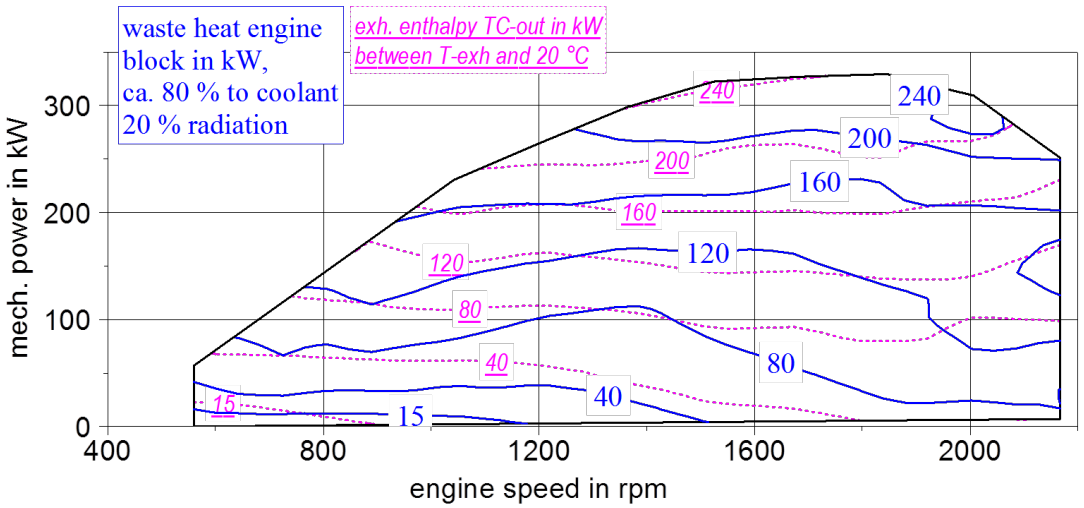

Figure 4. Breakdown of engine heat losses into waste heat to block (blue) and exhaust enthalpy (violet)

The radiation heat (approx. 20 % of waste heat to engine block) and the coolant heat (approx. 80 % of waste heat to engine block) can hardly be recovered. The temperature level of the coolant heat is between 80 and 100 °C. If one assumes a heat sink at an environmental

[9] The alternator is not mounted (or at least not operated) on the engine test bed. Hence, the engine fuel map and the fuel consumption measured in the WHTC do not cover the electrical power required to operate the engine-related electrical systems. This electrical power consumption is considered in VECTO in the generic power demand to be delivered by the alternator (in addition to the electrical power consumed by the vehicle). If a specific engine technology consumes additional electrical power (e.g. electric water pump), the power consumption measured during the WHTC has to be added to the alternator load in the VECTO calculations. For systems producing electrical energy (e.g. electric turbo-compound), the alternator load is reduced in the VECTO calculations according to the measured power consumption in the WHTC.

[10] (exhaust enthalpy) = (mass flow diesel) * (lower heating value) - [(mechanical power) + (waste heat block)]

temperature of 20 °C, the Carnot efficiency would be around 19 %. Thus, a real heat engine would work at very low efficiencies. In addition, a second low temperature coolant circuit at 20 °C would be necessary.

Another possible heat source is the waste heat from the EGR line. But this cannot be simulated with the VECTO approach, since the engine is depicted via a stationary consumption map and a correction factor for the transient behaviour. The engine-internal fluid flow EGR, its temperature, and transient behaviour are not covered by the applied methodology.

Thus, the focus of the first step shall be on the use of the exhaust downstream from the aftertreatment. There, the exhaust mass flow and the transient temperature can be simulated. The temperature downstream from the turbocharger, which is the entry value for the simulation, is given in Figure 5.

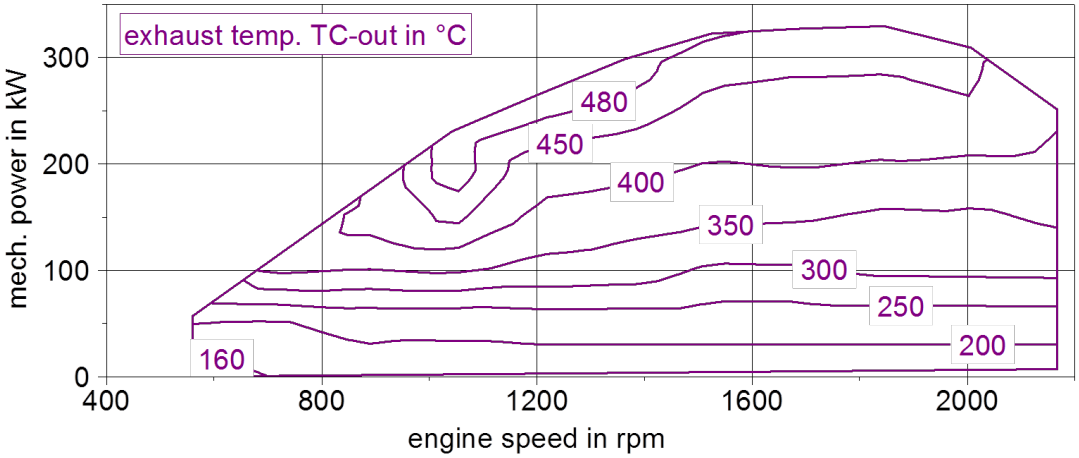

Figure 5. Exhaust temperature downstream from the turbocharger

When the heat sink temperature is 90 °C (average temperature of the main coolant circuit), the Carnot efficiency ranges from 14 to 53 %, so no second low-temperature coolant circuit is necessary, because the main coolant circuit can act as a heat sink for the ORC (Dold, 2013-06). This *can* lead to an economically efficient recuperation module in terms of surcharge, reduction of fuel cost, and payback duration.

In the following subsections, current approaches for waste heat recovery are presented. Ways for integrating these measures into the CO_2 certification process are also discussed.

4.2.1 Mechanical and electrical turbo-compound

The basic idea of turbo-compounding is that a second turbine is installed downstream from the turbocharger and converts a fraction of the thermal power from the exhaust gas into mechanical power (see Figure 6).

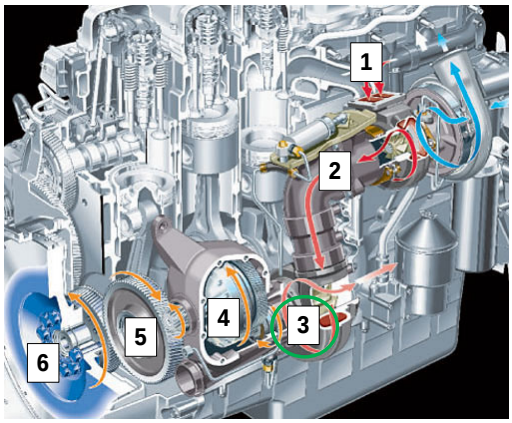

1: turbocharger, inlet
2: turbocharger, outlet
3: turbocompound turbine
4: hydraulic clutch
5: gear drive
6: engine crankshaft

© *Scania*

Figure 6. Turbo-compound

This turbo-compound system is coupled with the crankshaft to support the engine. In other constructions, the second turbine is connected to a generator, or the generator is integrated in the turbocharger. The FC reduction is reported to be from 1 to 5 % (Briggs, 2012-03), (Mamat, 2012-10), (Sendyka, 2004-08).

è In any case, the resulting FC reduction or the electrical power generation of a turbo-compound engine shall be measured together with the engine on the test bench during the component test procedure. The second turbine is fully integrated into the engine and influences the exhaust backpressure and charge exchange and thus the whole engine behaviour. The test results can be used in VECTO as outlined in 4.1.2.

4.2.2 Organic Rankine cycle and thermoelectric generator

An Organic Rankine Cycle (ORC) is a steam power process, driven by the exhaust heat from the engine. The working fluid is typically a mixture of organic fluids, e.g. refrigerants like R123 of R245fa. The specific evaporation heat of these liquids is much smaller than for water, which leads to higher vapour mass flow at equal heat absorption. This results in less specific gap losses of the fluid in the turbo-machine between rotor and housing. Due to the low power, these machines are very small compared to power stations. The operation of small turbines with water steam would result in high specific gap losses, due to the unavoidable minimal clearance between rotor and housing. This clearance results from the production process of a pairing turbine-housing, and a certain part of the thermal energy of the working fluid is wasted due to losses through this gap. The bigger the fluid flow is, e. g. due to a low specific heat of evaporation at equal heat absorption, the smaller these specific gap losses become, related to the total thermal absorbed energy.

Options for the working machines are turbines, scroll expanders, or piston machines. Piston machines, on the other hand, can be operated with water as a working fluid. In this case, the sealing between piston and cylinder is better than that of rotors and housing.

Two projects for waste heat recovery via steam processes have already been finished at IVT (Almbauer, 2012-02), (Almbauer, 2013-11).

A flow scheme of an ORC process is shown in Figure 7.

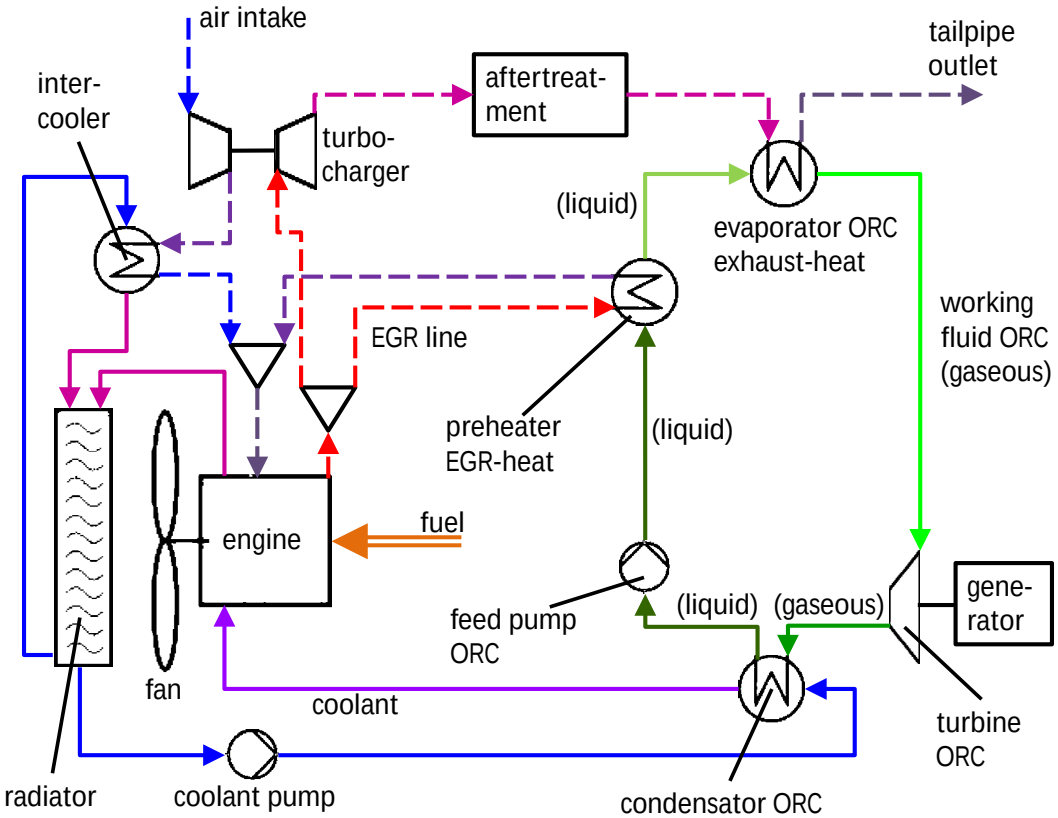

Figure 7. Flow scheme of an ORC process, coupled to a diesel engine
brighter colours within a circuit mean a higher temperature level

In this scheme, the working fluid is preheated by the EGR heat, in addition to the main evaporator downstream from the exhaust after treatment. As explained above, the EGR heat cannot be simulated in VECTO, so only the green ORC circuit with the exhaust gas as heat source and the main coolant circuit as heat sink will be analysed.

Pictures of an ORC prototype are provided in Figure 8.

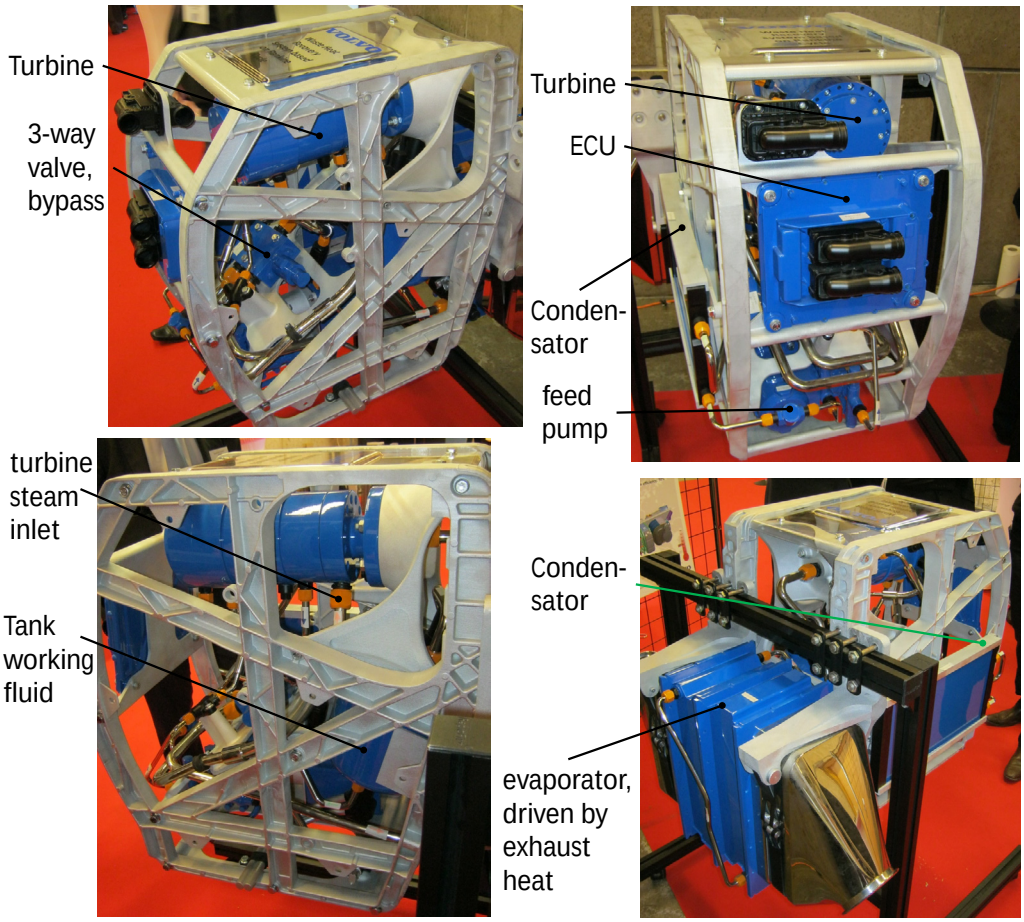

Figure 8. ORC prototype, Volvo trucks (Espinosa, 2012-11)

This system is a good example of a separate device, which can be mounted as a box behind the exhaust after treatment.

4.2.3 Thermoelectric Generator

A thermoelectric generator (TEG) uses the Seebeck effect to generate electrical power from heat. The best-known application is thermocouples for temperature measurement. Bigger devices can be used to recuperate waste heat. An example of a heat exchanger with an integrated TEG from semiconductor material is given in Figure 9.

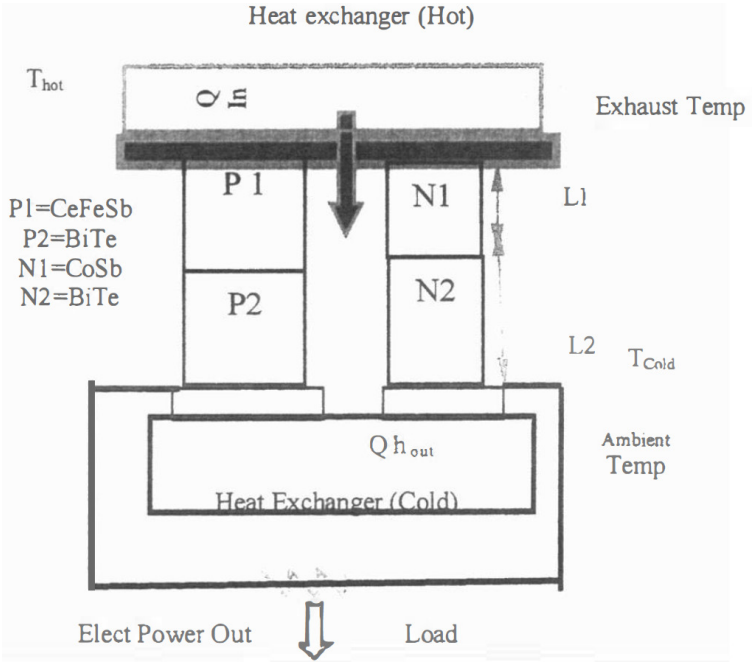

Figure 9. Heat exchanger with integrated thermoelectric generator. (Srinivasan, 2005-11 p. 980)

The electrical efficiency of a TEG is dependent on the figure of merit (ZT) and the temperatures of the heat source and the heat sink. An example of the temperature dependency of the efficiency, calculated from published measurements, is shown in Figure 10.

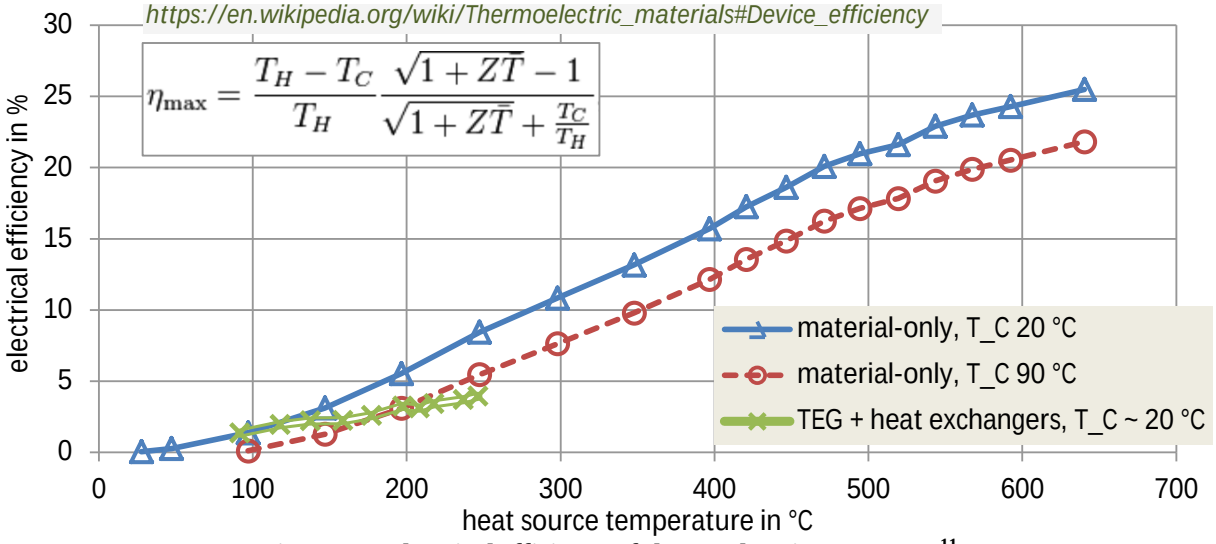

Figure 10: Electrical efficiency of thermoelectric generators[11]
calculated from **(Biswas, 2012-09 pp. 414, fig. 1) (Brito, 2011-11 p. 6 fig. 8)**

The curves with the high efficiency values (blue, red) result from measurements of the characteristics of advanced thermoelectric materials (Biswas, 2012-09). For a real TEG from standard material (green curve), the losses in the heat exchangers lead to lower efficiency

[11] h_{max} - max. electrical efficiency, T_H - heat source temp., T_C - heat sink temp., ZT - figure of merit

values between 2 and 5 % (Brito, 2011-11). Four TEGs were mounted on a hot copper pipe as heat source and cooled via water heat exchangers as heat sink (Brito, 2011-11 p. 5 fig. 5).

As shown in Figure 7, the EGR heat can be used as an additional heat input for the ORC. Another approach is to mount a TEG heat exchanger at this position and a stand-alone ORC behind the exhaust after treatment.

è If a waste heat recuperation device is integrated into the engine-internal fluid flows, its power generation shall be measured together with the FC map on the engine test bench. The heat absorption is heavily dependent on the control of the EGR and/or coolant valves, which determine the amount of fluid flow and temperature. Also, a measurement standard for the transient behaviour of the system is necessary. If the measurement during the highly transient WHTC test is sufficient for elaborating a simulation method for the urban cycles shall be elaborated further. In principle, we assume that the test results can be used in VECTO as outlined in 4.1.2.

4.2.4 Option for WHR component testing

If an exhaust heat recuperation system, ORC, or TEG is foreseen as a stand-alone device downstream from the exhaust after treatment, depicting it as a separate module in the simulation also seems possible. A possibility for component testing is explained below. To test if such a test can be done without an engine but with any exhaust source, e. g. an oil burner, the influence of different exhaust gas compositions is analysed.

The tractor engine presented in Figure 4 and Figure 5 allows for a heat sink temperature of 90 °C (engine coolant circuit) and a theoretical heat recuperation of up to 210 kW_{therm} at rated power, see Figure 11.

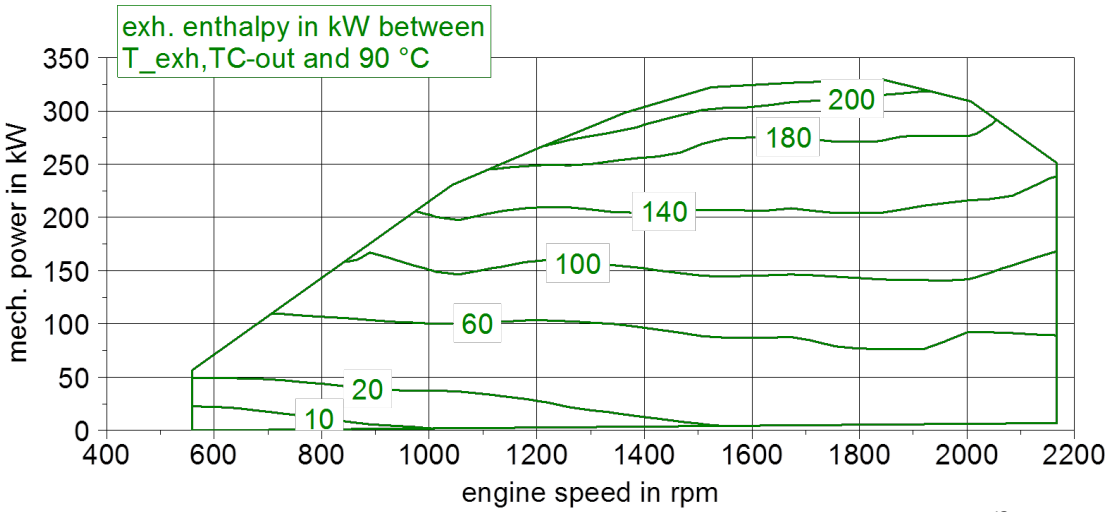

Figure 11. Exhaust enthalpy between temperature TC-out and heat sink 90 °C[12]

The shown absolute enthalpy difference between exhaust gas temperature and 90 °C is the product of the exhaust gas flow and its specific enthalpy. The specific enthalpy is dependent on the exhaust gas composition (varying fractions of CO_2, H_2O, O_2, N_2) and the temperature, (see *Equation **1***).

Equation 1

$$\Delta\dot{H}_{exh,\vartheta.sink} = \dot{m}_{exh} \times \left(h_{m,exh,\vartheta.exh} - h_{m,exh,\vartheta.sink}\right) = \dot{n}_{exh} \times \left(h_{n,exh,\vartheta.exh} - h_{n,exh,\vartheta.sink}\right)$$

$$\text{with} \quad h_{n,exh,\vartheta.i} = \sum_j \left(X_{j,exh} \times h_{n,j}(\vartheta_i)\right)$$

where:

$\Delta\dot{H}_{exh,\vartheta.sink}$	Exhaust enthalpy flow between exhaust gas temperature and heat sink temperature [kW_{therm}]
$\dot{m}_{exh}$	exhaust mass flow [kg/s]
$h_{m,exh,\vartheta.exh}$	mass-specific exhaust enthalpy at exhaust temperature ϑ_{exh} [kJ/kg]
$h_{m,exh,\vartheta.sink}$	mass-specific exhaust enthalpy at heat sink temperature ϑ_{sink} [kJ/kg]
$\dot{n}_{exh}$	exhaust molar flow [mol/s], $\dot{n}_{exh} = \frac{\dot{m}_{exh}}{M_{exh}}$, M_{exh}: molar mass exhaust gas [kg/mol]
$h_{n,exh,\vartheta.exh}$	molar-specific exhaust enthalpy at exhaust temperature ϑ_{exh} [kJ/mol]

[12] In this example, the enthalpy difference of the exhaust gas between temperature TC-out and 90 °C (average main coolant circuit temperature) is energy content of the waste heat which cannot be converted totally into mechanical work (only the exergy of the energy flow can in theory be converted). The electrical efficiency of WHR systems like thermoelectric generators and Organic Rankine cycles is temperature-dependent and ranges from 1 to 8 %.

$h_{n,exh,q.sink}$	molar-specific exhaust enthalpy at heat sink temperature q_{sink} [kJ/mol]
$X_{j,exh}$	molar fraction of gas component "j" (CO_2, H_2O, O_2, N_2) $X_{j,exh}$ is calculated from the air-fuel ratio
$h_{n,j}(q_i)$	molar-specific enthalpy of gas component "j" at temperature "i" [kJ/mol] [13]

This map is valid for the stationary case on the engine test bench. The chemical reactions in the exhaust after treatment system, SCR catalysis, and particle filtration, do not affect the exhaust temperature much during normal driving (see Figure 5). Only the heat loss from the tubes to the environment needs to be considered. But the engine block, the tubes, and the after treatment systems act as heat storage. Thus, the exhaust temperature course at the tailpipe outlet is heavily damped and to a large extend decoupled from the engine operation points. The simulated temperatures for the "turbocharger-out", from the stationary map, and for the "tailpipe-out", with all the damping effects, are given in Figure 12.

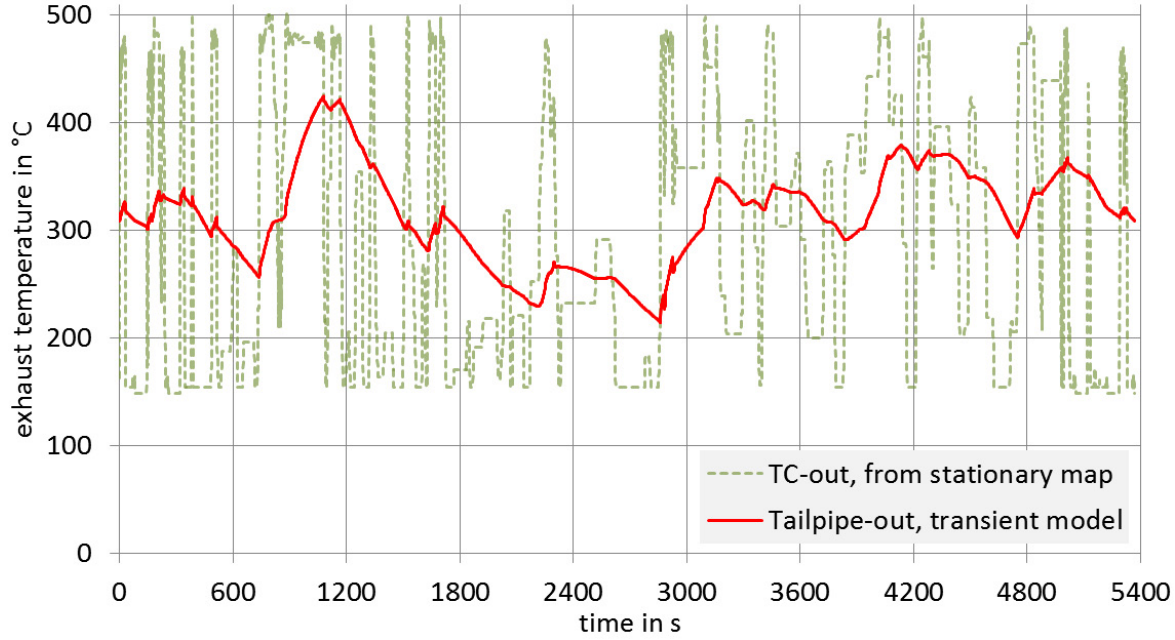

Figure 12. Exhaust temperatures, simulated with the PHEM model[14].
TC-out and tailpipe-out, for a tractor-trailer on the long-haul cycle

Thus, the exhaust mass flow and gas composition from the engine operating points enters the ORC system downstream from the tailpipe at different temperatures, depending on the thermal history of the engine. Most times, the temperature at the tailpipe outlet is above 250 °C.

[13] http://webbook.nist.gov/chemistry/fluid

[14] PHEM (Passenger Car and Heavy Duty Emission Model) is an emission model developed at the FVT, which also includes zero-dimensional modeling of the temperatures in the exhaust system. PHEM was the starting point for the development of the VECTO tool. In its current version, VECTO does not cover the modelling of temperatures in the exhaust system.

The limit cases are:

- Full-load acceleration after long idling at cold exhaust tract

  For example, after a long standstill. The exhaust system is cold at approx. 150 °C and the full-load exhaust gas is flowing through it. At the tailpipe outlet, the gas composition of full load is combined with the low idling temperature of the exhaust system. The whole exhaust system is heated up slowly, e.g. at + 0.5 K/s, (cf. Figure 12 from 900 to 1050 s).

- Idling engine and hot exhaust tract.

  After a long uphill section, the engine falls to idle during the following downhill rolling. The exhaust system is hot at 500 °C, but the gas composition of high or low idle is flowing through it. The exhaust tract cools down slowly, e. g. at - 0.3 K/s, (cf. Figure 12 from 1200 to 1500 s).

Thus, the ORC or TEG system should be measured over the whole possible operational envelope:

- Low exhaust flow, low temperature (continuous idling)
- Low exhaust flow, high temperature (engine idling after long full-load operation)
- High exhaust flow, low temperature (full load at drive-off after long idling)
- High exhaust flow, high temperature (continuous full load, e.g. during long uphill)

The exhaust volume flow [m³/s] from the stationary engine map was chosen as the basis value, because this number determines the gas flow velocity in the tubes and the heat exchanger and therefore influences the heat transfer to the ORC. The exhaust volume flow and l [15] are shown in Figure 13.

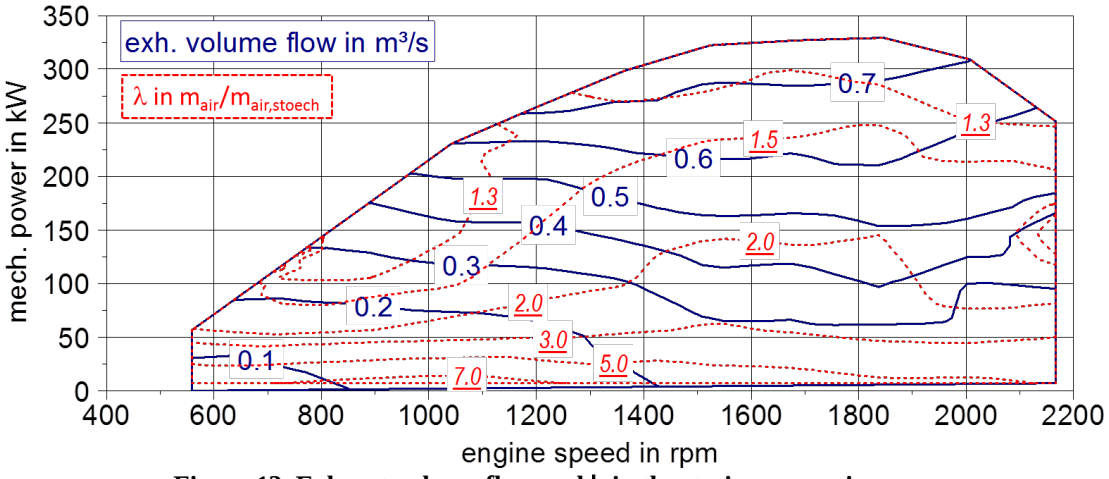

Figure 13. Exhaust volume flow and l in the stationary engine map

[15] l = (mass air) / (mass air stoichiometric)

The volume flow ranges from approx. 0.05 to 0.8 m³/s and λ is around 1.5 in the main operation area.

Because the measurement burden would be much too high for an ORC system for all combinations of all possible values of air-fuel ratio, volume flow, and temperature that can appear in reality, a simplification was analysed theoretically:

- The ORC system is mounted on a test bench and powered by the hot exhaust gas from an oil burner.
- To reproduce the presented engine, the burner operates at an idling volume flow of 0.05 m³/s at λ = 7 to match the idling exhaust composition. Idling occurs often during standstill and coasting.
- At high idling with an exhaust volume flow of 0.1 m³/s, the burner is set to λ = 3.
- For the rest of the map with an exhaust volume flow > 0.1 m³/s, the burner is set to λ = 1.5
- For every volume flow, the temperature is varied from 150 to 500 °C (cf. the temperature range in Figure 5) using a controlled heat exchanger. To cool down the highest exhaust flow at rated speed from the adiabatic burning temperature at λ = 1.5 to 150 °C, the controlled heat exchanger would need to transfer 1.1 MW_{therm} from the hot exhaust gas, so cheaper options should be investigated.

The deviation of the exhaust enthalpy of the oil burner to the real engine is reasonably low, (see Figure 14).

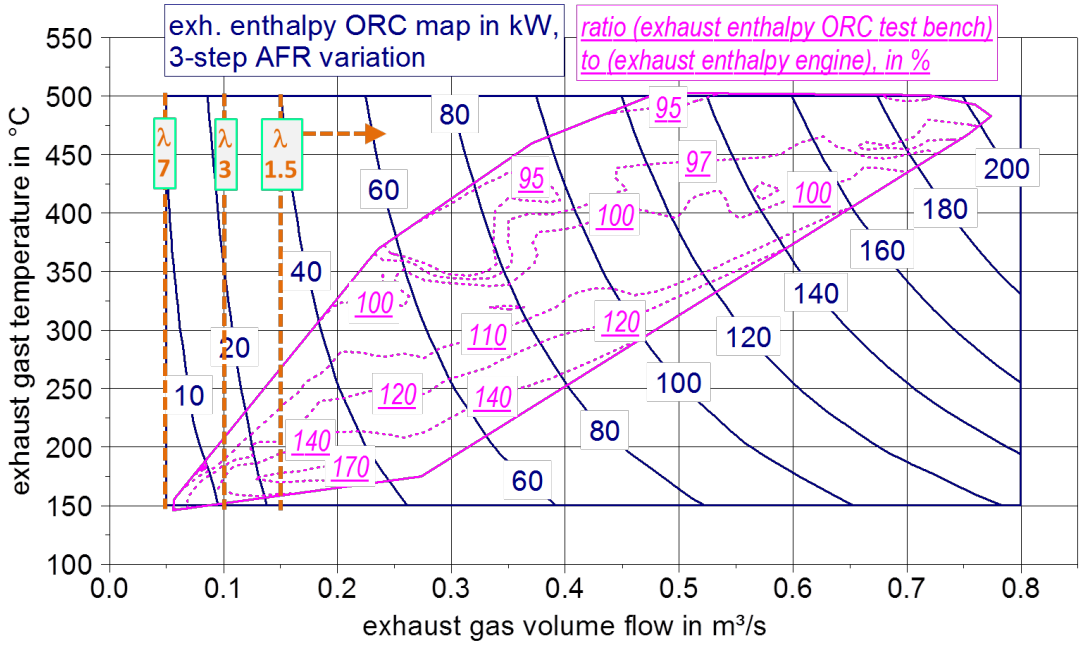

Figure 14. Blue map: Exhaust enthalpy between q_{exh} and 90 °C from the oil burner of the ORC test bench, 3-step λ variation.
Magenta: Ratio of exhaust enthalpy from oil burner to real exhaust enthalpy from stationary engine map (Figure 11), varying λ from 1.2 to 8.[16]

It is evident that at the engine outlet, which is shown in the magenta map in Figure 14, the low temperatures occur only at low exhaust flows and the high temperatures at high flows. However, due to the heat storage by the exhaust tract, the corners high temperature / low flow and low temperature / high flow also need to be considered, which would be using an oil burner in the component test.

It can also be seen that the deviation in terms of enthalpy between the exhaust gas from the burner and the real exhaust from the engine ranges from - 5 to + 20 % in the biggest part of the engine map (magenta). Only points with high exhaust flow and low temperature are not matched due to a higher AFR deviation.

[16] Creation of the magenta map: Take the exhaust enthalpy from the stationary engine map, Figure 11. Map this over the exhaust gas volume flow (x-axis) and the exhaust gas temperature (y-axis), both also from the stationary engine map. Divide the exhaust enthalpy of the oil burner (blue map, Figure 14) by these values. The result is the ratio (exhaust enthalpy ORC test bench) / (exhaust enthalpy engine). This ratio in % is the z-value of the magenta map in Figure 14.

The engine map provides a better impression of the impact of the enthalpy deviation, (see Figure 15).

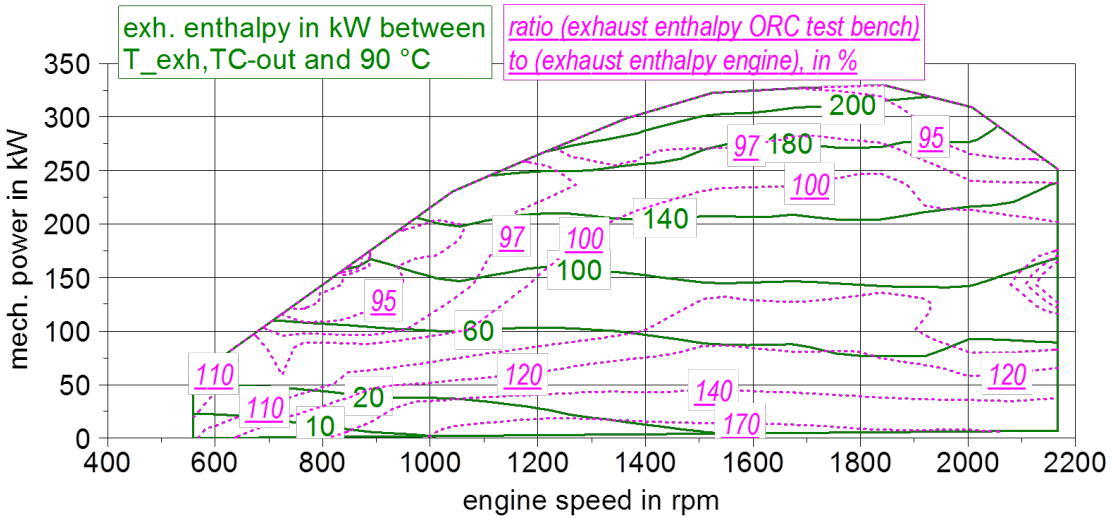

Figure 15. Green map: Exhaust enthalpy between temperature TC-out and heat sink 90 °C (Figure 11). Magenta: Ratio of exhaust enthalpy from oil burner (blue map, Figure 14) to exhaust enthalpy engine (the green map in this diagram)

In the main operation area of the engine above 75 kW_{mech}, the deviation from the oil burner exhaust enthalpy to the real engine exhaust enthalpy also ranges between - 5 to + 20 %. For the majority of operating points at high exhaust temperatures (cf. Figure 5), the oil burner exhaust enthalpy is close to 100 %. If low power at high engine speeds occurs often in the driving cycles, a correction factor for the simulation can be elaborated.

Thus, an ORC or TEG system for waste heat recovery can be measured in theory in an operating area as shown in Figure 14 (blue map). The necessary exhaust gas can be generated by an oil burner and the temperature can be set using a controlled heat exchanger. The result would be the map of the electrical power generation, dependent on exhaust volume flow and exhaust temperature.

Reported measurement results of ORC systems have shown an electrical efficiency at full load of the engine of approx. 10 %, with reference to the heat which is absorbed by the ORC system ($\dot{Q}_{absorb}$) (Hountalas, 2010 p. 333). If a heat exchanger efficiency of 90 % ($\dot{Q}_{absorb}$ / $D\dot{H}_{exh,q.sink}$) is assumed, this leads to a recuperation potential at full load of approx. 20 kW_{el} for the presented engine. In the main part of the operation map, this potential will be significantly smaller due to lower temperatures and exhaust flows. For example, for a 12 L HDV engine at the low-power operating point B25, a mechanical power output of the ORC turbine of 2.1 kW_{mech} is reported, and 9 kW_{mech} at B75 (Seher, 2012 p. 12).

Engine-independent, stand-alone exhaust heat recovery systems can be measured and certified separately from the engine. The electrical performance can be measured for gas compositions similar to the engine map. It is already possible to simulate the transient exhaust temperature at the tailpipe outlet in PHEM (see footnote 14 on page 31), so the values exhaust mass flow, gas composition, and temperature would be the input values for the ORC sub-model. Whether

transient effects of the ORC system need to be considered shall be the subject of further investigation.

4.3 Auxiliary systems

Auxiliary systems are devices that provide energy for functions other than propulsion. Auxiliaries are either needed for proper operation of the engine (e.g. engine cooling fan) or of vehicle related systems (e.g. compressor for pressurised air system). In conventional vehicles, auxiliary units are driven by mechanical power from the internal combustion engine.

The power consumption of some engine-related auxiliary components are already implicitly covered by the engine fuel map and hence do not have to be considered separately. These components are:

- engine oil pump
- coolant pump
- fuel delivery pump
- fuel high pressure pump

The remaining auxiliary units need to be covered in the fuel consumption modelling individually. These systems are:

- engine cooling fan
- alternator
- air compressor
- steering pump
- air conditioning system

The ranking of the average energy consumption of these five devices is dependent on the mission profile. Example results from the current VECTO model are shown in Figure 16.

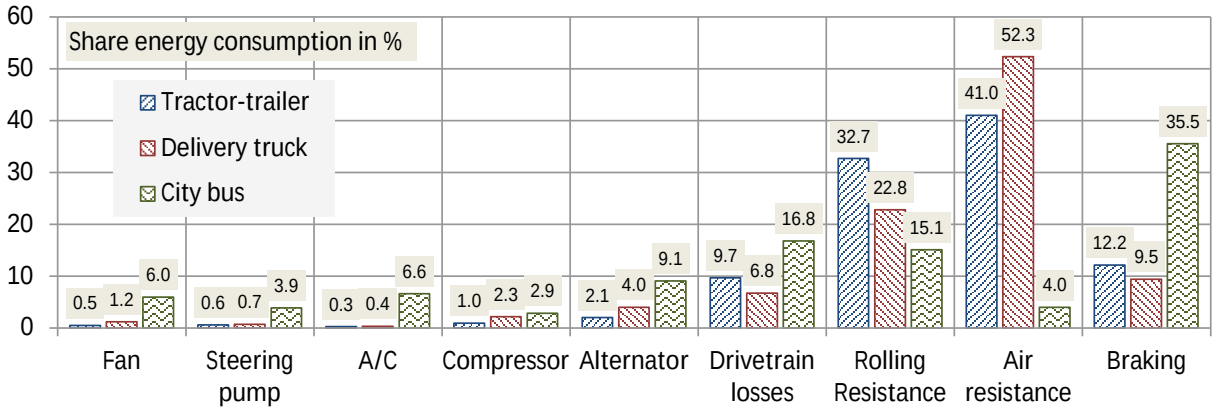

Figure 16. Share of auxiliary consumers, drivetrain losses, driving resistances, and braking at the energy demand of typical HDV

According to the current status of the EU HDV CO_2 certification procedure, the methods on auxiliaries are still not finalised. For truck applications, in which the influence on overall fuel consumption was assessed to be of secondary importance, rather simple approaches are under development. For buses, the impact of auxiliary performance was found to have a significant impact. Hence, a separate project ordered by DG Clima on related models and test procedures

for bus auxiliaries will be started in 2014. Some of the methods elaborated there might also be introduced also trucks at a later point in time.
In this report, first an overview on the "simple" methods under development for trucks is given. Then, advanced auxiliary models elaborated in this project are presented which might serve as a basis for further differentiation of auxiliary technologies or – if combined with component testing – for consideration of OEM-specific performance.

4.3.1 Current draft for general approach in VECTO

The current draft approach for the simulation of auxiliaries in VECTO foresees a three-step approach for the quantification of the mechanical power required from the engine:

1.) The determination of the necessary "supply power" to be delivered by the auxiliary unit based on the vehicle specifications (e.g. vehicle type or vehicle equipment)

Example (electrical system): Determination of average electrical power based on a list of electric consumers

2.) The calculation of the required mechanical power demand of the auxiliary unit from the internal combustion engine from "performance maps" in the format:

$P_{mech,\ aux} = f\ (n_{aux}, P_{sup,aux})$

with:

$P_{mech,\ aux}$ … mechanical power demand from the internal combustion engine

n_{aux} ..... operating speed of the auxiliary

$P_{sup,\ aux}$ .... supply power to be delivered by the auxiliary

The performance maps can be either generic or component-specific. For the use of the latter, a standardised test procedure is required.

Example (electrical system): Alternator efficiency map

3.) Optional: Consideration of applied technologies by the application of lump-sum factors

Example (steering pump): applying factors to baseline mechanical power demand which differentiate between technologies (hydraulic, electric, …)

The resulting mechanical power is then added in VECTO to the load pattern of the internal combustion engine. Figure 17 shows the general scheme approach for simulating auxiliaries in VECTO. The methods are still under development. The applied approach will most probably differ somewhat depending on the auxiliary type.

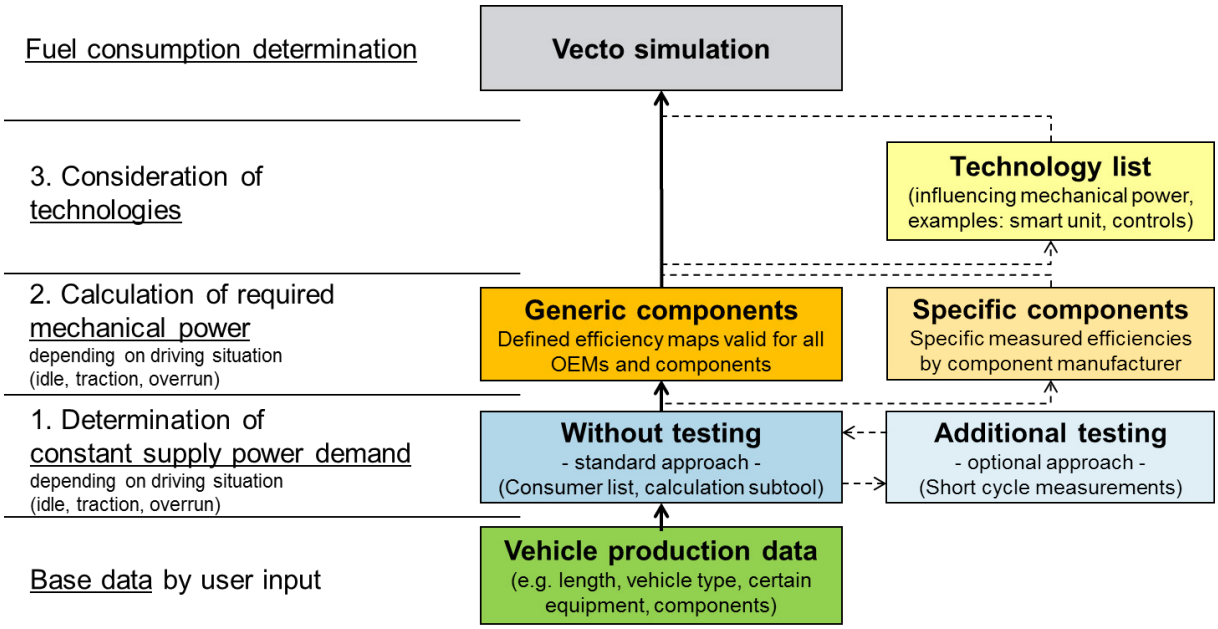

Figure 17: Scheme of current status for simulating auxiliaries in VECTO (source: ACEA; adapted by TUG)

This approach already allows for a good baseline quantification of the contribution of auxiliaries on overall fuel consumption if representative baseline data for supply power demand and performance data are available. ACEA promised to compile these baseline generic datasets to be applied for all truck categories.

The different auxiliary units and the models elaborated in this project are described in detail below. It was agreed to exclude air conditioning systems from this project because this type of system will be the main focus of the project dealing with bus auxiliaries.

4.3.2 Engine Cooling Fan

The engine fan is used to generate an additional air flow through the main radiator. This becomes necessary when the coolant begins to get too hot because the air flow from the vehicle's velocity is too low to dissipate the waste heat from the coolant system. An example of the average power demand of the engine fan for a long haul truck is 350 W and for an interurban bus 1400 W (data provided by ACEA).

Today, cooling fans are connected to the engine either by

- a viscous clutch, which increases the fan speed at increasing temperature levels or by
- a mechanical on/off clutch, which (dis-)connects the fan to the engine at a defined coolant temperature.

In future, if more than a 24 V supply system is on board, an

- electric driven fan

could be installed. In heavy duty trucks, the fan can consume > 10 kW_{mech}, (cf. Figure 22). This would be > 11.8 kW_{el} power demand of an electric motor, which results in > 420 A at 28 V. The maximum starter current of a 14 L truck engine is 250 A (Reif, 2010-12 p. 540 fig.

20), so the current low voltage systems would be overstressed. But in the case of (micro-hybrid) electric HDV with a high voltage system, e.g. a tractor with ZF Traxon Hybrid at 650 V, the fan can be powered electrically. The advantage would be that its speed can be fully controlled, in contrast to the on/off clutch, but without high losses up to 3 kW_{mech} as in the case of a viscous clutch, (see Figure 25).

4.3.2.1 Current draft approach

The current draft approach is based on generic values for constant mechanical power demand according to HDV class and mission profile. These values are defined as “supply power” using a “virtual” performance map with 100% efficiency. The need for differentiation between different fan technologies has not been decided yet.

4.3.2.2 Advanced VECTO cooling fan model

The advanced VECTO cooling fan model was developed in this project in cooperation with BEHR. Possible applications of the model are:

- Calculation of a generic baseline mechanical power demand of the engine cooling fan for all HDV classes in all mission profiles
- Differentiation between fan technologies: viscous clutch, on/off etc. (e.g. calculate correction factors for the baseline mechanical power demand for advanced technologies)
- Differentiation between fan control strategies (suitability of the model to be verified)

4.3.2.3 Model description

Due to complex physics and multiple input parameters, modelling of the engine cooling fan requires complex model structures. The basic assumptions made in the current model are

- Assume the air path as pipe flow:
  grille *(entrance)* - radiator - fan - engine compartment - vehicle under-surface *(outlet)*
- Use generic drag coefficients to depict the single flow resistances in the air path
- Set up a radiator model: dependence of heat transfer (coolant à air) from air flow velocity and coolant temperature
- Calculate the air flow for every time step, differentiate between cases of "fan off" (pressure drop) and "fan on" (pressure increase)
- Calculate the coolant temperature by a simplified energy balance of engine and coolant
- Apply a generic control strategy for the fan operation
- Consider the power losses in the transmission crankshaft - fan

The air path from grille to under-surface is shown in Figure 18.

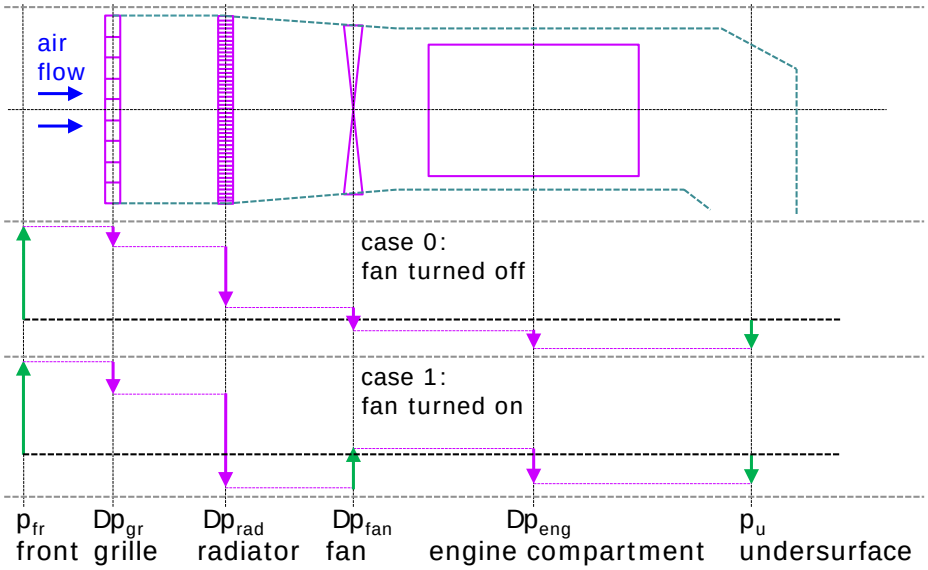

Figure 18: Air path from grille to under-surface

The calculation scheme for dealing with the single flow resistances is described in section 7.1, Equation 15 to Equation 17.

The radiator characteristics are depicted via maps. Some general properties of radiators are shown in Figure 19.

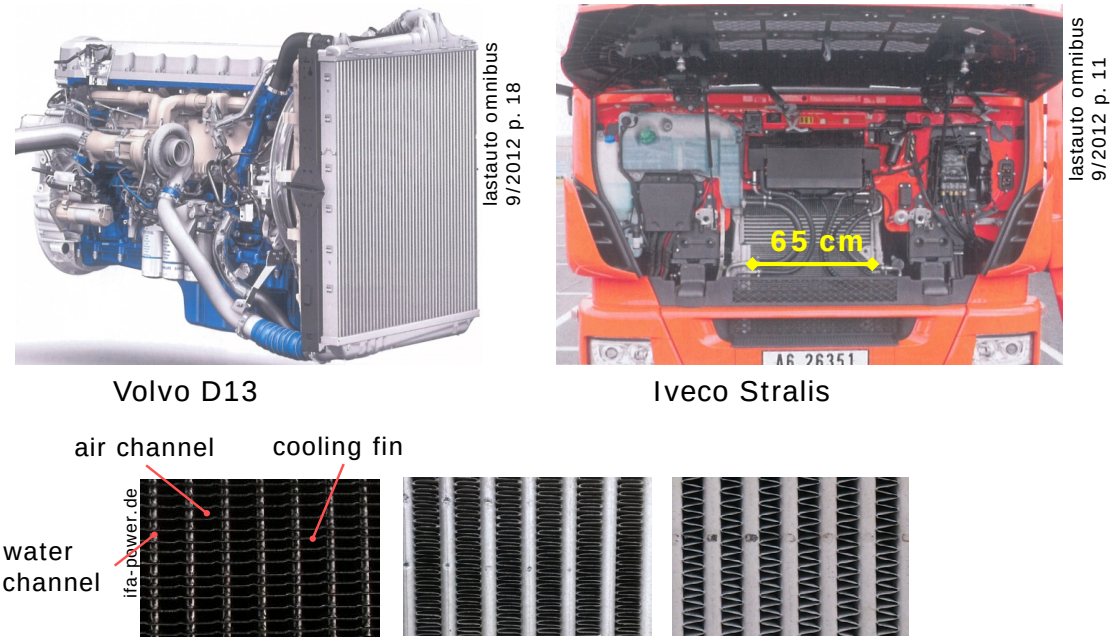

Figure 19: Installation space and detailed geometry of HDV radiators

The following assumptions were made for a simplified radiator model:

- Main- and EGR cooler treated as one combined cooler unit: 90 cm · 90 cm · 12 cm
- Disregard of air conditioning radiator
- 41 x 450 air channels, 1.7 cm · 0.18 cm (size w/o water channels and fins)
- Air temperature at air channel inlet constant: $\vartheta_{air,in}$ = 20 °C
- Heat transfer coefficient on water side constant: α_{water} = 11 kW/(m²·K)
- Thermal conductivity of radiator material constant: λ_{Alu} = 200 W/(m·K)
- Heat transfer coefficient on air side variable with air flow velocity:
- α_{air} = f(geometry, Re, Nu, $\vartheta_{air,avrg}$, η_{fin} ...), range approx. 30 to 120 W/(m²·K)
- overall heat transfer coefficient $k_{water-air}$, range approx. 160 to 500 W/(m²·K)

  à with reference to outer surface of water channels, fins included via fin heat transfer efficiency η_{fin}

- pressure loss estimated: losses of diameter reduction at air channel intake (factor $A_{cr,rad,flow}$ / $A_{cr,rad}$) and tube flow through single channels

In every single air channel, heat is conducted from the coolant to the flowing air, and the summarized heat conduction of all air channels is the total waste heat water-to-air of the radiator. The calculation scheme for this virtual radiator is given in section 7.2, Equation 20 to Equation 61.

The relevant parameters of the radiator are

- the mean air flow velocity in the air channels
- the coolant temperature
- the total heat transfer coolant-to-air
- the air density at the radiator outlet

The workflow of the calculation is listed below:

1) The coolant temperature is calculated according to Equation 10
2) The desired fan speed is determined by the control strategy, (in this case, the curve in Figure 26). The speed is always between the lower limit 1/4 • n_{ICE} [17]and the upper limit, (cf. Figure 25).
3) Using the values "average air flow velocity in radiator flow cross-section" and "coolant temperature" *of the last time step* (t - 1 s), the air density of the actual time step (ρ_{fan}(t)) is interpolated, (see Figure 20). Air density is a slowly changing factor, so this

[17] This lower boundary speed is caused by the losses in the viscous clutch and a component-specific characteristic.

is tolerable. Otherwise, a circular reference between air density and pressure drop would occur, (see Equation 18).

4) The average air density in the radiator air flow channels is calculated by ρ_{fan} and the ambient air density ($\rho_{air,amb}$):

Equation 2 $$\rho_{air,rad,avrg} = \frac{\rho_{air,amb} + \rho_{fan}}{2}$$

5) If the fan is turned off (mode 0), the "air flow velocity in fan cross section" ($v_{fan,0}$) is calculated via Equation 18.

6) If the fan is turned on (mode 1), the "air flow velocity in fan cross section" ($v_{fan,1}$) is calculated via Equation 19.

7) With v_{fan}, the fan cross sectional area ($A_{cr,fan}$), the air density there (ρ_{fan}), the average air density in the radiator air flow channels ($\rho_{air,rad,avrg}$) and the radiator air flow cross sectional area ($A_{cr,rad}$), the average air flow velocity in the radiator air flow channels ($v_{air,rad,avrg}$) is calculated:

Equation 3 $$v_{air,rad,avrg} = v_{fan} \times \frac{A_{cr,fan}}{A_{cr,rad}} \times \frac{\rho_{fan}}{\rho_{air,rad,avrg}}$$

8) With $v_{air,rad,avrg}$ and the coolant temperature, the waste heat coolant-to-air (Q_{rad}) is interpolated from the radiator map, (see Figure 20). These values ($v_{air,rad,avrg}$, ϑ_{cool}, Q_{rad}) are the initial values for the following calculation of the next time-step (t + 1 s), (see 1) in this list).

9) In the case of a running fan: With the known air flow velocity ($v_{fan,1}$) and engine speed (n_{ICE}), the pressure increase by the fan ($\Delta p_{fan,1}$) is calculated via Equation 5.

10) With $v_{fan,1}$ and $\Delta p_{fan,1}$, the fan power consumption at its hub ($P_{fan,hub}$) is interpolated from the map, (see Figure 24).

11) With the ratio of fan- to engine-speed (n_{fan} / n_{ICE}), the slip losses of the viscous clutch ($P_{cl,loss}$) are interpolated, (see Figure 25).

12) The total power consumption of the fan wheel at the crankshaft is

Equation 4 $$P_{fan,cranksh} = P_{fan,hub} + P_{cl,loss}$$

The following section gives a closer description of the single components of the model.

The behaviour of the radiator can be depicted via two 3-dimensional maps, (see Figure 20).

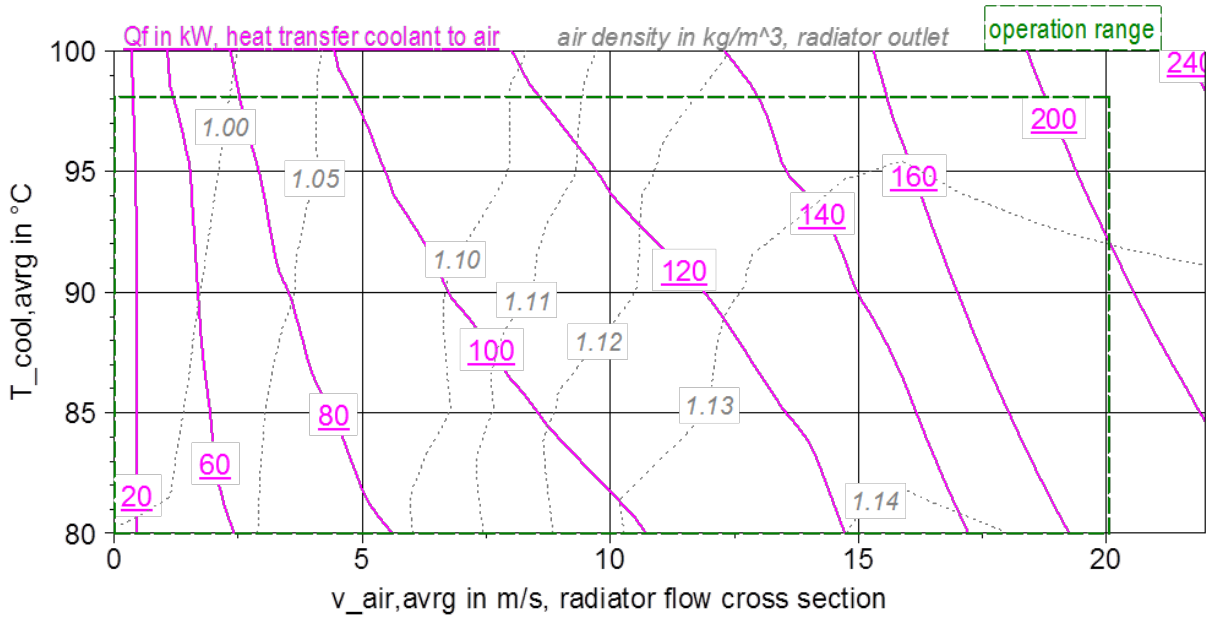

Figure 20: Radiator maps.
1 violet. average air flow velocity in radiator cross flow section - coolant temp. - heat transfer
2 grey. average air flow velocity - coolant temp. - air density outlet

The flow resistance coefficient of the radiator is dependent on the coolant temperature because the varying air density is part of the equation, (see Figure 21).

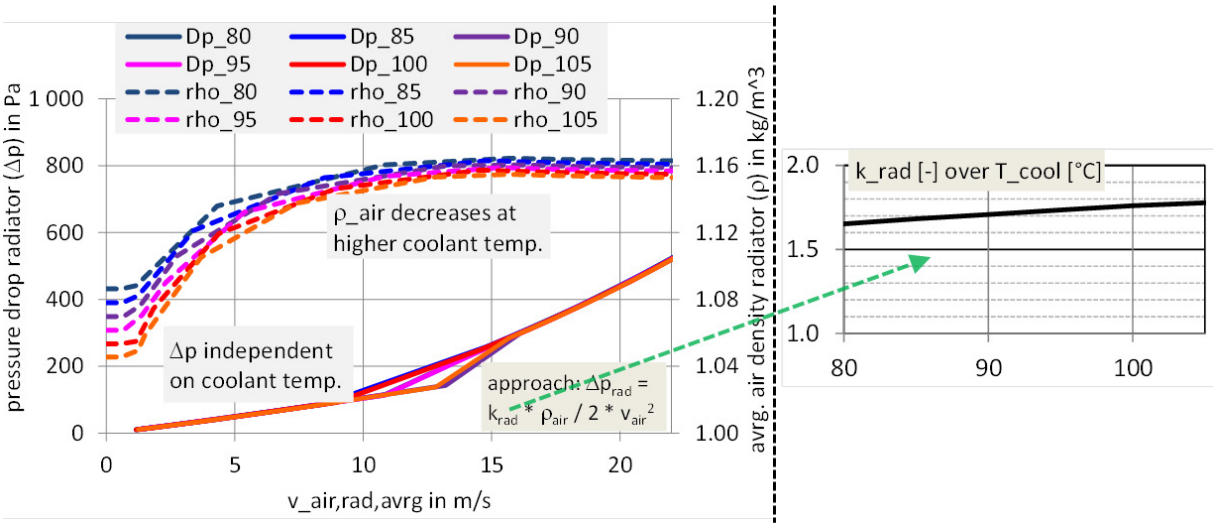

Figure 21: Left: Dependency of pressure drop (Dp) and avg. air density (rho) on air flow velocity and coolant temperature (80 to 105 °C)
Right: Resulting dependency of radiator flow resistance coefficient on coolant temperature

These results from the radiator model were chosen for the first setup of the fan-power calculation scheme, because no measurement data were available. For a later application, measured maps from existing radiators could be used as the input.

For the ventilator map, the technical data from an axial tube fan 93 cm, make Loren Cook 36 AFBV-C, were chosen, (cf. Figure 22).

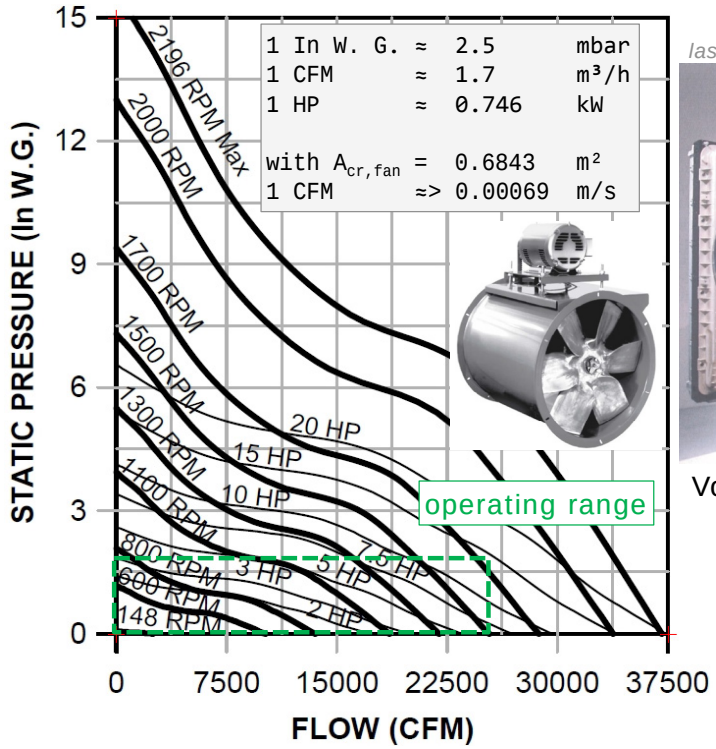

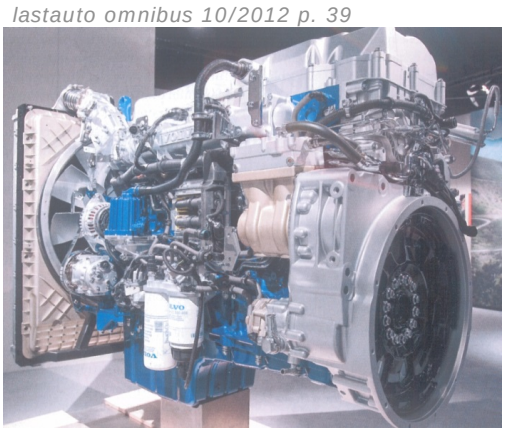

Volvo D13: Radiator, fan, engine

Figure 22: Left: maps volume flow - static pressure increase - ventilator speed and volume flow - static pressure increase - ventilator wheel power demand (LorenCook, 2004-09 p. 18) Right: Installation space of a real HDV fan between radiator and engine

It should be mentioned that the chosen 90 x 90 cm² radiator and the 93 cm fan are rather big for a real application but were simulated to show the general feasibility of this approach. Existing HDV fans have a maximum diameter of approx. 81 cm (Banzhaf, 2010-05-12 p. 7). For future tests, input data from existing devices can be taken, but in that case measurement standards for all devices need to be agreed upon.

To avoid interpolation in the 3D fan map later in the simulation, the characteristic curves [$\Delta p = f(v_{fan,avrg})$] = $f(n_{fan})$ were assumed to be 3rd order polynomials, which worked well, (see Figure 18).

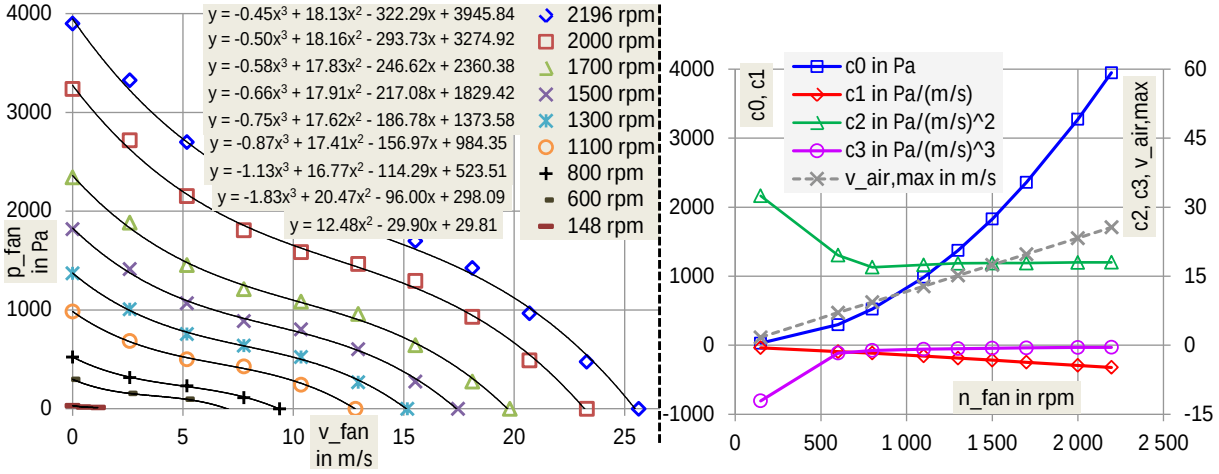

Figure 23: Left: Curve fitting to the ventilator map.
Right: Polynomial coefficients as functions of ventilator speed.

Thus, for every fan speed, a 3rd degree polynomial can be set up:

Equation 5 $$\Delta p_{fan} = c_3 \times v_{air,fan}^3 + c_2 \times v_{air,fan}^2 + c_1 \times v_{air,fan} + c_0$$

where Δp_{fan} static pressure increase by the fan

$v_{air,fan}$ air flow velocity in the fan cross sectional area

$c_{0,1,2,3}$ polynomial coefficients from characteristic curves

This equation describes the dependency between pressure increase and air flow velocity. The polynomial coefficients are read-out from characteristic curves.

The two 3D fan maps with $n_{fan}(v_{air,fan}, Dp_{fan})$ und $P_{mech,fanhub}(v_{air,fan}, Dp_{fan})$ are shown in Figure 24. It is the original map from Figure 22, but reduced to the operational area.

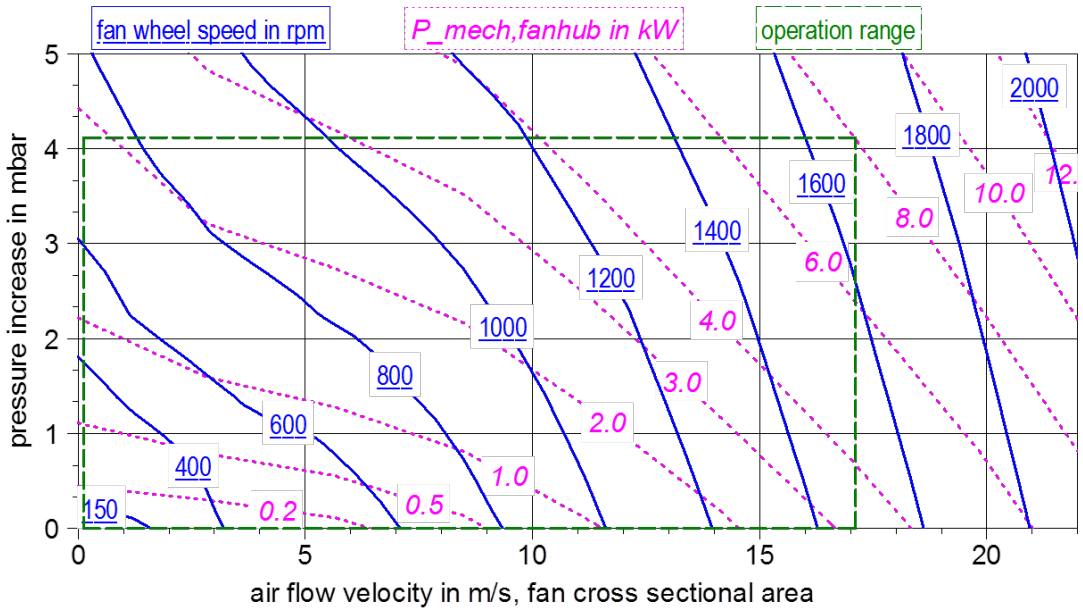

Figure 24. Example of fan, dependency on air flow velocity and pressure increase. Blue: fan wheel speed. Violet: power at fan wheel hub.

The first simulations showed that the virtual cooling system was slightly oversized, so the fan ran only in a small part of its operational area.

The characteristic of a viscous clutch, the dominating power transmission device connecting the crankshaft and the fan hub, is given in Figure 25.

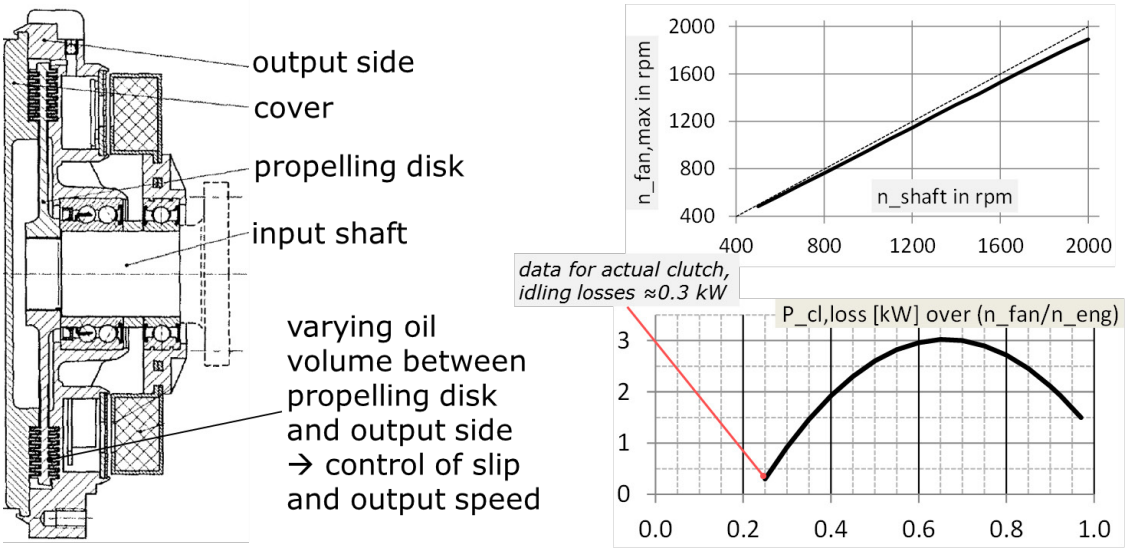

Figure 25. Left: Working principle of a viscous clutch. Right above: Max fan speed determined by crankshaft speed and min. clutch slip (both (Martin, 1993)). Right below: Clutch power loss dependent on speed ratio $n_{clutch,out}$ / $n_{clutch,in}$(Info from MAHLE Thermomanagement)

In the case of a simple on/off clutch, only the idling losses need to be set to zero.

Depending on the coolant temperature, a simple speed control curve for the fan is applied, (see Figure 26).

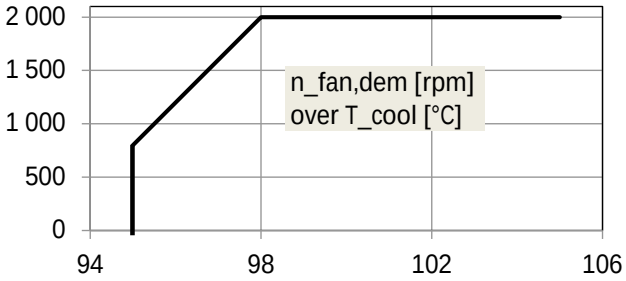

Figure 26. Demanded fan speed as a function of coolant temperature.

This control curve could be replaced by manufacturer-specific data, e.g. an on/off control with a switching hysteresis. The suitability of the model approach proposed here for such a purpose would need some verification (e.g. comparison with OEM data).

To calculate the coolant temperature, a simplified heat balance around the engine was applied. The heat- and energy flows are shown in Figure 27.

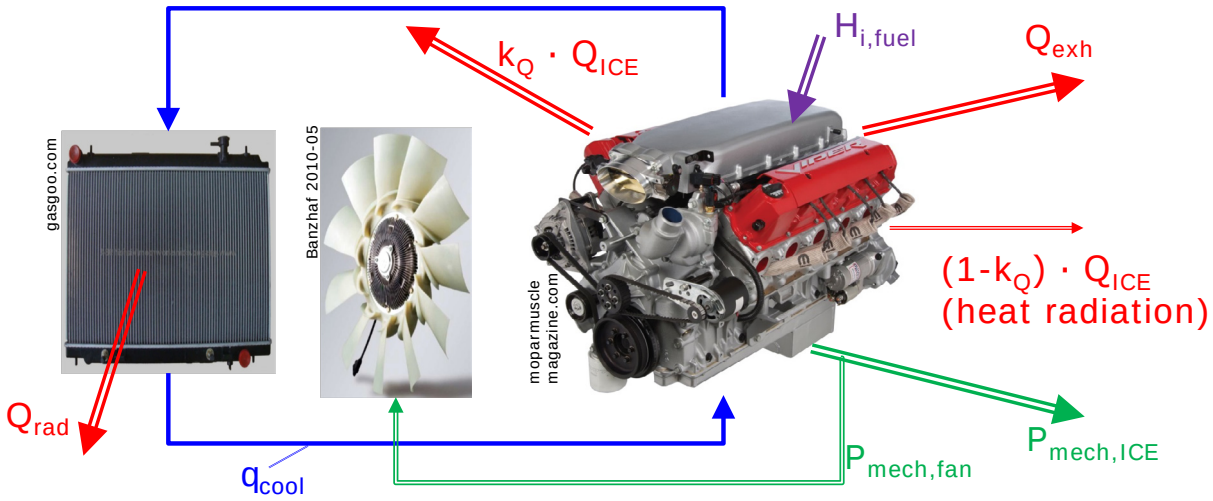

Figure 27. Energy balance around the engine

where

$H_{i,fuel}$	lower heating value of fuel
Q_{exh}	heat loss exhaust
Q_{ICE}	waste heat from combustion chamber to engine block
k_Q	fraction of Q_{ICE} which is conducted to the coolant, the rest its radiation
$P_{mech,ICE}$	mechanical power output of the engine
$P_{mech,fan}$	power demand of the fan, idling or running
Q_{rad}	heat transfer from coolant to air by radiator
q_{cool}	coolant temperature

The exhaust heat loss $\dot{H}_{exh}$ can be interpolated from a map, (see Figure 28).

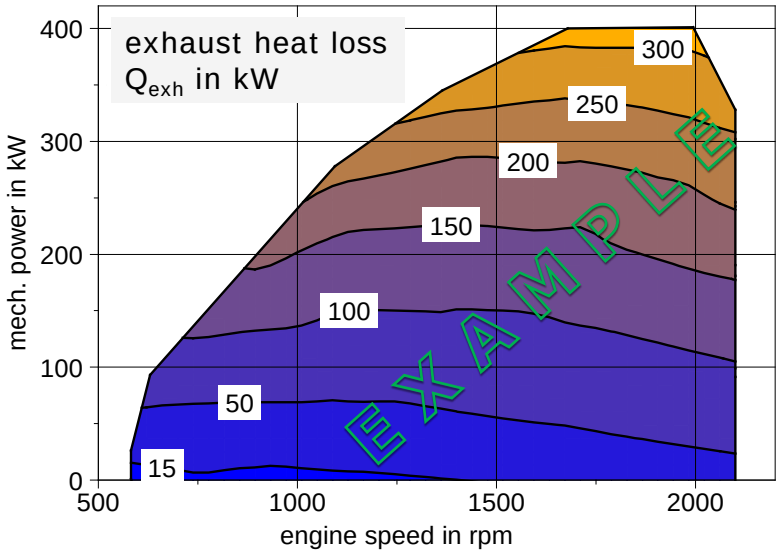

Figure 28. Map of exhaust heat loss. Example of typical tractor engine 400 kW_{mech}

In that case, the waste heat to the engine block is

Equation 6 $\dot{Q}_{ICE} = \dot{H}_{i,fuel} - P_{mech,ICE} - \dot{H}_{exh}$

If such a map is not available, for a diesel engine it can be estimated in good approximation that about half of the overall heat loss of the engine is conducted to the engine block, the rest is exhaust heat loss.

Equation 7 $\dot{Q}_{ICE} \approx \frac{\dot{H}_{i,fuel} - P_{mech,ICE}}{2}$

The energy balance around the coolant is in general

Equation 8 $\Delta\dot{H}_{cool} = C_{ICE,subst} \times \Delta T_{cool} = k_Q \times \dot{Q}_{ICE} - \dot{Q}_{rad}$

where $\Delta\dot{H}_{cool}$ change of enthalpy of coolant kW

$C_{ICE,subst}$ substitutional absolute heat capacity of engine block, oil and coolant [kJ/(kJ·K)]

ΔT_{cool} change of coolant temperature [K]

The substitutional absolute heat capacity of the engine block, oil and coolant is calculated via

Equation 9 $C_{ICE,subst} = m_{cool} \times c_{p,wat} + m_{oil} \times c_{p,oil} + k_{mass} \times m_{ICE} \times c_{cast.iron}$

where m_{cool} mass of coolant water

$c_{p,wat}$ specific heat capacity of water (= 4.2 kJ/(kJ·K))

m_{oil} mass of lubricant

$c_{p,oil}$ specific heat capacity of mineral oil (= 2 kJ/(kJ·K))

k_{mass} mass factor, which considers that not all of the engine block is part of the heat storage

m_{ICE} overall dry mass of the ICE, including all parts and auxiliaries. Simplification: The whole engine is one "homogeneous component" at equal temperature.

$c_{cast.iron}$ specific heat capacity of cast iron (= 0.54 kJ/(kJ·K))

Thus, the coolant temperature is calculated in 1Hz by

Equation 10
$$\vartheta_{cool}(t) = \vartheta_{cool}(t - 1s) + \frac{k_Q \times \dot{Q}_{ICE}(t - 1s) - \dot{Q}_{rad}(t - 1s)}{C_{p,ICE,subst}}$$

where (t) actual time step t

(t-1s) last time step, one second before

$\dot{Q}_{rad}$ heat transfer radiator to air

This simplified formula was validated with the heating-up process of a bus engine, (see Figure 29).

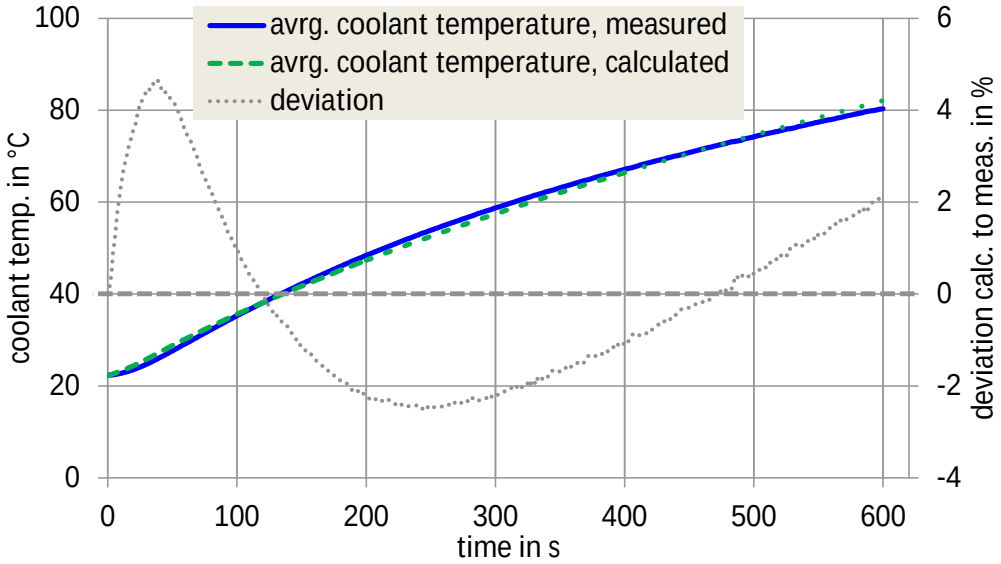

Figure 29. Comparison between measured and calculated coolant temperature during heating-up[18]

The process of heating up an engine from a cold start is a difficult case, because the fraction of radiated heat (factor (1 - k_Q), see Figure 27) is changing constantly due to the transient temperature of the engine block. Since this temperature curve could also be approximated well, the approach is found suitable to match the coolant temperature curve of a hot engine between 80 and 105 °C.

[18] cold start of a bus engine: in-line 6, V_{displ} 10.5 L, m_{ICE} = 980 kg, $P_{mech,const}$ = 85 kW, n_{ICE} = 1300 rpm, Q_{rad} = 0 (cold start, thermostat closed), m_{wat} = 30 kg, m_{oil} = 36 kg, k_{mass} = 0.95, k_Q decreases linearly from 1 to 0.78 until the engine is hot at 600 s (no radiation at cold engine)

With some reasonable assumptions for the flow resistance coefficients along the air path, the approach described above works well. For testing reasons, the standard VECTO model of a 40 t long haul truck was simulated on a highway with an ascending slope of 8 %. The resulting numbers for vehicle velocity, engine speed, engine power output, and fuel consumption were taken, and the above-described calculation scheme was applied in MS Excel as post-processing.

The results are shown in Figure 30.

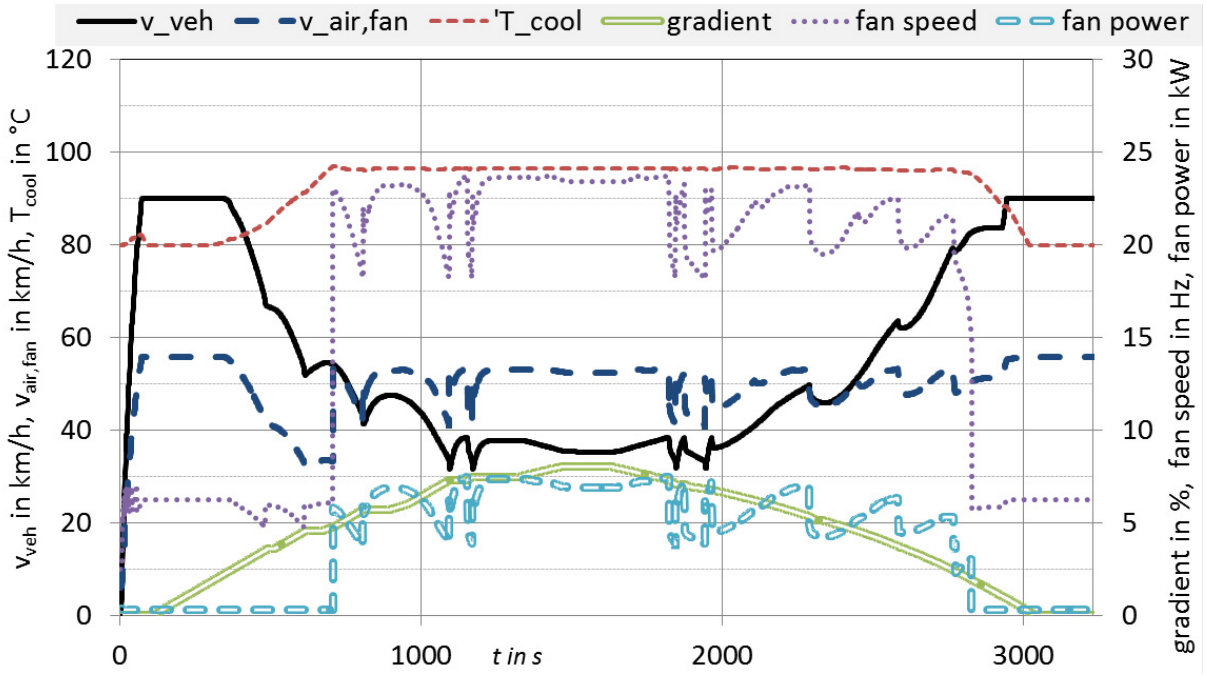

Figure 30. Simulated fan operation of a long haul truck.

When the slope begins, the coolant temperature increases and the vehicle gets slower. As the coolant temperature rises above 97 °C, the fan is turned on and the temperature stays between 96 and 97 °C. The fan speed is around 1400 rpm (23.4 Hz) and the maximum total power consumption is 7.5 kW_{mech}. When the slope ends and the vehicle recovers speed, the coolant temperature sinks below 95 °C and the fan is turned off (slight hysteresis to avoid continuous shifting).

The same procedure was applied to the VECTO results of the draft HDV CO_2 long haul cycle, (see Figure 31).

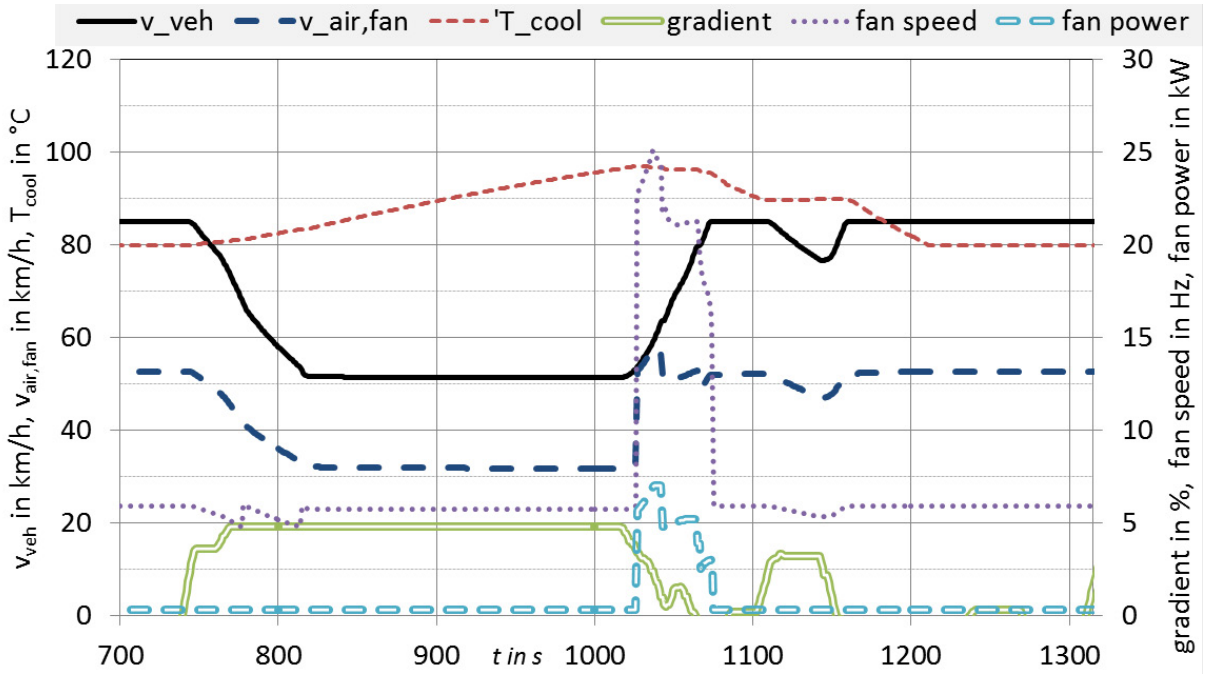

Figure 31. Simulated fan operation, extract from the draft HDV CO_2 long haul cycle.

The fan is only turned on once, at the end of a 5 % slope. The discussion with a manufacturer of engine cooling systems, MAHLE Thermomanagement (formerly BEHR), led to the same result: That during normal driving on highways the fan of trucks is normally switched off.

On the regional and the city bus urban cycle, the fan of the 40 t long haul truck is not running.

This behaviour is reasonable. The fan is idling most of the time and only turned on in heavy urban traffic or on steep slopes. The fact is that the whole cooling system is totally oversized for most driving situations, but it must fit for the worst case:

- mid-engine speed with only mid-fan speed
- full load with high heat output
- very slow vehicle velocity on steep slopes, in low gears without headwind
- high ambient temperature

If the cooling system did not fulfil these demands, the engine would be heavily damaged, e.g. by piston jamming.

Summary Fan

It can be summarized that a detailed model for coolant temperature, fan speed, and fan power needs a lot of input data from several components comprising physical parameters (flow resistance coefficients, radiator dimensions ...), as well as information on the applied control strategy. The use of such a model for a particular vehicle in the framework of the CO_2 certification would require that all these parameters have to be determined by a certified process. Thus, the incorporation of a detailed fan model in VECTO seems to be too complex.

However, the presented approach could be used to establish "technology-specific" generic values for the fan power demand in VECTO. ACEA has already provided tables with such generic values for several fan technologies.

4.3.3 Air compressor

The air compressor is an intermittently operated auxiliary. It boosts the pressurized air for the pneumatic braking system, the clutch, and gearbox actuators. In the case of city buses, it is also used in the operation of the doors, the kneeling mechanism, and all other pneumatic consumers.

4.3.3.1 Current draft approach

The current draft approach for trucks as proposed by LOT 3 and ACEA foresees the use of generic air delivery rates (with reference to the supply power demand) per vehicle class and mission profile and the use of default efficiency maps for the compressor. Details shall be elaborated by the beginning of 2014.

4.3.3.2 Advanced model approach

A more detailed method for depicting the power demand from the air compressor is presented below. This approach is to a large extent similar to the method proposed by ACEA for the simulation of city buses but is extended by simulating the charging level of the reservoir for pressurized air.

In the model, only two working modes of the compressor are considered: “idling” or “delivering” (=full load). The mechanical power demand in these two modes can be depicted by two characteristic curves. As an example, the power demand and the air delivery rate for the Voith LP 490 are shown in Figure 32.

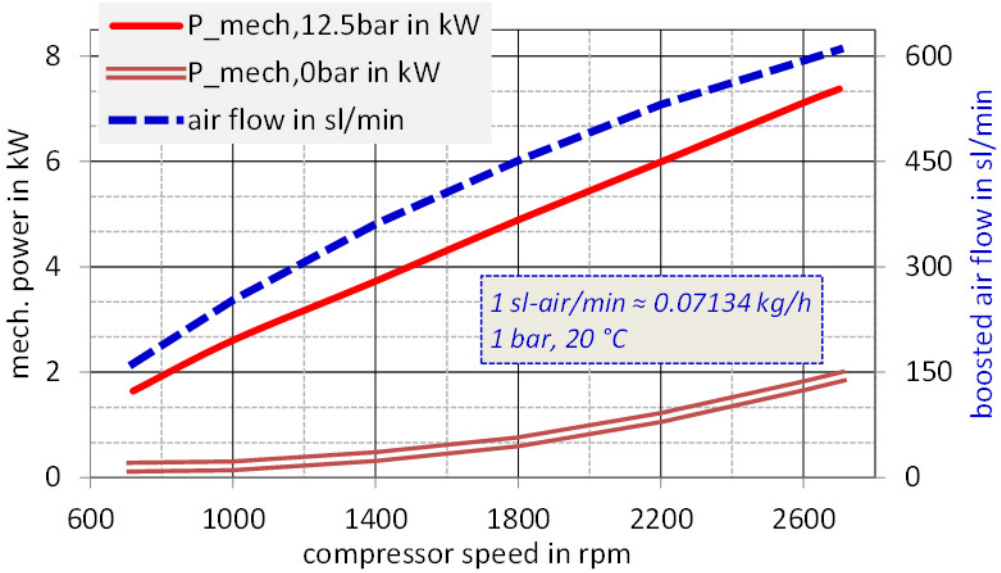

Figure 32: Power demand and air delivery rate of compressor Voith LP 490 (Voith, 2013-12)

A draft for a measurement standard for the compressor's operational characteristic in terms of preconditioning, backpressure, oil temperature etc. has already been elaborated by ACEA.

All technical measures which influence the mechanical power demand for a given operational state (compressor speed, idling or delivering) can be described based on the curves above:

- Measures for the reduction of idling losses like clearance volume add on, the control system or using a clutch between power transmission and compressor shaft result in a lower power curve at “idling”.
- Measures for the reduction of boost power at full load like fluid cooling, multistage compression with intercooling or using two or three cylinders (one per compression stage) result in a reduction of the mechanical power demand at “delivering”.

For the air compressor system, the “supply power” can be specified as the air demand at standardised conditions. The unit “sl” (= standard litre) used here refers to one litre of dry air at (1 bar, 20 °C). The air demand for a particular vehicle in a particular mission profile can be calculated based on the vehicle specifications and the cycle characteristics. The air consumers and devices/controls which influence the air demand are given in the following list, according to ACEA:

- **brakes** consumption per brake actuation and vehicle mass [sl / kg]
- **retarder** (generic decrease of brake air demand for HDV with retarder)
- **clutch** fixed air volume per clutch actuation [sl]
- **gearbox** fix air volume per gear shift [sl], only in the case of pneumatic actuators
- **Ad Blue Doser** constant air demand for HDV with pneumatic Ad Blue doser [sl / h]
- a**ir suspension** constant air demand [sl / h], distinction of mechanical and electrical control, higher consumption for mechanical control (plus x %)
- **leakage** constant air loss [sl / h]. It is controversial whether this consumer should be considered or not. For HDV in new conditions, this is not important, but after one or two years the leakage may have an impact on overall air consumption. This is relevant, because 2-stage compressors with intercooling lead to lower leakage. In this case, the compressed air is cooler and causes less damage at the synthetic seals. Thus, 2-stage compressors could get a leakage bonus over 1-stage devices. But up to now there are no exact numbers on the leakage difference or even a standardized measurement procedure for 2-year-old HDV.
- **dead volume blow out** simplified constant air demand [sl / h]
- **bus doors** consumption per actuation of pneumatic double doors [sl]
- **bus stop brake** consumption per brake actuation and vehicle mass [sl / kg] (only city buses)
- **kneeling mechanism** consumption per actuation, vehicle mass and vertical lift [sl / (kg • mm)] (only city buses)

- **overrun** preferred compressor operation during overrun phases, where the engine is driven by the coasting vehicle (not during freewheel phases with declutched engine): yes/no
- **air dryer regeneration** (simplified to a constant air consumption):

  smart control (blow out dependent on effectively passed air flow and humidity): fix volume flow [sl / h]

  standard control (blow out after every x^{th} boost phase): lump-sum percentage increase of smart regeneration air demand: + x %

Example results for the share of the different air consumers are given in Figure 33.

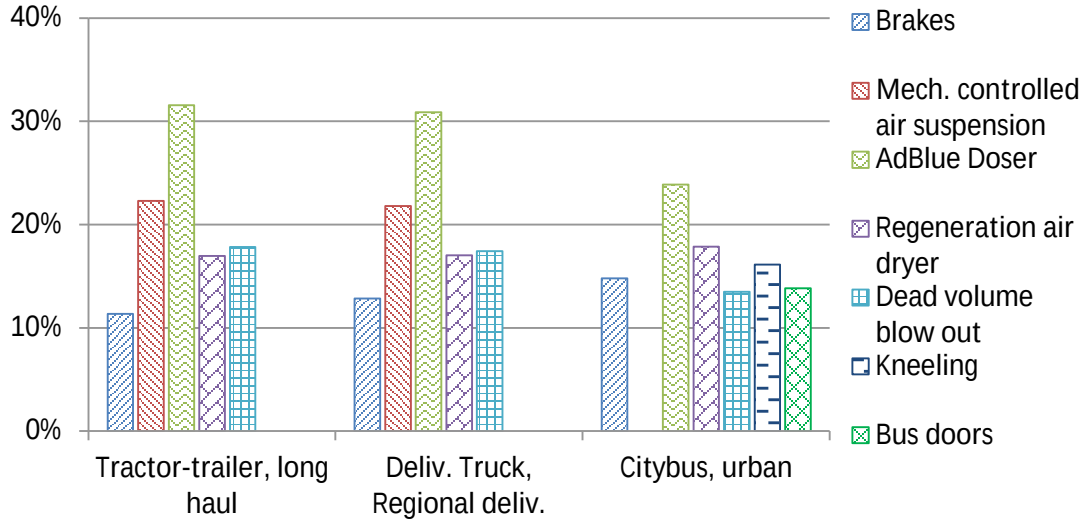

Figure 33. Share of the single air consumers of the total demand of pressurized air. Calculated with actual values from ACEA for EURO V SCR technology with a pneumatic AdBlue dosing system.

Thus, the air demand on the consumption side can be calculated in terms of the time course over the CO_2 driving cycle to be simulated as the sum of the constant and intermittent air consumption. Also, the air delivery characteristic of the compressor is known, (see Figure 32). With these values, the pressure in a virtual air reservoir with constant values for volume and inner temperature (simplification!) can be calculated.

The model structure is shown in Figure 34.

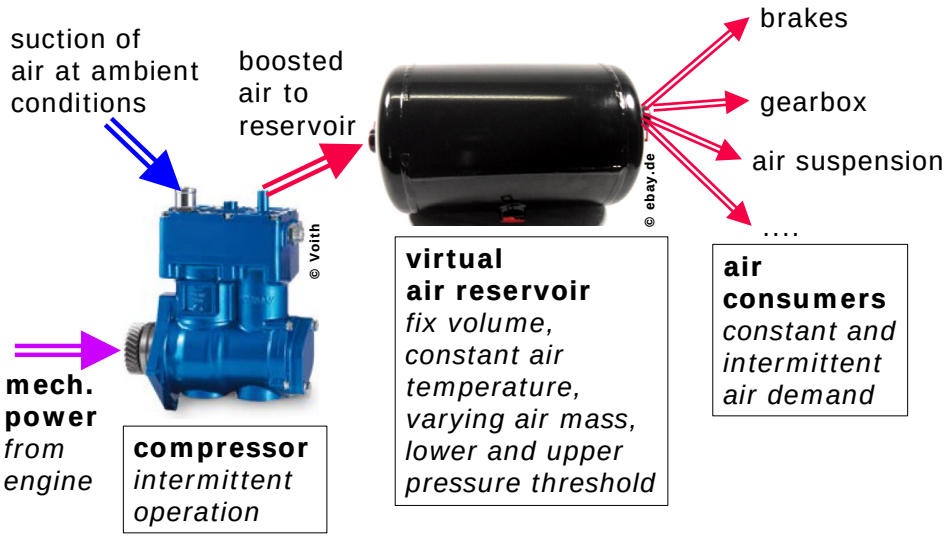

Figure 34. Simplified model of pneumatic system for simulation of reservoir pressure. Assumption: isothermal and isochoric change of state on reservoir.

The 1Hz time course of the reservoir pressure can be calculated via *Equation 11*.

$$p_{res}(t) = p_{res}(t - 1s) + \Delta p_{res}(t)$$

Equation 11

$$\Delta p_{res}(t) = \left(\dot{V}_{air,compr} - \dot{V}_{air,consum}\right) \times \frac{\rho_{air,std} \times R_{air} \times T_{air,res}}{V_{res}}$$

where $p_{res}(t)$ reservoir pressure at current time step (t)

$p_{res}(t\text{-}1s)$ reservoir pressure at last time step (t-1s)

$\Delta p_{res}(r)$ pressure change in actual time step

$\dot{V}_{air,compr}$ flow of delivered air from compressor [sl/s], = 0 when compressor turned off

$\dot{V}_{air,consum}$ air demand by consumers [sl/s], sum of constant and intermittent demand.

$\rho_{air,std}$ air density at standard conditions (= 1.189 kg/m³)

R_{air} specific gas constant air (= 287.06 J/(kg·K))

$T_{air,res}$ constant temperature of air in reservoir (e. g. 323.2 K = 50 °C)

V_{res} volume of virtual air reservoir

Thus, when the reservoir pressure falls under the lower limit, e.g. 8 bar, the compressor is turned on, the reservoir pressure increases, and when the upper limit, e.g. 12 bar, is reached, the compressor is turned off. Then, air is only taken off the reservoir, its pressure decreases until the lower limit, and the cycle restarts.

Summary air compressor

A detailed model for the pressurised air system offers the possibility to simulate the intermittent operation of the compressor but needs substantial input data in terms of reservoir volumes and control strategies. For the simulation of the official CO_2 values for trucks, the use of generic values for pressurised air consumption and generic technology-dependent compressor efficiencies might be sufficient (however, ACEA has not come up with a final proposal on this issue yet). A model as presented above could be used for elaborating tables with generic data for the different truck classes and mission profiles. For buses, where the power consumption of the compressor has a significantly larger impact on overall fuel consumption, the use of a detailed simulation approach e.g. as drafted above and consideration of component-specific input data too might be reasonable. Such methods are actually under development in a separate project on bus auxiliaries in the HDV CO_2 certification funded by the DG CLIMA.

4.3.4 Alternator

Alternators generate the electrical power required by the vehicle and the engine.

4.3.4.1 Current status

Standard controlled alternators, which simply keep voltage constant, can be simulated based on an electrical energy demand (the “supply power”) based on a consumer list for each produced HDV and an efficiency map of the alternator (mechanical power demand over rpm and electrical power demand). The mechanical power demand computed for the alternator is then added to the 1Hz power demand computed for the combustion engine by VECTO. This approach has already been implemented in VECTO. The typical power demand of alternators is approx. 1.1 kW_{mech} for long haul applications. For buses, work on the standard values is still in progress.

Table 1 gives an example of the consumer list as elaborated in the Lot 3 project. The simplification has been made that every single consumer has an average constant current demand, e.g. it is not separated between headlights on or off. Thus, a mean value based on a “usage factor” value is elaborated. For every single consumer, agreed table values for different technology stages are already available or are being worked on: lighting (bulbs and LED), basic power demand of the vehicle (controller units, sensors and actuators, cockpit instruments), air conditioning, wipers, heating, audio system, and bus displays.

Table 1: Example of electric consumer list, motor vehicle lighting front and side

$P_{effect} = quant. \cdot P_{single} \cdot \%use$

			bulb		LED	
Light	**quant.**	**% use**	**P_{single} in W**	**$P_{effect.}$ in W**	**P_{single} in W**	**$P_{effect.}$ in W**
motor vehicle front and side						
headlamps lowbeam	2	50%	70	**70**	25	**25**
headlamps highbeam	2	25%	70	**35**	25	**12.5**
front fog lights	2	5%	70	**7**	25	**2.5**
front turn signal lights	2	5%	21	**2.1**	2	**0.2**
front corner marker lights	2	50%	5	**5**	0.9	**0.9**
front clearance lights	2	50%	5	**5**	0.5	**0.5**
front daytime running lights	2	50%	21	**21**	5.5	**5.5**
lateral turn signal lights	2	5%	21	**2.1**	2	**0.2**
lateral marker lights	2	50%	5	**5**	1	**1**

Regarding the efficiency map of the alternator, in a first step, the use of generic data is foreseen. It is open whether a differentiation between alternator technologies will be made in a first step. In a later step of the legislation, the use of component-specific efficiency maps is expected. As a starting point for a related standardized test procedure, the Bosch standard, based on ISO 8854:2012, chapter 5.6, could be used. In this test procedure, measurements are made at 9 points in the operating range of an alternator for the following parameters:

- rotational speed
- current output at self-regulated voltage
- input torque

In addition, ACEA is currently validating an extended approach which shall allow for the depiction of the benefits of KERS (“kinetic energy recovery”) systems. For this purpose, a procedure based on a standardized “short test” on a test track is under investigation. From this short test, the share of electrical energy produced in different driving conditions (motoring, traction, idle) can be computed, and these shares can then be used as input parameters for VECTO. In VECTO, the measured shares are then used to distribute the alternator power output demand accordingly in the simulated mission profile of the bus. A vehicle with a well-operating KERS system maximizes the production of electricity in motoring phases (where no extra fuel is required).

Unfortunately, the share of the different driving conditions depends on the mission profile, as well as the vehicle and engine specifications (maximum acceleration level, driving resistances). To guarantee that the produced electrical energy is in line with the demanded value would require correcting the overall consumed fuel e.g. by an adapted Willans approach [19], or making several iteration loops in VECTO, which should be avoided for a complex simulation.

4.3.4.2 Application of the status quo VECTO alternator model

The additional fuel demand of the electrical system was simulated for the long haul cycle of a typical 40t articulated truck with average loading for different configurations of the electrical system:

- alternator maps "bad" (worst-case) and "good" (state-of-the-art technology) provided from a supplier
- summarized current demand of standard and LED lighting
- different solutions for power transmission from the crankshaft to the alternator: V-belt (mechanical efficiency 95 %) and toothed belt (mechanical efficiency 98 %)

[19] A simple approach for correcting the overall fuel consumption in order to compensate for a difference between the electrical energy produced in the simulation and the target electrical energy could look as follows:

1) From all 1Hz data points of the VECTO simulation, a linear regression curve (y=k*x+d) for fuel consumption (unit: grams per hour) over engine power (unit: kilowatt) is calculated.

2) From the difference between the electrical energy produced in the simulation and the target electrical energy (unit kilowatt-hours), a cycle average change in mechanical power "ΔPe" (unit kilowatt) of the internal combustion engine is calculated (using an average alternator efficiency and the cycle time with running engine).

3) The correction of the cycle average fuel consumption is performed using:

ΔFC (unit: grams per hour) = ΔPe * k * s_trac

where: k… gradient in the regression from 1)
s_trac …. time share of engine in traction conditions in the cycle
(in motoring condition, the fuel consumptions is assumed to be zero)

The alternator maps for the main operating area during the cycles are shown in Figure 35 and Figure 36.

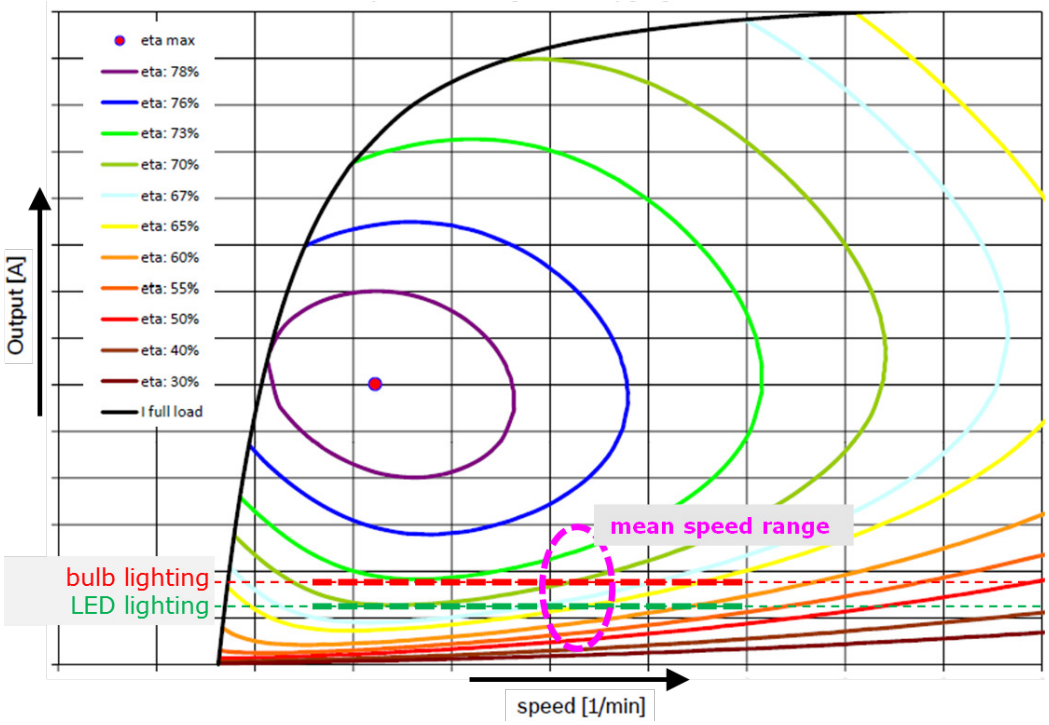

Figure 35. Performance map of alternator "good" and avg. total electrical power consumption of tractor-trailer with bulb- or LED lighting

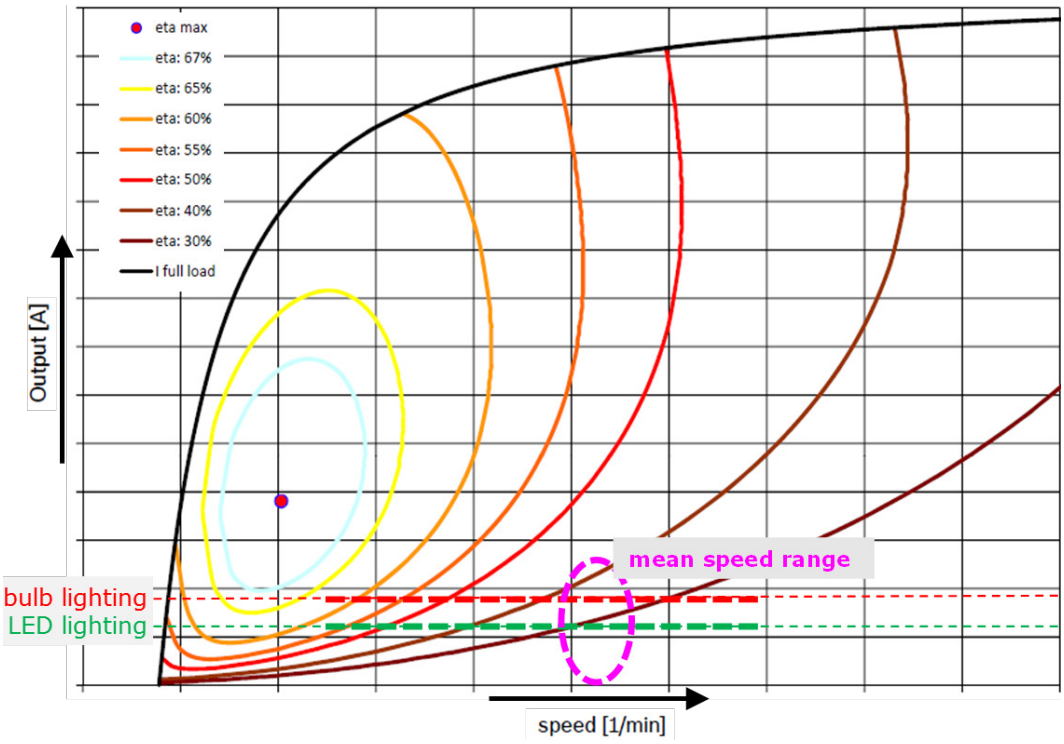

Figure 36. Performance map of alternator "bad" and avg. total electrical power consumption of tractor-trailer with bulb- or LED lighting

The cumulated results on fuel consumption are shown in Figure 37. Compared to the “worst case” technology, a total fuel benefit of 1.1% was determined.

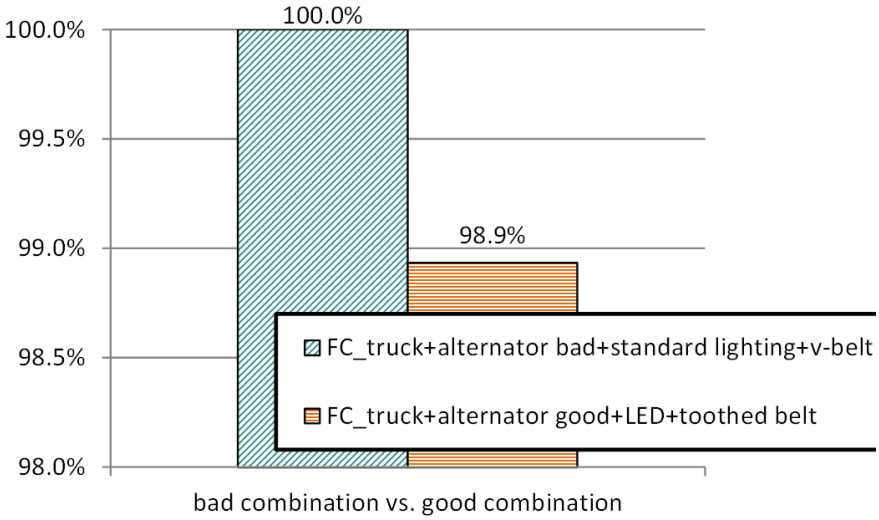

Figure 37. Fuel-saving potential of the electrical system.

The single contributions to the overall FC reduction of 1.1 % are toothed belt 0.1 %, alternator "good" 0.8 %, and LED lighting 0.2 %.

4.3.4.3 Elaboration of a more detailed model for the electrical system

As an alternative to the ACEA proposal for external testing of the benefits of a KERS system, a more detailed model of the electrical system was elaborated. If validated, such a model could also allow for a differentiation between a standard charging strategy and a “smart alternator strategy”. The component-specific input data would be:

- the battery capacity (limits the energy which can be stored, most likely relevant for downhill passages)
- the inner resistance and the voltage, and
- (optional) the alternator efficiency map.

The threshold levels for charging would be rather generic data.

The main idea is that the alternator operation (I_{alt}) follows the state of charge (SOC) of the battery and/or supercapacitor.

- In "traction" mode, when the vehicle is powered by the ICE, the electric consumers are fed only from the battery (I_{disch}) when the SOC is high. When the SOC decreases, the alternator is partly engaged, and below a certain limit only the alternator supplies the consumers (I_{cons}). When the SOC is very low, the alternator loads the battery in addition to supplying the consumers ($I_{ch} + I_{cons}$).
- At standstill ("Stop"), the battery supplies the consumers as long as possible (I_{disch}). Only if the SOC falls under the lowest possible limit is the ICE turned on, and the alternator takes over (I_{cons}).
- In the case of coasting or braking ("Overrun"), the alternator(s) run(s) at maximum generator power and load the battery up to the maximum (I_{ch}).
- The SOC-dependency of the alternator operation is modelled using characteristic curves.
- The battery is depicted via a simple model of (dis-)charge voltage curves and internal losses.

The alternator speed (n_{alt}) is calculated second-wise by the VECTO model, and its power demand is added to the ICE load, including transmission losses ($P_{mech,alt} + P_{loss,transm}$). In this way, the alternator model interacts with the rest of the vehicle model.

Figure 38 shows a scheme of this model.

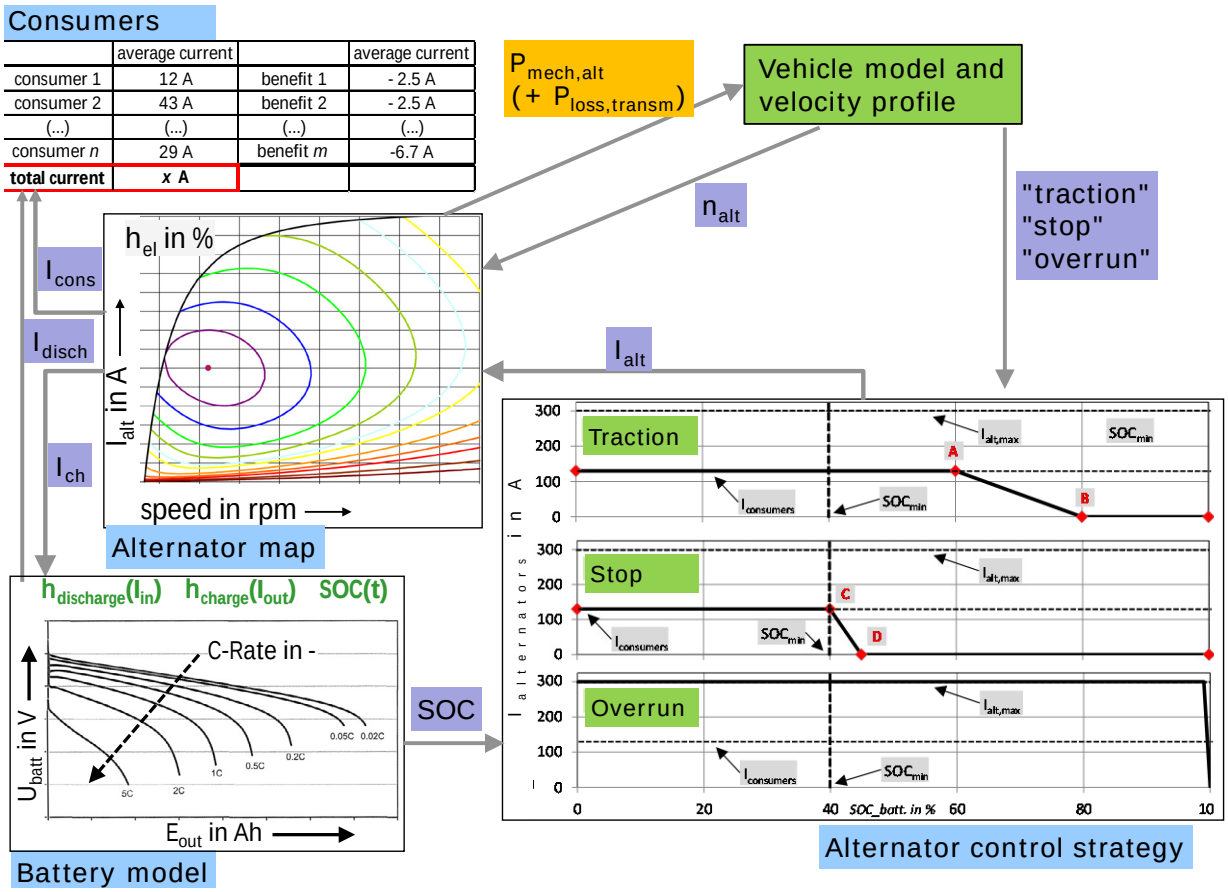

Figure 38. Model structure for the simplified control strategy of the electrical system.

An example of the (dis-)charge curves of the terminal voltage of lead-acid batteries is given in Figure 39.

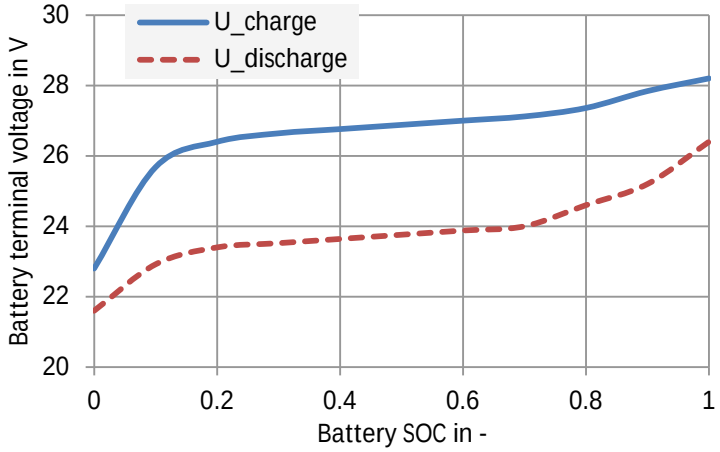

Figure 39. Terminal voltage of lead acid batteries, charging and discharging[20]

To get the electrical power of the battery at cell level for the stepwise SOC calculation, the power loss at the internal resistor of the battery is calculated via *Equation 12* (Renhart, 2010-06) *eq. 2*.

Equation 12 $P_{batt,cell,in/out} = P_{batt,terminal,in/out} \; -/+ \; I^2 \times R_{batt,internal}$

where

$P_{batt,cell,in/out}$	electrical power at battery cell level
$P_{batt,terminal,in/out}$	terminal electrical power at battery clamps
I	electrical current
$R_{batt,internal}$	internal resistor of battery (e. g. 0.05 W)

The simplified energy control model was applied via post-processing on the VECTO output of a standard city bus model on the heavy urban bus cycle. A constant electrical power of 1.4 kW was assumed; in addition, the effect of a clutch to eliminate the alternator idling losses was investigated.

[20] http://www.kleinwindanlagen.de/Forum/cf3/upload/avatars/utool_f_1325438921_61.jpg

The calculated theoretical FC-saving potential is shown in Figure 40.

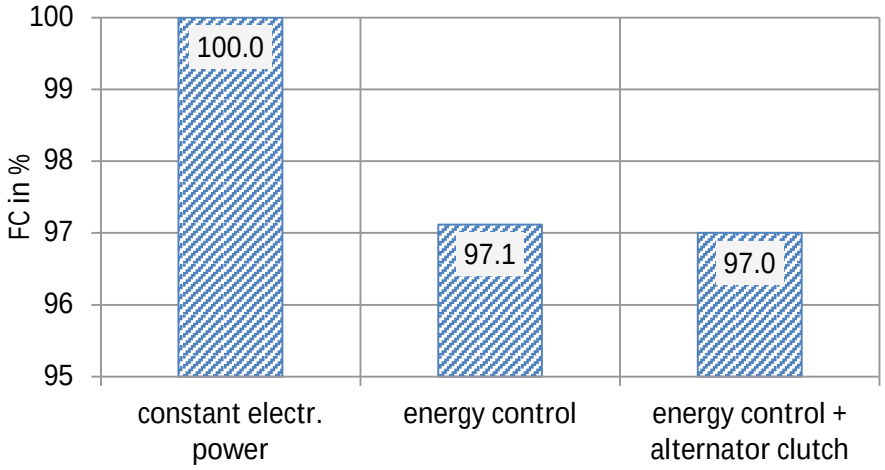

Figure 40. FC reduction potential of a simplified energy control strategy Bus model on the heavy urban cycle, constant electrical power of 1.4 kW_{el}

The controlled use of the battery as buffer storage for a fraction of the braking work offers a fuel consumption reduction potential of approx. 3 % for city buses, according to these first simulation results.

Whether the application of such a standardized and simplified energy control system is possible for the upcoming CO_2 certification procedure shall be discussed with the OEMs.

4.3.5 Steering Pump

The steering pump is a hydraulic machine which supplies the steering gear with pressurized hydraulic oil to turn the front wheels. The structure of the whole system is shown in Figure 41. A typical steering pump in a long haul truck consumes approx.. 0.5 kWmech, (cf. Figure 46), and in a city bus approx. 0.9 kW_{mech} (ACEA, 2013-12 p. 193).

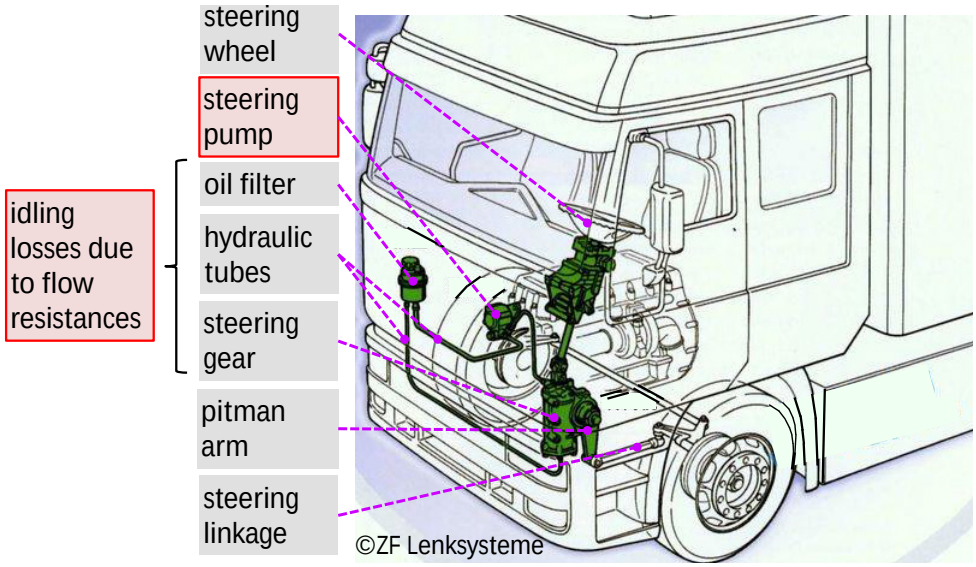

Figure 41. Steering system of a HDV

4.3.5.1 Current status

As the contribution of the steering systems to overall fuel consumption is assessed to be much smaller than 1%, in the current draft HDV certification the steering system is considered in the VECTO calculations only by a generic lump-sum power demand value. The corresponding values, which are a function of HDV class, mission profile, and technology type of the steering system, are currently being elaborated by ACEA.

4.3.5.2 More detailed model

In this project, in cooperation with steering system suppliers (ixetic, ZF Lenksysteme), a more detailed approach was elaborated, which would allow for the depiction of system-specific saving potential. This method and exemplary results for fuel reduction potential are described below.

For the simulation of the power demand of the steering system, the consideration of the idling losses is most important, as this operational state predominates in real world driving. Measurements performed by TU Graz on a city bus (12 m) in and around Graz showed a typical actuation pattern of the steering system (Figure 42):

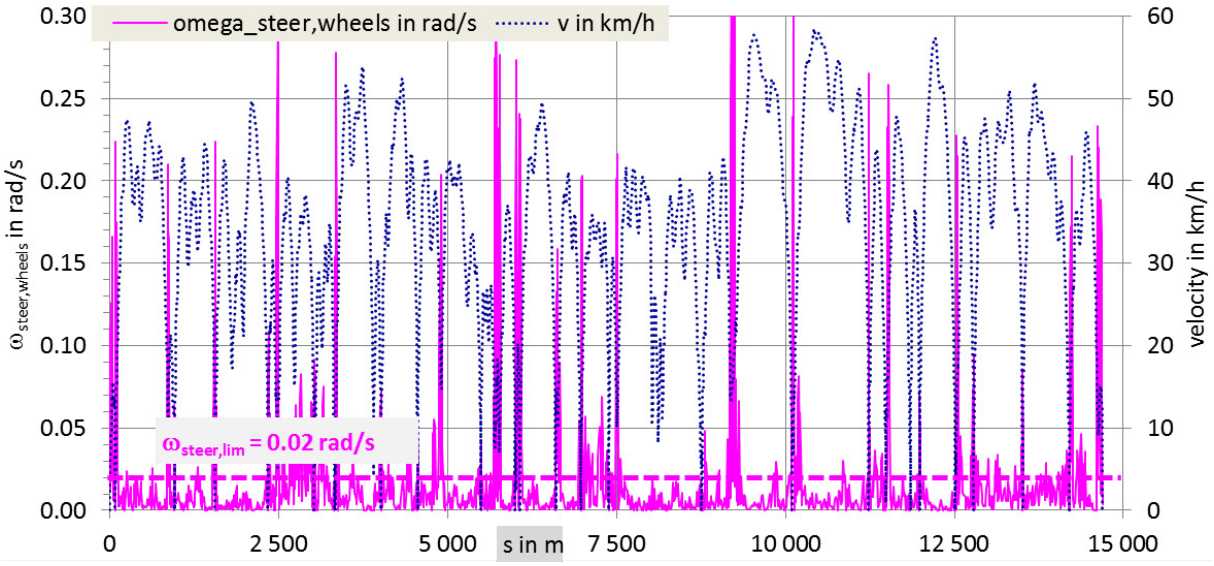

Figure 42. Actuation of the steering system. Measurement city bus 12 m, Graz 03/2013, urban driving.

When a "steering action" is defined by a minimum angular front wheel steering velocity of 0.02 rad/s, the steering system is actuated only during 21 % of the overall driving time, including standstill. On a longer ride with one part consisting of faster rural traffic, the distance share of steering was 18 % of the total driving time.

Based on further discussions with component suppliers, it was concluded that generic average values for the steering power during steering phases are sufficient for the simulation in VECTO. These values are in the same magnitude for all steering pump types, because the absolute work to turn the steering wheels must be generated and the technologies (hydraulic constant, hydraulic variable, electric ...) do not differ much in overall steering efficiency. The main difference in energy consumption of the different steering systems is the power loss in the steering system during idling.

To calculate a first estimation of the possible fuel-saving potential, four combinations of steering systems have been analysed. These four systems consist of two steering pump technologies ("standard", "improved") and two designs of the hydraulic systems ("low" pressure drop, "high" pressure drop).

For this exercise, example data were available from a supplier. One pump is "standard design", and the other is slightly improved in efficiency. The data are shown in Figure 43 (only the operating range relevant for idling is shown).

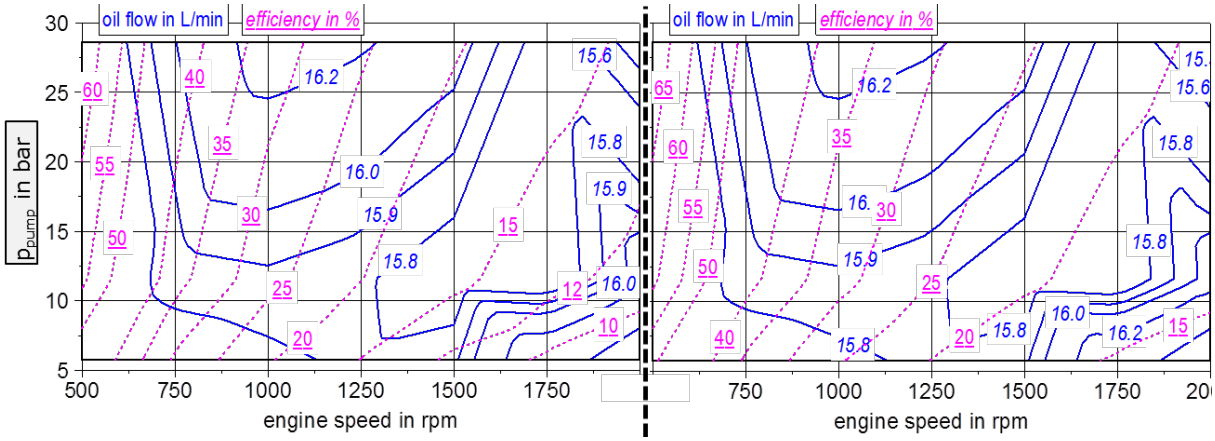

Figure 43. Performance maps of hydraulic steering pumps. Left: standard, Right: improved
data slightly distorted due to confidentiality reasons

The pressure drop of the idling steering system can be modelled to be quadratic over the oil volume flow. The losses of all components in the systems are combined into one big throttle. Typical values for the pressure drop in the hydraulic systems are around 5 bar at 16 l/min[21], so the following flow resistance coefficients ("k_{steer}") were assumed in the calculations:

pressure drop "low" (optimised system), 4 bar: $k_{steer,low} = 0.016$ bar/(L/min)²

pressure drop "high" (non-optimised system), 6 bar: $k_{steer,high} = 0.023$ bar/(L/min)²

[21] Information from ZF Lenksysteme, Schwäbisch Gmünd.

For articulated buses, this idle pressure drop can be up to 30 bar ($k_{steer} \approx 0.117$ bar/(L/min)²), due to long tubes from the rear engine to the front wheels and additional throttles, which avoid oscillation of the oil mass.

Based on this data, a simple model was set up to quantify the impact on fuel consumption. In a first step, vertical cuts were taken from the performance maps to get the dependency of oil flow on pump pressure for each node speed, (shown in Figure 44).

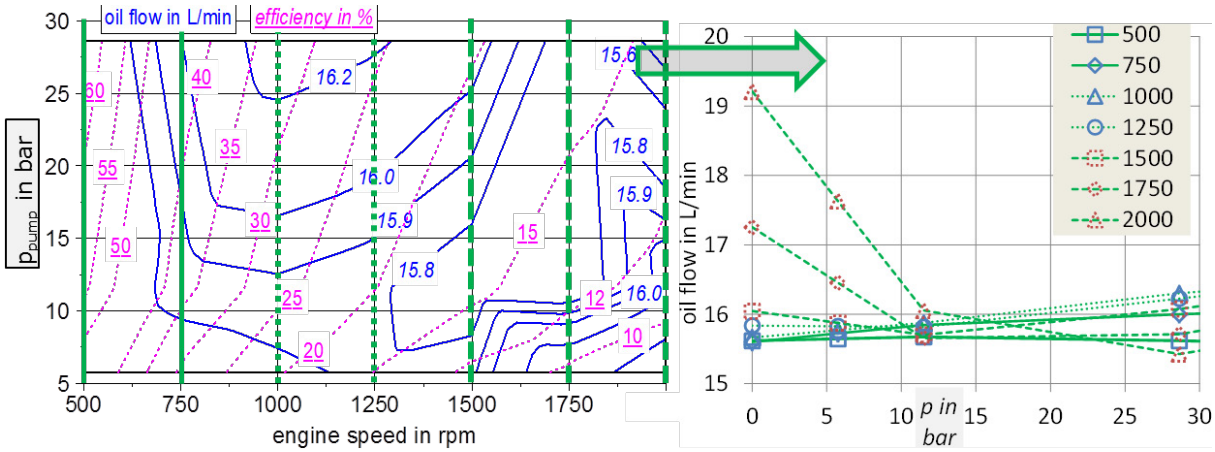

Figure 44. Dependency of oil flow on pressure for node speeds

To get the working point at idle for each node speed, where the pressure drop of the idling steering system equals the available pump pressure, the pressure drop over oil flow is calculated by Equation 13.

Equation 13 $$\Delta p_{drop,steer} = k_{steer} \times \dot{V}_{oil}^{2}(p_{pump})$$

where $\Delta p_{drop,steer}$ pressure drop of idling steering system

k_{steer} flow resistance coefficient steering system

$\dot{V}_{oil}(p_{pump})$ oil flow at node speed dependent on pump pressure

The result for every pump node speed is the working point in terms of oil flow and pump pressure, (see Figure 44).

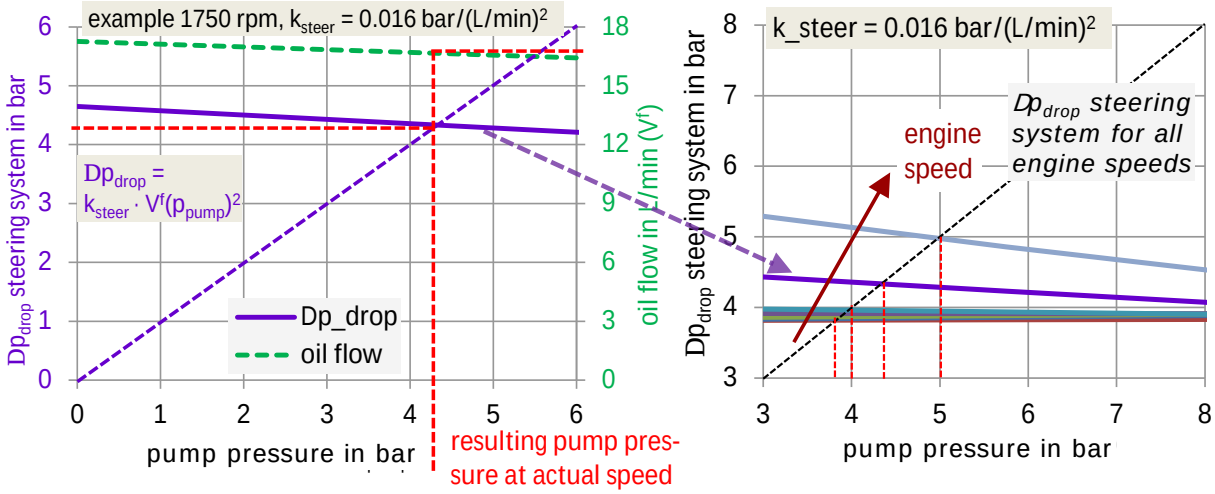

Figure 45. Workings points of pump and idling steering system, in engine speed range

Now, for every combination of pump (performance map) and idling steering system (flow resistance, k_{steer}), the pump pressure and volume flow for the node speeds are known. Via Equation 14:

Equation 14 $$P_{mech,pump} = \frac{\dot{V}_{oil} \times p_{pump}}{\eta_{hydr,pump}}$$

where $P_{mech,pump}$ mechanical power demand of steering pump

$\eta_{hydr,pump}$ hydraulic efficiency of steering pump, from performance map, (see Figure 43)

the curve "steering pump power, idling" over "engine speed" is calculated, (shown in Figure 46).

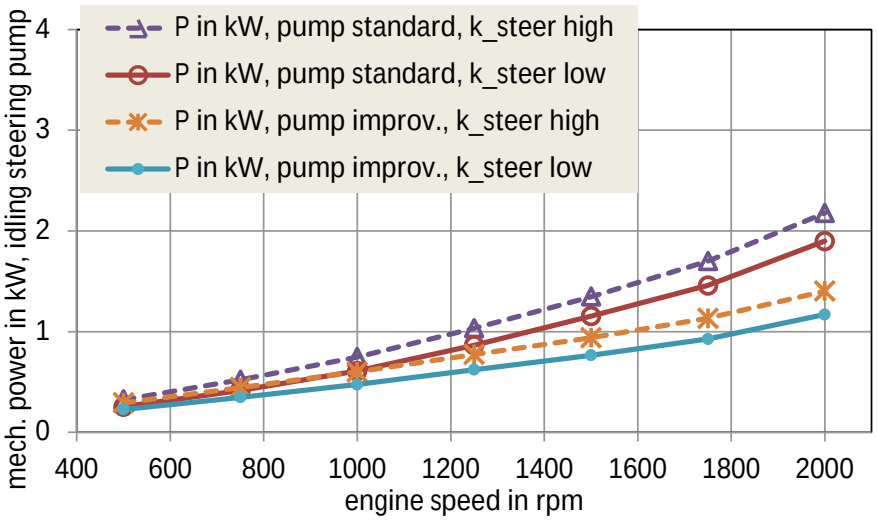

Figure 46. Steering pump power over engine speed idling steering system, for different combinations of pump and steering system.

These curves were applied in a post-processing calculation to the VECTO results of an articulated truck on the long haul cycle to estimate the FC reduction potential, (see Figure 47).

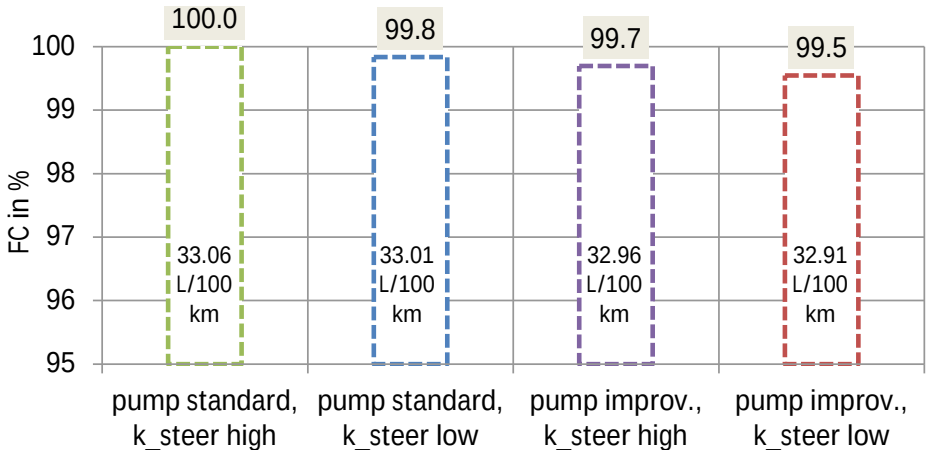

Figure 47. Results for FC reduction potential of different pump types and flow resistances of idling steering system.

In this calculation example, a benefit of 0.5 % in fuel consumption of an optimised steering system compared to a low performing system was determined.

To implement such a more detailed depiction of the steering system in the HDV CO_2 certification, the following tasks would be required:

1. Elaboration of a measurement standard for the hydraulic pressure drop in the steering system in “steering idling” conditions
2. Elaboration of standard values for the generic power demand of the steering system in “steering operation” conditions
3. a) Elaboration of (technology-dependent) default performance maps for steering pumps (if the steering pump is considered in the detailed approach also by generic data) or
3. b) Elaboration of a standardised test procedure for the measurement of performance maps for steering pumps if component-specific performance shall be covered by the procedure
4. Implementation of the calculation steps used above into the VECTO software.

The results of this advanced approach would then have to be compared and aligned with the results for the generic method (as described in 4.3.5.1). Whether the potential fuel savings depicted by the advanced simulation approach for optimised systems are worth the additional effort in the certification procedure has to be discussed with the industry.

4.4 Hybrid Vehicles

This chapter describes a possible approach for determining CO_2 emissions for heavy-duty hybrid vehicles (HDH) using the European CO_2 simulation tool VECTO.

The distribution of propulsion power between the combustion engine and the alternative energy converter is handled by the vehicle-specific hybrid control strategy. This hybrid control strategy, as the decisive influence factor on CO_2 emissions, is designed very specifically for a particular vehicle or powertrain concept and realized very differently for diverse vehicle manufacturers. As the distinctive feature in hybrid system performance and fuel efficiency, the control strategy will most likely not be disclosed by the vehicle manufacturer. Also, due to its complexity and dependency on various parameters, which are different for every vehicle manufacturer, the specific control strategy would also not fit into a predefined, simplified control strategy dependent on only a few parameters without adding too much inaccuracy. In order to include the vehicle-specific hybrid control strategy in a simulation, the real control units as the hardware have to interact with the simulation tool and decide about the distribution of propulsion power between the combustion engine and the alternative energy converter. This setup is called a hardware in the loop system (HILS), where the control units are present as hardware. This approach only works for simulation tools which can be coupled with a real-time development environment in order to communicate with the connected hardware control units. Such a setup is planned to be used for emission certification of HDH and shall be implemented as an amendment to the GTR No. 4 procedure that addresses heavy-duty vehicle exhaust emissions certification (Six, 2013). This setup, called the GTR HILS procedure, could then also be used for determining CO_2 emissions of HDH.

An HILS system requires a real-time simulation and a specific interface between the simulation model and the hardware parts. The specific interface consists of two layers: a software layer and a hardware layer. The software layer handles the signal conversion between the simulation model and the control units for the different units and signal levels used, as well as handling the simulation of the remaining signal bus of the vehicle for control units that do not contain hybrid control functionalities and are thus not connected as hardware. The hardware layer converts the virtual signals from the software layer to physical signals that are transmitted to the connected control units and also provides the wiring harness for the physical connection between the hardware control units.

If the VECTO tool would be changed to a real-time forward simulation approach, this would most likely require switching from proprietary software to commercial software packages (e.g. Matlab Simulink or Dymola). This would mean forcing the usage of one specific commercial software through the legislative process, since the same database of component and vehicle models would have to be used by all vehicle manufacturers. Another general issue is the required model validation of an HILS system. As soon as manufacturer-specific input parameters and specific control units are used, the representativeness of the real life operation of the simulation model has to be proved by comparing data from vehicle measurements on the chassis dyno to data produced by the simulation model.

Since the effort for setting up an HILS system is very high, especially the construction of the interface and the model validation, it is not ensured that all HDH will be certified for pollutant emissions using an HILS system in the near future. Therefore, basic interim options for handling HDH in CO_2 certification are also being discussed until the HILS approach is evaluated in its practical application and fully established.

Interim option 1 would be to use generic models of HDH in the VECTO tool and input a few manufacturer-specific parameters (e.g. RESS capacity, alternative energy converter maximum power, SOC range) in order to allow limited adaption of the generic simulation models to the specific hybrid system. A simple generic hybrid control strategy (e.g. charge the RESS during decelerations as much as possible within system limits, use all available energy as fast as possible) would be used to run the simulation. The few manufacturer-specific input parameters could be determined easily from datasheets of the components and this approach would not require a validation of the simulation model since a generic model and control strategy is used. Certainly, the resulting fuel consumption would not be accurately representative of the real vehicle, but nevertheless the simulation would show a realistic fuel saving compared to a conventional vehicle. In order to better align the generic hybrid control strategy with the specific one, some manufacturer-specific parameters for the control strategy could be introduced (e.g. threshold for energy buffer in the RESS, which is used for pure electric driving below a certain power demand, SOC dependent discharge curve for the RESS). A similar generic hybrid control strategy in simulation has already been used in a previous project at TU Graz dealing with the optimization of operation strategies of hybrid passenger cars (Luz, 2011-05).

Interim Option 2 would be to define generic table values for fuel savings in percent compared to a conventional vehicle with the same vehicle parameters. Therefore, global generic values for the reduction in fuel consumption as a function of several parameters (e.g. RESS capacity, alternative energy converter maximum power, normalised to a suitable vehicle parameter, for example, mass or available free kinetic energy from the mission profile, etc.) would have to be agreed on and used in order to calculate the fuel saving of a specific HDH compared to the same vehicle with a conventional engine.

A possible long-term solution using an interaction between the VECTO tool and GTR HILS, which would deliver more accurate results but would also require essentially higher effort and resources from both vehicle manufacturers and certification authorities, is discussed in the following sections.

Since vehicle-related CO_2 emissions shall be directly comparable for HDH and for conventional HDV, a harmonisation of the approaches for CO_2 testing for both vehicle categories is important. Since the existing approaches for conventional HDV around the world are not harmonised and certainly will lead to different results when applied for the same vehicle, the GTR HILS method can hardly be made comparable to all existing methods. Therefore, an interaction between the CO_2 simulation tool and the GTR HILS simulator with defined interfaces is needed.

The following chapter describes a suitable interaction between the European CO_2 simulation tool VECTO and the GTR HILS simulator, but the methodology can be applied for other CO_2 simulation tools as well.

4.4.1 Methodology for coupling VECTO with the HDH HILS simulator

For calculating the vehicle-specific CO_2 emissions for a conventional HDV in VECTO, vehicle-specific component test results and a speed cycle which is representative of the HDV class are used as input for the simulation tool.

The basic idea for obtaining the CO_2 emissions of a HDH is to use the same component test results and vehicle parameters from VECTO in the GTR HILS tool, together with the same vehicle speed cycle. But since the cycle is defined as target speed over distance, a conversion into actual vehicle speed over time as the input for the GTR HILS tool is needed since the HILS model is not capable of simulating target speed cycles with all the features VECTO includes. In addition to that, the VECTO tool also has some advanced driver functionalities implemented (e.g. look-ahead cruising before mechanical braking, overspeed functions, acceleration demand limits), which are not available in the GTR HILS model. The following steps are necessary to perform a simulation of vehicle-specific CO_2 emissions for a HDH:

1. Perform the vehicle-specific component tests according to the European CO_2 test procedure for HDH
2. Define a virtual combustion engine in the VECTO tool that represents the full load curve of the hybrid power pack
3. Run the VECTO tool with the vehicle-specific component test results and the respective vehicle speed cycle as input

4. Use the same data from the vehicle-specific component test results that were used in VECTO as input for the GTR HILS tool
5. Run the GTR HILS tool with the converted actual vehicle speed cycle from VECTO
6. Use the resulting combustion engine operation from the GTR HILS tool to calculate the fuel consumption using the “Engine Only Mode” in VECTO
7. Use the resulting total fuel consumption value from “Engine Only Mode” in VECTO and the resulting cycle work delivered by the hybrid power pack from the GTR HILS tool to calculate the fuel consumption per work delivered by the hybrid power pack (i.e. specific fuel consumption in g/kWh)
8. Use the specific fuel consumption from Step 7 and the original cycle work delivered by the combustion engine from the VECTO tool in step 3 to calculate the total fuel consumption and CO2 emissions, respectively. (Both values for delivered cycle work, power pack and combustion engine need to be calculated for the same reference point, e.g. wheel hub).

In Step 6, the resulting operation points of the combustion engine in HILS are used as the input for a separate operation mode – the “Engine Only Mode” – of the VECTO tool. In this operation mode, VECTO calculates the actual fuel consumption of the engine for a given load cycle using a fuel consumption map depending on engine speed and torque. This procedure can be thought of as a simulated running of the engine as a stand-alone system on an engine test bed. The only inputs needed for this calculation are the engine operation over time (i.e. speed and torque), the engine inertia, and a fuel consumption map. The VECTO tool calculates the total torque that is needed to follow the transient engine operation cycle, taking engine acceleration and deceleration into account. With this total torque and the given engine speed, the resulting fuel consumption value is interpolated from the fuel consumption map. This is necessary because VECTO uses a more accurate interpolation routine for calculating the fuel consumption from the fuel consumption map than the one available in the GTR HILS tool.

Since the GTR HILS driver is not able to follow the speed profile from the VECTO tool exactly and the operation of the vehicle is more dynamic due to forward calculation and a driver model acting in a feedback loop, Steps 7 and 8 are performed to compensate for the resulting difference in total cycle work between the GTR HILS and the VECTO tool.

An overview of the methodology described above is given in Figure 48.

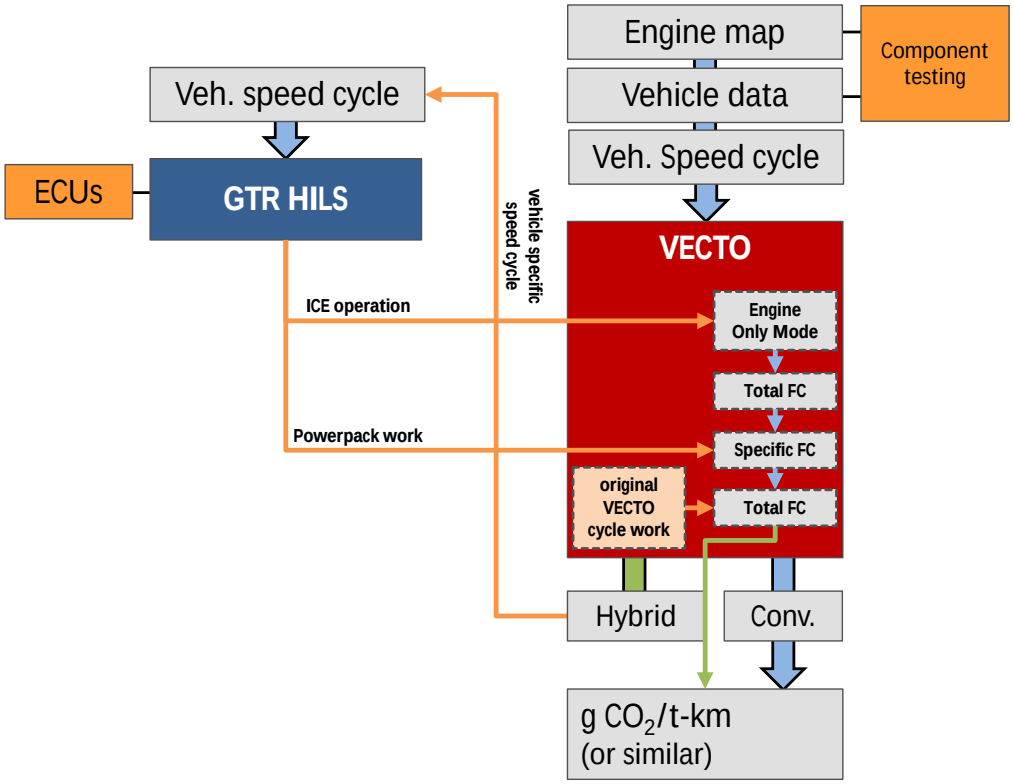

Figure 48. Overview of interaction between VECTO and HILS GTR

4.4.2 Example of application

In this subchapter, the indicated methodology is applied for one generic demonstration vehicle as an example. This demonstration vehicle is a 12 t, parallel electric hybrid delivery truck, which is simulated in the GTR HILS model using a simplified hybrid control strategy in the software instead of connecting real hardware ECUs.

The basic parameters used in both the VECTO and GTR HILS simulation tool are listed in Table 2.

Table 2. Vehicle parameter settings for simulation of a parallel hybrid truck

Parameter	VECTO	GTR HILS
vehicle mass [kg]	9870	9870
aerodyn. drag coefficient [-]	0.6	0.6
frontal area [m²]	8.8	8.8
rolling resistance coefficient[22] [-]	axle 1: 40% load, 0.0083 (Fz ISO 20800) axle 2: 60% load, 0.0094 (Fz ISO 20800)	0.0088
final gear ratio [-]	4.3	4.3
wheel radius [m]	0.43	0.43
wheel inertia [kgm²]	39	39
gearbox ratios [-]	[6.696, 3.806, 2.289, 1.48, 1, 0.728]	[6.696, 3.806, 2.289, 1.48, 1, 0.728]
engine max. power [kW]	185	185
electric machine max. power [kW]	-	52

Since no real hardware ECUs were available for this demonstration example, the decisions on how to divide the requested propulsion power between the combustion engine and the electric machine had to be made by a simple software ECU implemented in the simulation model. This simple control strategy can be described as follows: “The control strategy is to use the electric machine below a certain vehicle speed and the combustion engine above that. If the energy level stored in the battery is lower than a certain value, the electric machine is used as the generator and is then driven either by the combustion engine or purely by the available kinetic energy of the vehicle. The electric machine is used for braking the vehicle when possible. If the brake torque of the electric machine is not sufficient, the mechanical brakes are used additionally. The electric machine is also used for power assist when the desired torque, interpreted from the accelerator pedal position, is larger than the combustion engine can deliver.”

[22] VECTO uses rolling resistance coefficients determined under standardized wheel load as input parameters for the different axles. These values need to be converted according to the actual wheel loads depending on the mass of the vehicle and the mass distribution on the different axles in order to get a general average rolling resistance coefficient that is used for calculating the rolling resistance of the vehicle.

GTR HILS uses the same general average rolling resistance coefficient directly as an input parameter.

The simulation results are shown in the following graphs:

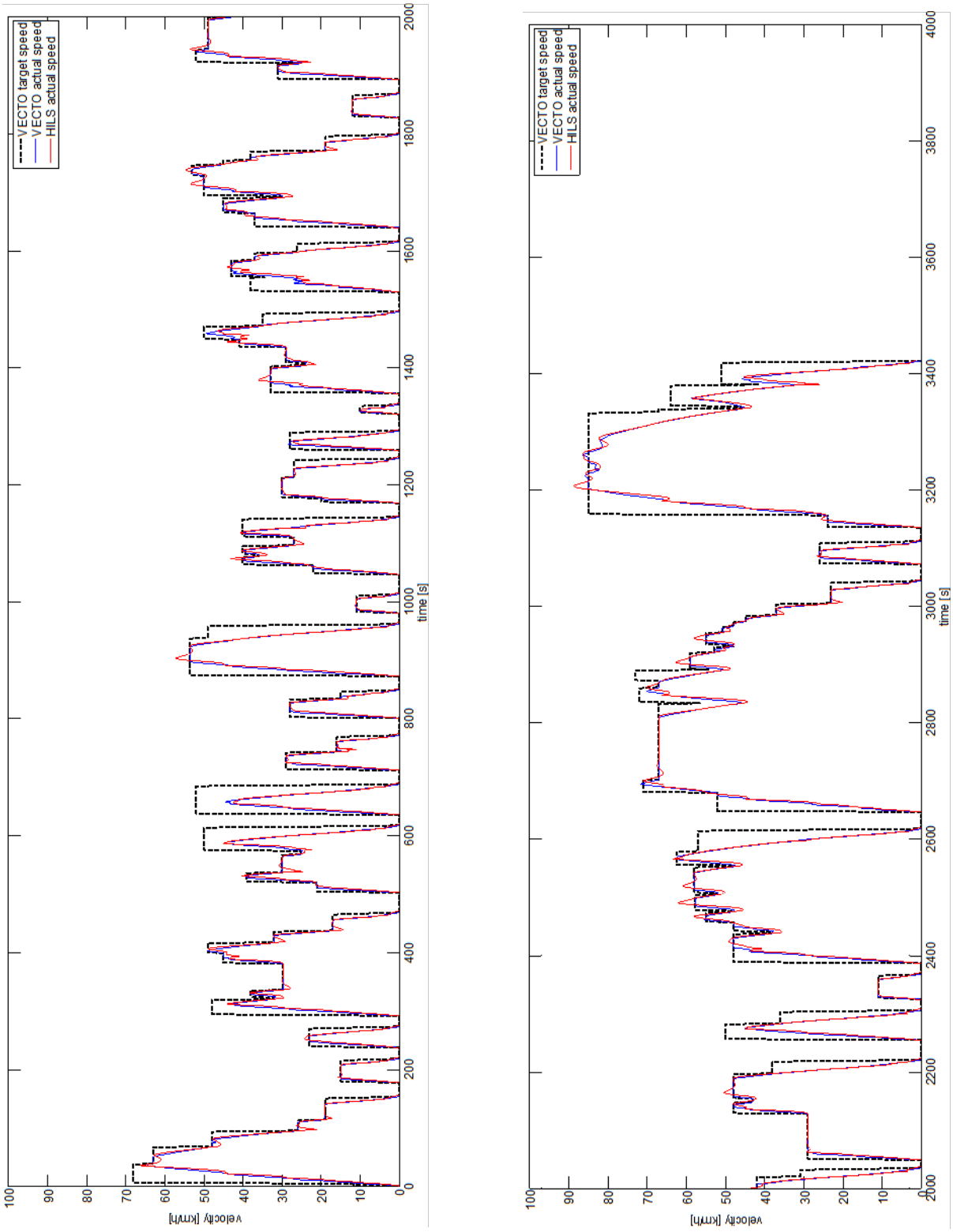

Figure 49. Vehicle speed traces over cycle

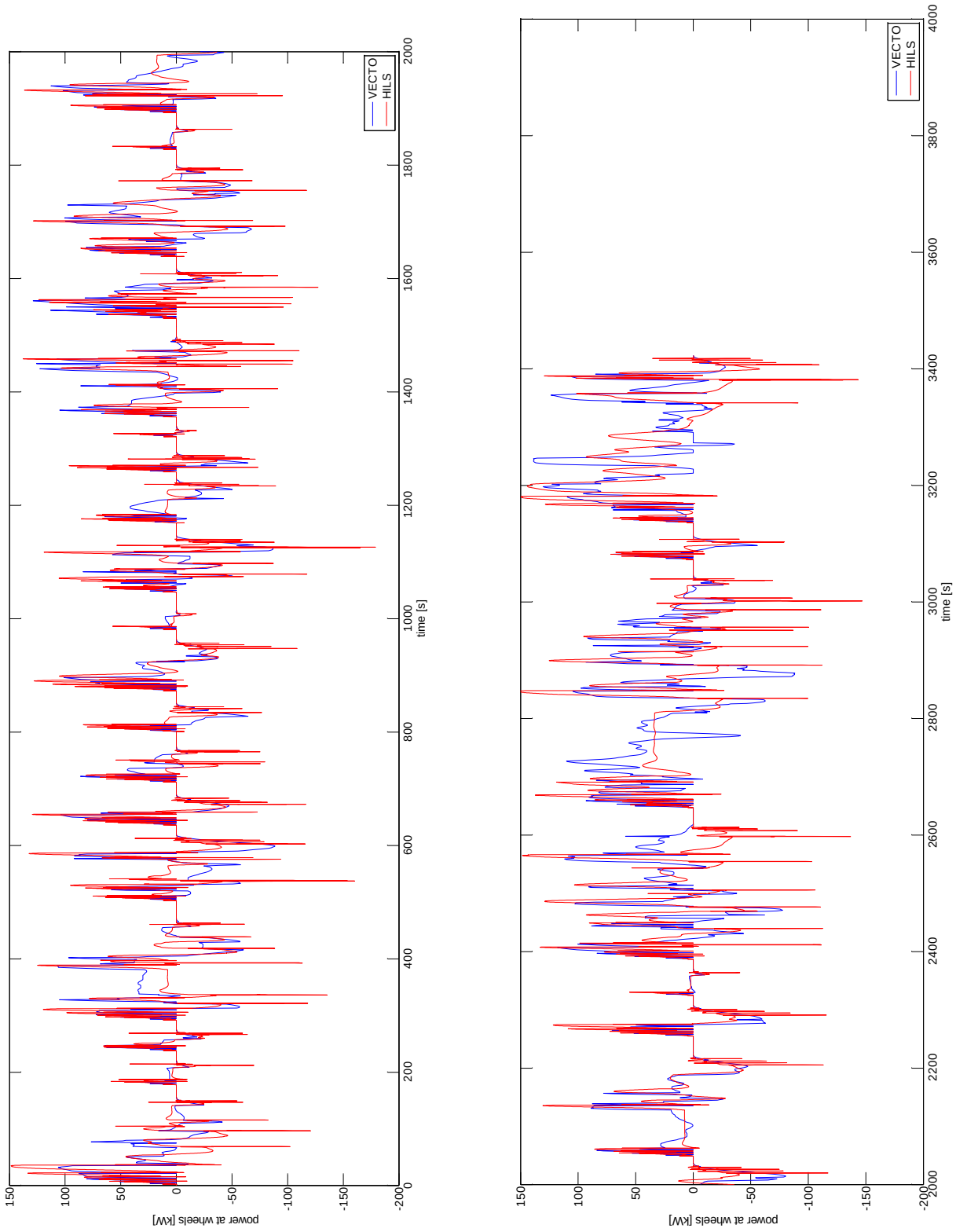

Figure 50. Wheel power traces over cycle

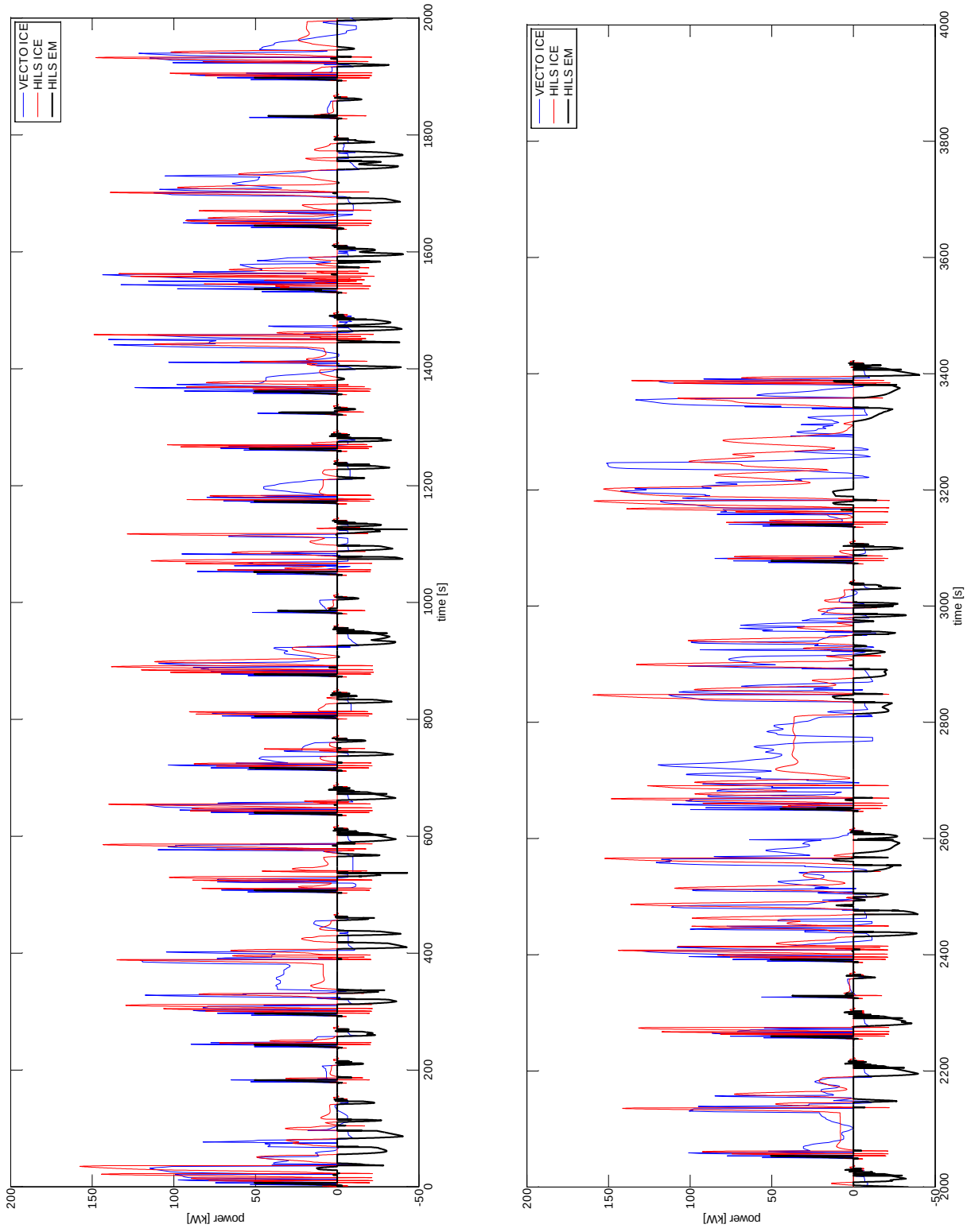

Figure 51. Engine and electric machine power traces over cycle

Figure 52 shows the SOC of the battery over the test cycle. For several simulation runs with a different initial value for the SOC, the value at the end of the cycle was always converging to

100%. In order to keep the SOC neutral over the test cycle, 100% was also chosen as the initial value for the final simulation run.

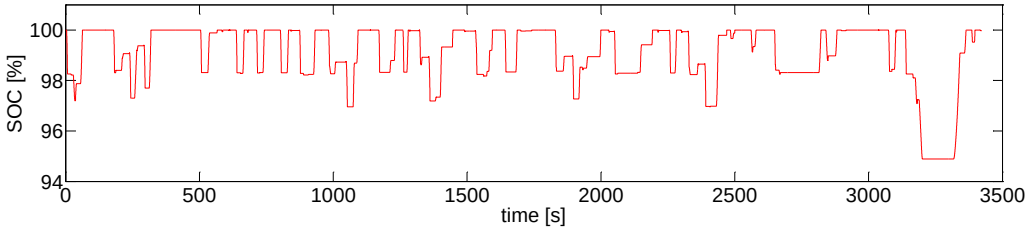

Figure 52. SOC trace over cycle

Table 3 shows a comparison of the results over the test cycle between VECTO and GTR HILS.

Table 3. Integral and average simulation results

Parameter	VECTO	GTR HILS
average velocity [km/h]	29.25	28.73
total distance [km]	27.81	27.31
total positive work at wheels [kWh]	17.92	16.42
total negative work at wheels [kWh]	6.41	5.40
total positive ICE work [kWh]	20.14	16.52
total recuperation energy of EM [kWh]	-	3.85
FC HILS in Engine Only Mode [g]	-	4061.90
original specific FC HILS [g/kWh] (HILS FC divided by HILS work)	-	247.37
corrected FC [g/cycle] (specific FC HILS x VECTO tot. pos. work)	-	4432.96
final FC value for cycle [g]	4578.74	4432.96

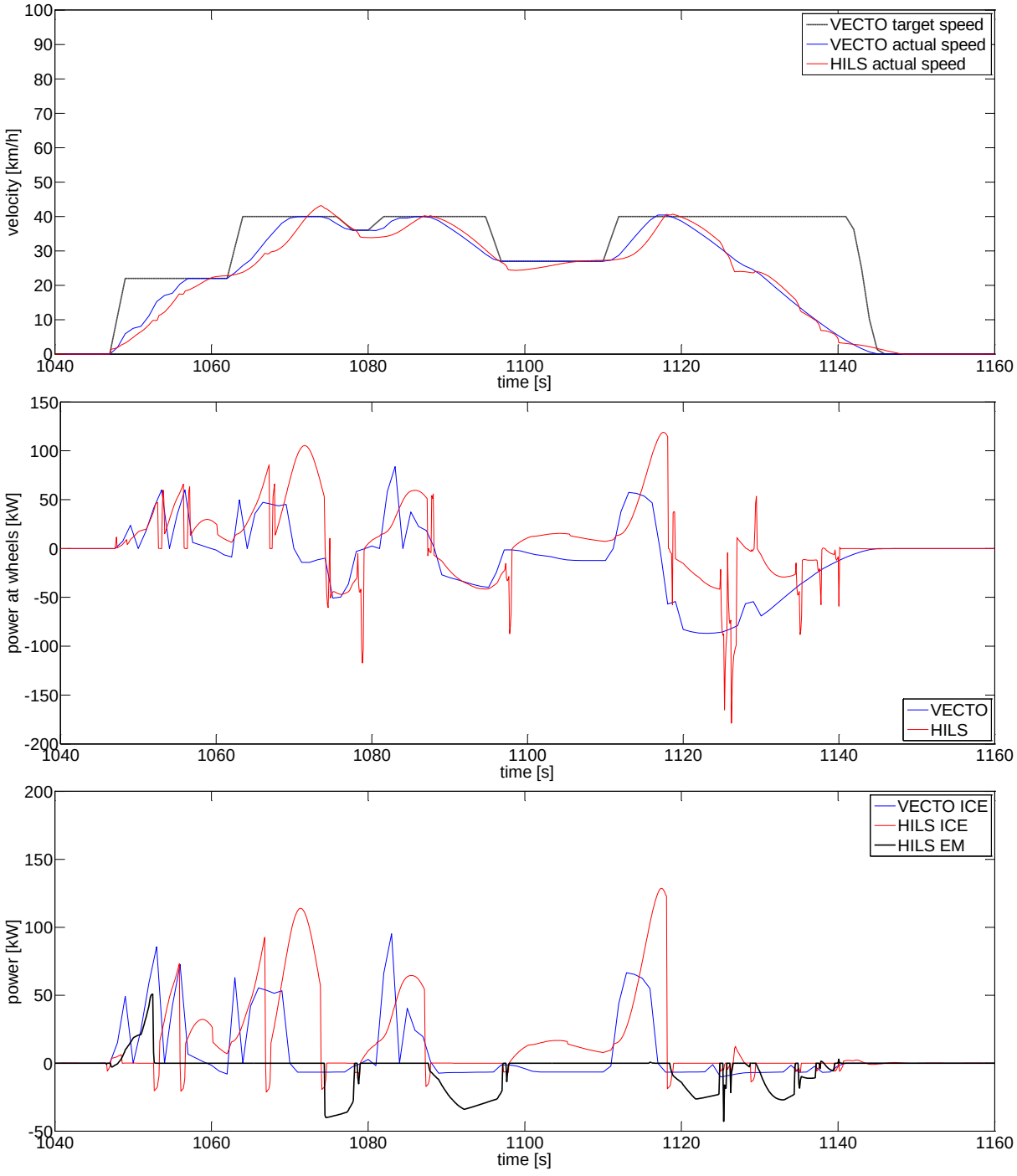

Figure 53: Detailed traces over test cycle

The conclusions that can be drawn from this demonstration example are the following:

- In principle, the suggested methodology was successfully applied and delivered reasonable results.
- The existing simple driver model in the GTR HILS tool is not able to follow the given reference vehicle speed trace from the VECTO tool exactly (see Figure 53). Due to the

dynamic system behaviour of the forward calculating GTR HILS model with the driver model engaged in a feedback loop, there is a time delay and the system cannot react immediately on the requested reference speed. Additionally, overshoots of the vehicle speed occur at points in the cycle where phases of acceleration or deceleration transition directly into cruising phases. In order to improve this behaviour, the possibility and feasibility of an advanced driver model with some kind of look-ahead functionality could be investigated.

§ As shown in Figure 53, the simple driver model also leads to a very transient operation of the hybrid power pack with high load changes compared to the much smoother operation of the VECTO tool which just calculates an average power demand over one second. This very aggressive pedal actuation is not representative of a normal driver but simply due to the simple controller used for the driver model. A more advanced driver model could also improve this behaviour and lead to smoother operation, especially of the combustion engine. This would result in less transient and more realistic load points for the combustion engine, thus getting a realistic improvement in fuel consumption compared to the conventional vehicle.

The issues mentioned lead to unrealistically low fuel savings of only 3.2% for the generic demonstration vehicle (see Table 3). Nevertheless, the proposed methodology is a good basis for further development and improvement. Besides, this approach has already been successfully tested by one of the participating OEMs in the “Validation Test Program 2” of the informal working group on heavy-duty hybrids with real ECUs as the software version connected to the GTR HILS tool.

In order to get a clearer picture of what needs to be changed inside the driver model, a detailed analysis of the resulting deviations between the VECTO and GTR HILS tool needs to be performed. On this basis, a profound conclusion can be drawn for adapting and improving the final methodology for the interface between VECTO and GTR HILS.

4.4.3 Analysis for different hybrid technologies

The GTR HILS tool is capable of representing several layouts of hybrid powertrains due to its modular structure. A specific HDH can be modelled according to the powertrain layout by using components that are available in a library.

In order to connect different components, two types of interfaces between the powertrain components are defined:

1. the physical interface is related to how different components are connected together physically
2. the signal interface is related to control/sensor signals needed to control the components for an ECU

The component structure is divided into two parts: the physical model and the local controller (see Figure 54). Every model includes a local controller, which converts the signals from the respective ECU (if existing) into local control signals. The block also sends sensor signal values to the control system, i.e. it handles the communication between the control system (ECU) and the physical model. The physical model block includes the implementation of the model equations.

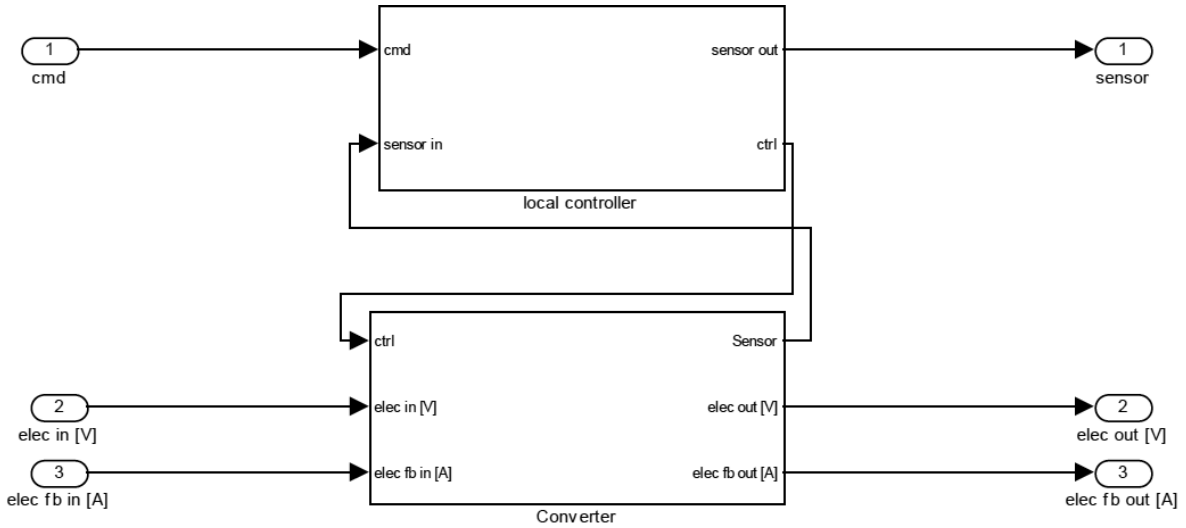

Figure 54. Component structure (example) (Six, 2013-10 p. 35)

The idea in the HILS model is to use a port-based modelling paradigm. The communication signals between the different components are physical signals, like electric wires, mechanical joints etc. These interfaces or connectors are based on energy flow to and from the component, or through a port. A port is characterized by one across- and one through variable, also known as flow- and effort variables in Bond Graph modelling. The interfaces are key to the exchangeability of component models.

For hybrid powertrains, four different physical interfaces are available in the GTR HILS simulation tool: electrical, mechanical (rotational and translational), chemical, and fluid. Table 4 below gives an overview of the physical interface signals used.

Table 4. Classes of physical interfaces

	Electrical	**Mechanical (rotational and translational)**	**Chemical**	**Fluid**
Flow	Voltage	Torque, Force	Specific energy	Pressure
Effort	Current	Rotational Speed, Velocity	Mass flow	Flow

As forwarding is used, feedback signals that go into a block come from the block directly downstream of the actual component block. This means that from an energy perspective the power that goes into a component block is given as the product of the input signal (flow port) and the feedback output signal (effort port). Similarly, the power that goes out from a component block is given as the product of the output signal (flow port) and the feedback input signal (effort port).

As an illustrative example, consider the model in Figure 54.

The incoming energy (energy flow = power) is determined as

P_{in} = elec in [V] · elec fb out [A]

and the outgoing energy is given as

P_{out} = elec out [V] · elec fb in [A]

The fact that the input voltage of the block shown in Figure 54 is multiplied with the feedback output current to get the electrical input power, and vice versa to get the output power, is a general characteristic of port-based modelling for forward calculation. The *feedback output port* represents, in this case, the *input current* of the block. The *feedback input port* is the *output current*. Further explanations can be found in (Six, 2013-10) pp. 32.

Due to these physical interfaces, where the energy flow is directed from one component to the next, the simulation tool is very flexible and every vehicle layout can be modelled by using the respective component blocks from the library. Figure 55 shows examples of a parallel and a series hybrid vehicle.

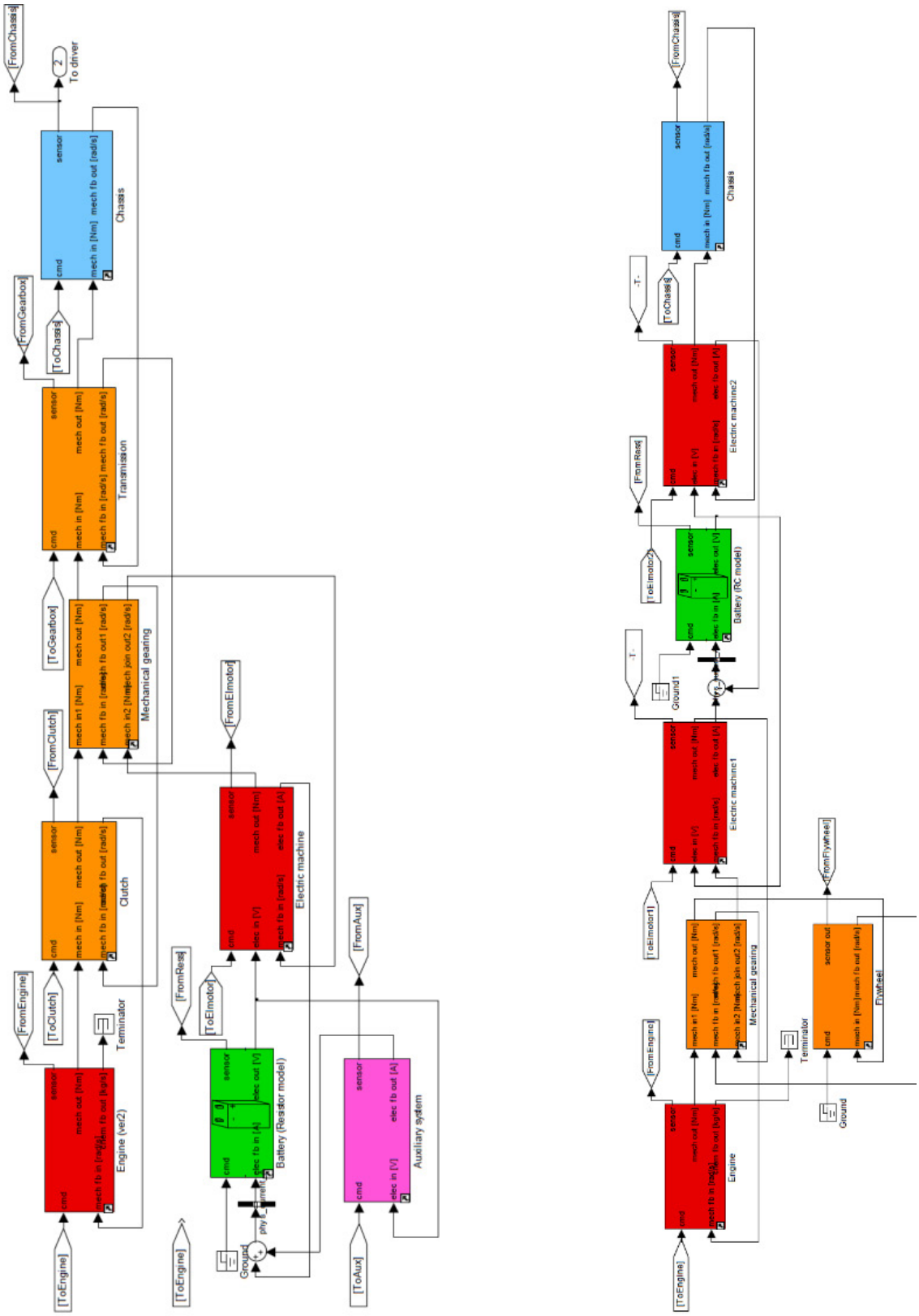

Figure 55. Example model layout of a parallel and series hybrid powertrain (Six, 2013-10 pp. 43, 40)

The top level of the GTR HILS model looks the same for all vehicle topologies. It includes a driver model, an ECU model block, its corresponding input/output interface block for converting ECU signals into the proposed signal interface, and the vehicle model block (see Figure 56). The ECU block is replaced by the real ECU when performing a HILS simulation. The input interface block is modified in order to convert HILS model signals into desired/needed ECU signals in order to be able to run the ECU. The output interface block is modified in order to convert the ECU signals into signals required by the HILS model in order to be able to run.

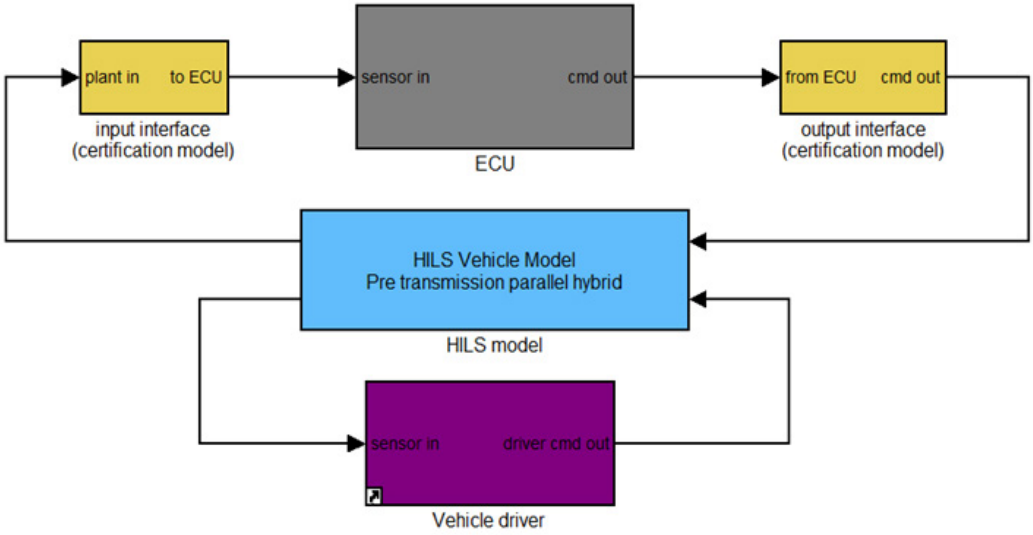

Figure 56. Top level of GTR HILS model (Six, 2013-10 p. 59)

The following components are available in the library of the GTR HILS tool:

- Auxiliary system
  - Mechanical auxiliary system
  - Electrical auxiliary system
- Chassis
- Driver
  - Driver for automatic gearbox (without clutch operation and gearshift strategy)
  - Driver for manual gearbox (with clutch operation and gearshift strategy)
- Electrical components
  - DC/DC converter
- Energy converters
  - Electric machine
  - Internal combustion engine
  - Fluid mechanical machine (hydraulic/pneumatic pump/motor)
- Mechanical components
  - Clutch
  - Continuously variable transmission
  - Flywheel
  - Summation gear
  - Retarder
  - Spur gear pair

- Hydraulic torque converter
- Gear box

§ Rechargeable energy storage systems
- Battery
- Super Capacitor
- Fluid accumulator
- Flywheel

For a detailed description of the models, parameters, and interfaces, see (Six, 2013-10) or (UNECE, 2013-12).

4.5 Fuels

The fuel properties are already covered by the engine fuel flow map included in the VECTO model. The conversion from fuel flow to CO_2 mass emissions is done by the fuel-specific carbon content. From the (measured) carbon mass fraction, the CO_2 emissions per kg fuel can be computed simply by the ratios of molar masses from CO_2 (44 kg/kmol) and C (12 kg/kmol).

$$m_{CO2} = m_{fuel} \times m\%_{CO2} \times \frac{M_{CO2}}{M_C}$$

Table 5 shows as an example of the properties for different fuels. The CO_2 test procedure shall require the use of the reference fuel qualities also defined in the EURO VI procedure and a certified fuel analysis for the carbon content. Thus, the $kgCO_2/kg_{fuel}$ value will vary somewhat depending on the test fuel.

Table 5: Example of fuel-specific density and CO_2 emissions

	Energy density [kWh/kg]	Density [kg/l]	$kgCO_2/kg$
Gasoline	11.59	0.742	3.153
Diesel	11.78	0.832	3.153
LPG	12.8	0.54	2.29
CNG	9.94	0.73	2.79

In the case of dual fuel systems, such as pilot injection systems, for the engine map the fuel flow of both fuels (e.g. diesel and CNG) would have to be measured and stored in the map file as the input for VECTO. Then, the same method that is already implemented for conventional engines is applicable, but it has to be done in parallel for 2 fuels (interpolation from the engine fuel map and correction with the WHTC correction factor). In this case, the WHTC correction factor needs to be computed for both fuels separately by just interpolating the fuel flow in the WHTC and calculating the ratios of measured and interpolated fuel flows for each fuel separately. Whether this approach is robust and accurate enough for all dual fuel systems would need to be tested.

In the case of a full electric vehicle, the engine map needs to contain the electrical energy consumption instead of the fuel flow. In this instance, a battery model similar to the one used

in the HILS GTR needs to be added to VECTO to simulate the recuperated brake energy in a realistic way and to consider losses during charging and discharging of the battery. The battery component test procedure could also follow the one already defined for the GTR HILS procedure for HDH.

4.6 Gear box

4.6.1 Improved transmission efficiency

VECTO uses “loss maps” to calculate transmission losses in the gearbox and the differential(s). These maps are foreseen to be measured for the make and model of gear box and axle mounted to the HDV under consideration. In addition, default efficiencies are provided by VECTO, which represent rather poor technology to incentivise the usage of better gear boxes. These maps describe the torque loss as a function of input speed and input torque for each gear. A detailed test procedure for measuring the torque losses has been elaborated by industry for Lot 3, which can be applied to determine the loss maps for the VECTO calculations. This method enables appropriately accurate consideration of the actual transmission losses.

Consequently, there is no need for additional model improvements to consider improved transmission efficiencies.

4.6.2 Automatic manual transmission

The gear shift model in VECTO is based on shift polygons that describe the engine speed thresholds for up and down shift as functions of the engine torque as shown in Figure 57.

Figure 57: Gear shift polygons in VECTO

For the VECTO simulations, these polygons are generated based on engine full load characteristics according to a standardised method. Manual Transmissions (MT) and Automatic Manual Transmissions (AMT) will use the same generic polygons, but in AMT

mode the VECTO gear shift model is allowed to shift inside the polygons (i.e. below the actual shift up threshold) whenever a certain torque reserve can be ensured, resulting in lower engine speeds and in a fuel benefit compared to the MT mode.

A much more complex approach would be to allow OEMs to implement their own gear shift strategies, either by using OEM-specific shift polygons or by connecting external components to the model, i.e. hardware-in-the-loop (HIL) to use their own gear shift controls directly in the simulation, which would allow more complex and realistic controls, not covered by the simple polygon approach, to be supported. However, this is not actually feasible with the current version of VECTO, since it would require the use of a forward approach simulation model. Additionally, a validation of the relevant control hardware, either on the chassis dynamometer or on-road, would be required, as it has to be ensured that the OEM control strategy in the simulation matches with real world operation.

4.6.3 Automatic transmission with hydraulic element

VECTO includes a model for Automatic Transmissions (AT) including the hydraulic torque converter. The basic gear shift control is the same as the one for MT and AMT as described in 4.6.2 with the exception that in AT mode only sequential gear-shifting is allowed, whereas (A)MT can skip gears under certain conditions.

The torque converter is designed to operate like a separate gear, i.e. the lock-up clutch is controlled by the gear shift polygons. When the lock-up clutch is open, the engine operation point (engine speed and torque) cannot be calculated based on the vehicle speed and transmission ratios. In this case, an iterative method is used based on the torque converter's characteristics, which are defined by its torque ratio and input torque as a function of the speed ratio, (Figure 58). The input torque is defined for a specific reference input speed (MP1000 = input torque at 1000 rpm) and is converted for the actual speed during runtime.

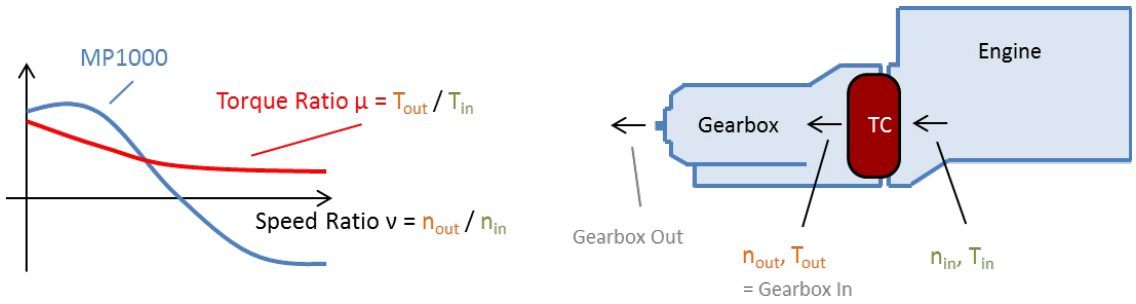

Figure 58: Torque converter characteristics

The torque and the speed at the torque converter output (gearbox side) are calculated using the backwards longitudinal approach. Using the torque converter characteristics, the torque and the speed at the input (engine side) can be calculated iteratively in such a way that the three parameters, speed ratio, torque ratio and input torque, match.

The torque converter characteristics can be derived from standardised component tests (test procedure not fully finalised yet) and should consequently allow an appropriate modelling of its efficiency.

4.6.4 Dual clutch transmission (DCT)

Compared with conventional transmissions, dual clutch transmissions (DCT) have the advantage of very short shifting times (practically zero). As a consequence, low shifting times allow the final drive ratio to be lowered, since the speed and torque loss during shifting is lower. A lower final drive ratio allows the engine to operate at a lower speed which is generally more fuel efficient. (Zeitzen, 2012-09 p. 38/39)

These effects can be quantified by the VECTO model via the "traction interruption" input parameter which considers speed and torque loss during the gear shift process Furthermore, the time between two gear shifts can be reduced when using a DCT, though generic values for this parameter have yet to be defined.

To demonstrate the fuel-saving potential of a dual clutch transmission, a VECTO simulation was set up representing an average 40t long haul truck with trailer, 350 kW rated power and 19.3 t loading (33.3 t total mass). The baseline vehicle was designed with an AMT gearbox with a shifting time of 0.8 s. The DCT version had zero shifting time and a lower final drive ratio as shown in Table 6.

Table 6: Long haul truck configurations for AMT and DCT and VECTO results in the long haul driving cycle

Version	Shifting time [s]	Final-drive ratio [-]	FC [g/km]	FC reduction
AMT	0.8	3.066	290.1	-0.6%
DCT	0	2.850	288.2	

The final drive ratio of the DCT version was designed to reduce the engine speed by 100rpm at a vehicle speed of 85 km/h.

Figure 59 shows speed (blue, left axis) and engine speed (right axis) for the AMT (red) and DCT (green) version.

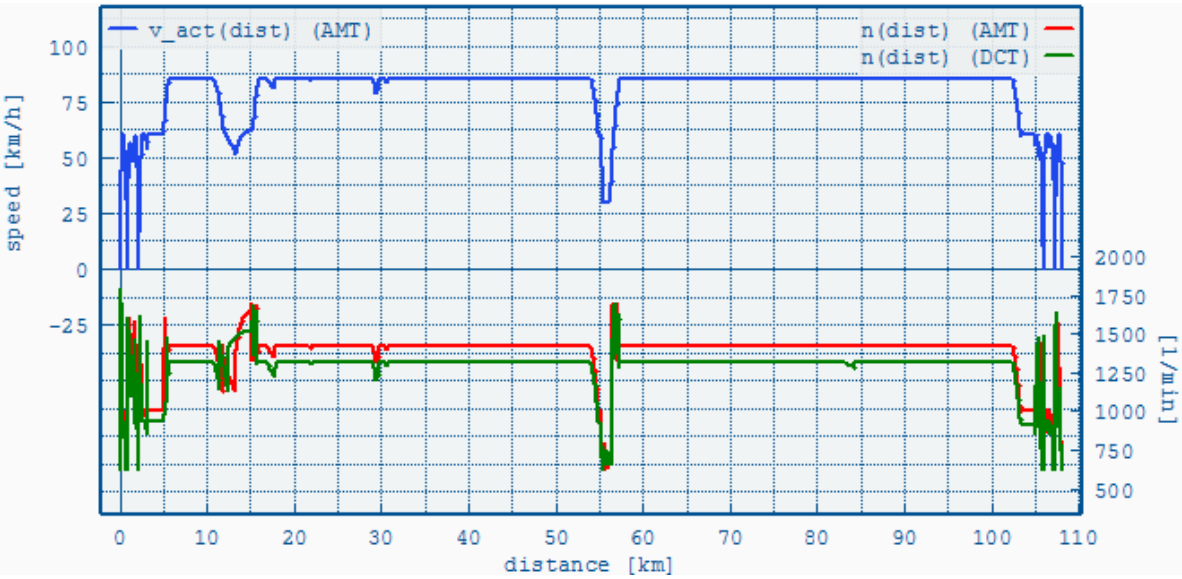

Figure 59: AMT and DCT version of a long haul truck calculated with VECTO

In long haul missions, the vehicle travels at the highway target speed of 85km/h almost the entire time, so the target rpm reduction of 100 rpm can be achieved for most of the vehicle's operation. In VECTO, the measure showed a 0.6 % reduction of fuel consumption in the long haul cycle.[23]

4.7 Vehicle Aerodynamics

The procedure for measuring the air drag coefficient of heavy-duty vehicles with standardised trailers and bodies is fully integrated in the VECTO approach. Constant speed measurements of the torque at the powered wheels shall be conducted, and the air flow velocity and the yaw angle shall be recorded. The result is the road load curve as a sum of the rolling resistance and the air drag as a function of the air flow velocity. The quadratic part of this curve is the air drag coefficient. The whole approach is described in (Hausberger, 2012-01) pp. 14. A description of more recent results will be published in April 2014 (Fontaras, 2014-04).

The same approach can be used to measure the effect of platooning. In this case, the distance between two HDV is reduced below 50 m, which is the actual safety distance in Germany. The effect is a reduction of the air drag for the following HDV. Measurements for two tractor-trailers resulted in an FC reduction of the second vehicle from 1 to 7 % (Al Alam, 2010-09 p. 311). For the measurement of the air drag, two HDV shall be measured according to the standard procedure, where the second HDV closely follows the lead vehicle.

Thus, improvements on vehicle aerodynamics are correctly considered by VECTO as long as the test for the aerodynamic drag measurement has been performed as elaborated in the HDV CO_2 test procedure. Whether it shall also be allowed to apply CFD simulation to calculate influences of small variations against a “parent HDV” is under consideration. So far, different CFD codes have resulted in different C_d reductions for the same measures on a vehicle. Thus, more standardisation work for CFD application is necessary.

For platooning, the reduced C_d value would need to be multiplied by a weighting factor, which represents that a HDV hardly drives all the time platooning behind another HDV.

4.8 Tyre rolling resistance

In the current version of the VECTO model, the influence of rolling resistance is already considered by a detailed approach. VECTO makes use of the “Rolling Resistance Coefficients” (RRC) values as measured on a test drum using the ISO 28580 test standard as applied for the EU tire labelling. In VECTO, the RRC value has to be specified for each axle of the entire HDV configuration (truck/tractor and trailer if applicable). The model also considers the non-linear influence of axle load on rolling resistance force by a generic model

[23] In reality, measuring engine down speeding also causes a reduction of the speed-dependent idling losses of the auxiliary units. In the VECTO calculation presented here, only the speed dependency of the power consumption of the alternator was considered (via the alternator efficiency map). The power consumption of all other auxiliary units (e.g. fan, compressor) was assumed to be constant. Thus, the calculation result might somewhat underestimate the overall fuel benefit of the DCT transmission in combination with a lower axle ratio. According to the current proposal for the calculation of official CO_2 values (which is for trucks based on constant auxiliary power consumption), this effect would also not be reflected in the HDV CO_2 certification.

elaborated based on tire manufacturer data. This feature improves the model quality with respect to the simulation of the influence of vehicle weight and/or vehicle load on overall fuel consumption. The entire modelling approach was successfully validated during the Lot 3 project by a comparison with measured rolling resistance forces on test tracks for several HDV configurations.

Currently, it is being discussed which RRC value shall be applied in the future HDV CO_2 certification. The Commission and the vehicle OEMs propose using the specific RRC values as measured in the ISO 28580 test of the tires sold with the new HDV. The tire manufacturers favour less strict regulation which allows them to use the average RRC values of the tire label bin as they fear more demanding responsibilities related to COP testing[24]. However, applying bin-average RRC values would only result in much less incentive to optimise tire technology as improvements would only be rewarded if a bin-class limit was skipped. A compromise could be that a certain transition period is foreseen in the legislation after which the declaration of the specific RRC values of each tire would become compulsory.

The tire equipment of the trailers is not known in the HDV CO_2 certification, as these vehicles are in most cases not sold in combination with the truck/tractor. For this purpose, standard RRC values for trailer tires will have to be defined for the simulation of the CO_2 values. To motivate truck operators to use low rolling resistance tire equipment also on the trailers, separate CO_2 values could be calculated for different trailer tire equipment (e.g. label classes from A to C).

4.9 Lightweighting

Reduced vehicle weight leads to benefits in fuel consumption and CO_2 emissions due to the following effects:

- reduced rolling resistance
- reduced power demand for accelerations
- reduced power demand for uphill driving
- and the possibility to operate the engine in lower engine speed ranges due to earlier upshifts

All these effects are already covered by the current model structure of VECTO with the vehicle-specific component test data (in this case, the vehicle mass). For this purpose, only the correct vehicle curb weight has to be specified.

An additional influence comes from the rotational inertias from the engine and clutch plate, as well as from the wheels (tires and rims). This effect is also considered in the VECTO model, but so far only standard values for rotational inertias (engine: function of capacity; wheels: function of tire dimension) are foreseen for use in the VECTO calculations. ACEA has indicated that a separate set of generic rotational inertias shall be elaborated at least for aluminium rims.

[24] COP … Conformity of Production: Legislative provisions which aim to ensure that the approved product can be produced with a constant quality in conformity with the type approval (usually done by regular testing of a small sample of products).

4.10 Driver support systems

Driver support systems are designed to increase efficiency and safety by assisting the driver either by displaying certain information, e.g. gear shift recommendations, or by directly acting on the controls like cruise control systems.

In the following chapter, it is discussed how certain driver support functions can be incorporated in the VECTO model.

4.10.1 Speed limiter

Since the mission profiles in VECTO are designed as target speed cycles, a speed limiter can easily be realized by adapting these cycles accordingly. Alternatively, the speed can be limited in the calculation routine itself using the speed limit as an additional input parameter.

The real issue of this function is not the implementation, but its relation to real driving. Limiting the vehicle speed in VECTO while real vehicles may potentially have this function disabled (or set to a different speed) would be inappropriate just like an 80 km/h motorway speed in the simulation would be inappropriate when the real life average driving speed is close to 90 km/h.

4.10.2 Acceleration controller

The current VECTO driver model limits the acceleration according to a predefined speed-dependent acceleration limit. It was implemented to ensure realistic acceleration behaviour when the vehicle loading is low or empty. Without it, the vehicle's acceleration would only be limited by the engine's full load torque, resulting in unreasonably fast accelerations when the vehicle is not fully loaded or the road gradient is negative (downhill).

This method could also be used to model an acceleration controller if necessary.

4.10.3 Eco-Roll

Eco-Roll is an advanced driver assistance function that aims for reduced fuel consumption by taking advantage of the vehicle’s kinetic energy during downhill driving. When enabled, the gearbox will be set to neutral gear with the engine in idling mode to roll downhill without braking unless a certain overspeed or underspeed is reached. The advantage of this system is the efficient use of the kinetic energy without losses by any form of braking (mechanically or engine brake).

Such a function was developed and successfully implemented in VECTO. If the vehicle is equipped with Eco-Roll, the Eco-Roll functionality is implemented to activate whenever the total driving power at the wheels is negative ($P_{wheel} < 0$), which means the downhill road gradient is high enough to allow the vehicle to roll out without losing speed. In this case, the gearbox will go into neutral gear with the engine in idling.

Figure 60 shows an example of how Eco-Roll operates in VECTO. On the left axis, the target and actual speed is shown over time in seconds. The right axis shows engine (P_e) and wheel power (P_{wheel}).

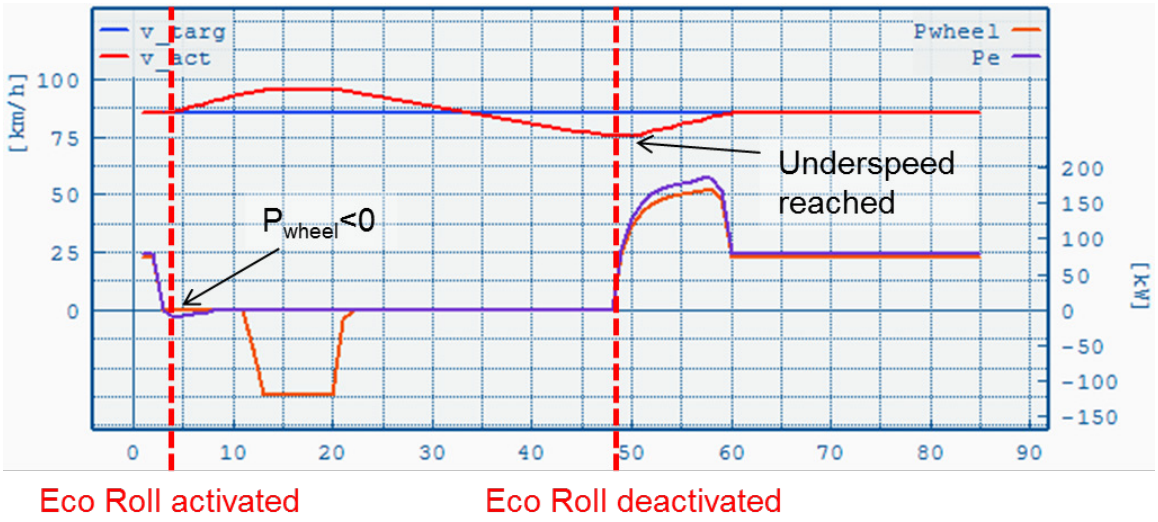

Figure 60: Eco-Roll in VECTO

In this example, Eco-Roll is triggered by $P_{wheel} < 0$ at t=4. The vehicle then rolls out until a predefined overspeed limit is reached (at t~13). Mechanical brakes are applied to keep the vehicle from accelerating over this limit. Eco-Roll remains active until a predefined underspeed limit is reached.

For comparison, VECTO calculations were performed in two versions: with and without Eco-Roll. The test vehicle represents an average 40 t long haul truck with trailer, 350 kW rated power and 19.3 t loading (33.3 t total mass). For comparison, the long haul driving cycle was used. Both the over- and underspeed limits were set to 5 km/h, which means at 80 km/h target speed with Eco-Roll active the vehicle will travel between 75 and 85 km/h.

Figure 61 shows vehicle speed over distance for the normal (red) and Eco-Roll (blue) version. The road gradient (green) is shown on the right axis.

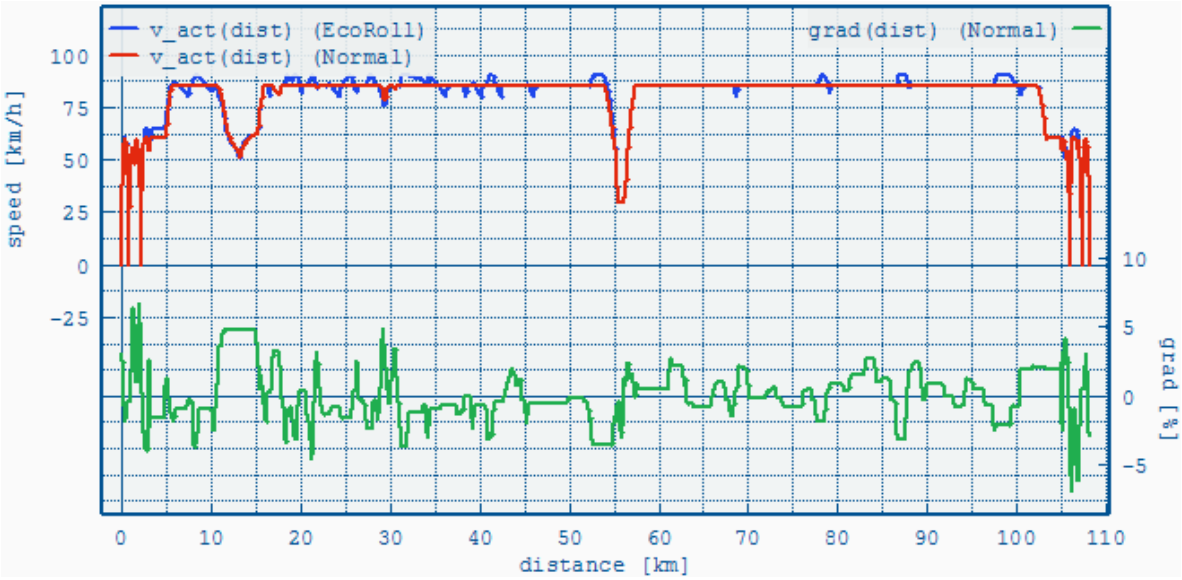

Figure 61: Long haul cycle with (blue) and without (red) Eco-Roll

Over the cycle's distance of about 108 km, there are several occasions where Eco-Roll is active. In this case, the effect of Eco-Roll on fuel consumption is a reduction of about 2.5 % as shown in Table 7.

Table 7: Calculated fuel consumption of a 40t long haul truck with and without Eco-Roll in the long haul driving cycle

Configuration	FC [g/km]	FC reduction
Normal	290.1	-2.5%
Eco-Roll	282.8	

5 Summary and outlook

In the project, options to consider advanced fuel-saving technologies in the future European CO_2 test procedure for HDV have been investigated. The European procedure is based on component testing in combination with a simulation of the entire vehicle using the simulation tool VECTO. Several future fuel-saving measures can already be considered by the combination of the component test procedures and VECTO or need only minor adaptations which have already been implemented in VECTO in 2013:

- ü Improved aerodynamic design
- ü Reduced rolling resistance
- ü Lightweight construction
- ü Reduced losses in the gear box, in the axle, and in the retarder
- ü Automated transmissions, dual clutch systems to reduce torque interruption at gear changes, automatic gear boxes (but all systems considered only with generic gear shift strategies; OEM-specific strategies can also be simulated, but no method for the validation of these strategies has been elaborated yet)
- ü Improved engine technologies including turbo-compounding, and waste heat recovery as long as the energy is fed back as mechanical power
- ü Alternative fuels for internal combustion engines (CNG, LPG, etc.)
- ü Automatic driver aids (speed and acceleration limiter, Eco-Roll)

Several technologies could be added with rather little effort in the simulation tool but need validation by testing:

- o Vehicle-specific alternator efficiencies and brake energy recuperation by intelligent alternator controllers (but much effort to validate to which extent the vehicle makes use of this potential)
- o Waste heat recuperation with electrical energy feedback if the device can be tested together with the engine
- o Dual fuel engines
- o Hybrid vehicles (as prerequisite the HILS GTR has to be finalised including the options suggested in this report. Then, however, quite extensive validation work would be necessary)
- o Electric vehicles (where instead of fuel consumptions and CO2 emissions the consumption of external electrical energy is simulated)

More effort would be necessary to simulate the following components based on component-specific performance data, so it is suggested to treat these components instead by generic values, where technology-specific differences could possibly be made (e.g. control type of the cooling fan):

- Demand-controlled engine cooling fan (difficult to simulate vehicle-specific cooling demand and corresponding fan speed)
- Efficiency of the air compressor with smart control (no test procedure available for component test, and additional model for pressurised air storage system would have to be elaborated in more detail than in the actual report).
- Steering pump (no test procedure available yet for component test)

In total, the HDV CO_2 test procedure seems to already be capable of including most of the technologies expected in the near future. The main difficulty appears to be including OEM-specific control strategies since this needs much effort for setting up the simulation (HILS or SILS) and for validation. Without proper validation whether the simulated control strategies are in line with the real world behaviour of the vehicle, the method would deliver rather unreliable results. This shortcoming is certainly not VECTO-related but a general problem in CO_2 testing. Even tests on a chassis dyno would not ensure that the controller would operate similarly on the road. This mainly concerns vehicle-specific gear shift strategies, smart operation of auxiliaries, such as brake energy recuperation by the alternator and the air compressor, and certainly hybrid power packs. For the latter, the combination of VECTO with the parallel developed HILS method for type approval of pollutant emissions from heavy-duty hybrids is a very promising approach, but it seems that especially the HILS method needs further validation and possibly an improved driver model. Since hybridisation and smart control of components have a reasonable fuel-saving potential which will become more attractive if the potential is visible in the CO_2 test result, further development of options to include these fuel-saving measures is suggested. A combination of SILS with a short test for validation which may be combined with the vehicle's aerodynamic drag test could be the most cost-efficient way to solve this topic in a cost-efficient and robust way.

6 Contact

Stefan Hausberger : hausberger@ivt.tugraz.at
Raphael Luz : luz@ivt.tugraz.at
Antonius Kies : kies@ivt.tugraz.at
Martin Rexeis : rexeis@ivt.tugraz.at
Gérard Silberholz : silberholz@ivt.tugraz.at

7 Appendix

7.1 Calculation of the air flow velocity

Dynamic pressure in front of grille

Equation 15 $p_{fr} = c_{p,fr} \times \frac{\rho_{amb}}{2} v_{veh}^2$

where p_{fr} dynamic pressure in front of grille

$c_{p,fr}$ dynamic pressure coefficient (≈ 0.9, almost full ram pressure)

ρ_{amb} ambient air density (= 1.188 kg/m³, standard ambient conditions)

v_{veh} vehicle velocity

Dynamic pressure at under surface

Equation 16 $p_u = c_{p,u} \times \frac{\rho_{fan}}{2} v_{veh}^2$

where p_u dynamic pressure at under surface

$c_{p,u}$ dynamic pressure coefficient (≈ - 0.2, slight underpressure)

ρ_{fan} air density at fan cross sectional area, directly behind radiator outlet. assumption: the air temperature changes only once on the air path, the increase in the radiator

Pressure drop over flow resistance "i", referred to reference cross sectional area "j":

Equation 17 $\Delta p_{i,j} = k_i \times \frac{\rho_j}{\rho_i} \times \left(\frac{A_j}{A_i}\right)^2 \times \frac{\rho_j}{2} \times v_j^2$ *, (Wagner, 2012) p. 148 eq. 324*

where $\Delta p_{i,j}$ pressure drop over flow resistance "i", referred to reference cross sectional area "j"

k_i flow resistance coefficient of flow resistance "i" ($\Delta p_i = k_i \times \frac{\rho_i}{2} \times v_i^2$)

ρ_j fluid density in cross sectional area "j"

ρ_i fluid density in cross sectional area "i"

A_j cross sectional area "j"

A_i cross sectional area "i"

v_j fluid flow velocity in cross sectional area "j"

Pressure balance mode "0", fan switched off (à idling fan as additional flow resistance)

Equation 18

$$p_{fr} - \Delta p_{gr} - \Delta p_{rad} - \Delta p_{fan,0} - \Delta p_{comp} = p_u$$

$$\Rightarrow \quad p_{fr} - p_u = \left[\left(c_{p,fr} \cdot \rho_{amb} - c_{p,u} \cdot \rho_{fan}\right)\right] \cdot \frac{1}{2} v_{veh}^2 = \ldots$$

$$\ldots = \left[k_{gr} \cdot \frac{\rho_{fan}}{\rho_{amb}} \left(\frac{A_{fan}}{A_{gr}}\right)^2 + k_{rad} \cdot \frac{\rho_{fan}}{\frac{\rho_{amb} + \rho_{fan}}{2}} \left(\frac{A_{fan}}{A_{rad}}\right)^2 + k_{fan} + k_{comp} \cdot \left(\frac{A_{fan}}{A_{rad}}\right)^2 \cdot \left(\frac{\rho_{fan}}{\rho_{amb}} - 1\right) \right] \cdot \frac{1}{2} \cdot \rho_{fan} \cdot v_{fan,0}^2$$

$$\Rightarrow \quad \frac{1}{2} \cdot \rho_{calc,fu} \cdot v_{veh}^2 = \frac{1}{2} \cdot \rho_{calc,fan,0} \cdot v_{fan,0}^2$$

$$\Rightarrow \quad v_{fan,0} = \sqrt{\frac{\rho_{calc,fu}}{\rho_{calc,fan,0}}} \cdot v_{veh}$$

where X_{gr} index for value X in grille cross sectional flow area

X_{rad} index for value X in radiator cross sectional flow area

X_{fan} index for value X in fan cross sectional flow area (w/o fan wheel)

X_{comp} index for value X in engine compartment cross sectional flow area

Pressure balance mode "1", fan switched on (à fan generates pressure increase)

Equation 19

$$p_{fr} - \Delta p_{gr} - \Delta p_{rad} + \Delta p_{fan,1} - \Delta p_{comp} = p_u$$

$$\Rightarrow \quad p_{fr} - p_u = \left[\left(c_{p,fr} \cdot \rho_{amb} - c_{p,u} \cdot \rho_{fan}\right)\right] \cdot \frac{1}{2} v_{veh}^2 = \ldots$$

$$\ldots = \left[k_{gr} \cdot \frac{\rho_{fan}}{\rho_{amb}} \left(\frac{A_{fan}}{A_{gr}}\right)^2 + k_{rad} \cdot \frac{\rho_{fan}}{\frac{\rho_{amb} + \rho_{fan}}{2}} \left(\frac{A_{fan}}{A_{rad}}\right)^2 + k_{comp} \cdot \left(\frac{A_{fan}}{A_{rad}}\right)^2 \cdot \left(\frac{\rho_{fan}}{\rho_{amb}} - 1\right) \right] \cdot \frac{1}{2} \cdot \rho_{fan} \cdot v_{fan,1}^2 - \ldots$$

$$\ldots - c_3 \cdot v_{fan,1}^3 - c_2 \cdot v_{fan,1}^2 - c_1 \cdot v_{fan,1} - c_0$$

$$\Rightarrow \quad \frac{1}{2} \cdot \rho_{calc,fu} \cdot v_{veh}^2 = \frac{1}{2} \cdot \rho_{calc,fan,1} \cdot v_{fan,1}^2 - c_3 \cdot v_{fan,1}^3 - c_2 \cdot v_{fan,1}^2 - c_1 \cdot v_{fan,1} - c_0$$

$$\Rightarrow \quad c_3 \cdot v_{fan,1}^3 + \left(c_2 - \frac{1}{2} \cdot \rho_{calc,fan,1}\right) \cdot v_{fan,1}^2 + c_1 \cdot v_{fan,1} + \left(c_0 + \frac{1}{2} \cdot \rho_{calc,fu} \cdot v_{veh}^2\right) = 0$$

$$\Rightarrow \quad a_3 \cdot v_{fan,1}^3 + a_2 \cdot v_{fan,1}^2 + a_1 \cdot v_{fan,1} + a_0 = 0$$

where $\Delta p_{fan,1} = c_3 \cdot {v_{fan,1}}^3 + c_2 \cdot {v_{fan,1}}^2 + c_1 \cdot v_{fan,1} + c_0$

$c_{0,1,2,3}$ coefficients of polynomial 3rd degree $\Delta p_{fan,1} = f(v_{fan,1})$
$c_{0,1,2,3} = f(n_{fan})$, dependent on the fan speed, (cf Figure 23).

Application of Cardano's formula (Cardano, 1545)

$$a_3 \cdot x^3 + a_2 \cdot x^2 + a_1 \cdot x + a_0 = 0$$

$$p = \frac{3 \cdot a_3 \cdot a_1 - a_2^2}{9 \cdot a_3^2} \qquad q = \frac{2 \cdot a_2^3}{54 \cdot a_3^3} - \frac{a_2 \cdot a_1}{6 \cdot a_3^2} + \frac{a_0}{2 \cdot a_3} \qquad D = q^2 + p^3$$

$$u = \sqrt[3]{-q + \sqrt{D}} \qquad v = \sqrt[3]{-q - \sqrt{D}}$$

$$\text{real part of solution:} \quad x = u + v - \frac{a_2}{3 \cdot a_3}$$

$$\Rightarrow \quad v_{fan,1} = u + v - \frac{a_2}{3 \cdot a_3}$$

7.2 Calculation of the virtual radiator

With formulas from the literature, the operational behaviour of a water-to-air heat exchanger was calculated in terms of air flow velocity, coolant temperature and pressure loss.

7.2.1 Geometry data of heat exchanger

Equation 20 $$h_{fin} = \frac{w_{air.ch}}{2}$$

where h_{fin} height of one cooling fin (one air channel shared by two water channels)

$w_{air.ch}$ width of air channel

Equation 21 $$A_{cr,air.ch} = h_{fin} \cdot (h_{air,ch} - t_{fin})$$

where $A_{cr,air.ch}$ cross sectional area of one air channel

$h_{air.ch}$ height of air channel including one cooling fin

t_{fin} thickness of cooling fin

Equation 22 $$A_{cr,air.ch,tot} = \frac{d_{fan}}{w_{air.ch} + w_{o,water.ch}} \cdot \frac{d_{fan}}{h_{air.ch}} \cdot (2 \cdot A_{cr,air.ch})$$

à assumption: the heat exchanger area is quadratic and in front of the fan.

where $A_{cr,air.ch.tot}$ total cross sectional area of all air channels in heat exchanger
à $A_{cr,air.ch}$ is calculated with the half air channels width $w_{air.ch}$, see above. Therefore, it is counted twice.

d_{fan} diameter of fan

$w_{o,water.ch}$ outer width of water channel

Equation 23 $C_{air.ch} = 2 \times (h_{fin} + (h_{air.ch} - t_{fin}))$

where $C_{air.ch}$ circumference of one air channel

Equation 24 $d_{hy} = \frac{4 \times A_{cr,air.ch}}{C_{air.ch}}$ *; (von Böckh, 2011) p. 96, eq. 3.19*

where d_{hy} hydraulic diameter of air channel

Equation 25 $A_{cr,fin} = L \times t_{fin}$

where $A_{cr,fin}$ cross sectional area of one cooling fin

L length of one air channel, equals outer length of water channel and depth of heat exchanger in driving direction

Equation 26 $C_{fin} = 2 \times (L + t_{fin})$

where C_{fin} circumference of cooling fin

Equation 27 $C_{o,water,ch} = 2 \times (w_{o,water.ch} + L)$

where $C_{o,water.ch}$ outer circumference of one water channel

Equation 28 $A_{o,water,ch} = C_{o,water.ch} \times h_{exch}$

where $A_{o,water.ch}$ outer surface of one water channel

h_{exch} height of heat exchanger

Equation 29 $A_0 = 2 \times h_{exch} \times L - 2 \times \left(\frac{h_{exch}}{h_{air.ch}} \times t_{fin} \right) \times L = 2 \times h_{exch} \times L \times \left(1 - \frac{t_{fin}}{h_{air.ch}} \right)$

(von Böckh, 2011) p. 114 eq. 3.49

where A_0 outer surface of one water channel, orientated to air channels, w/o cross sectional areas of cooling fins

Equation 30 $A_{fins} = 2 \times h_{fin} \times L \times \frac{h_{exch}}{h_{air.ch}}$ *; (von Böckh, 2011) p. 114 eq. 3.49*

where A_{fins} surface of cooling fins of one water channel

Equation 31 $n_{water.ch} = \frac{d_{fan}}{w_{o,water.ch} + w_{air.ch}}$

where $n_{water.ch}$ number of water channels in front of the fan

d_{fan} diameter of fan

Equation 32 $A_{o,water.ch} = n_{water.ch} \times C_{o,water.ch} \times d_{fan}$

where $A_{o,water,ch}$ outer surface of water channels

7.2.2 Heat transfer from coolant to air flow

Equation 33 $\dot{m}_{air} = v_{air.ch,in} \times A_{cr,air.ch,tot} \times \rho_{air,in}$

where $\dot{m}_{air}$ mass flow of air through heat exchanger

$v_{air.ch,in}$ flow velocity of air at air channel entrance

$\rho_{air,in}$ air density at air channel entrance (= 1.188 kg/m³, standard ambient conditions:
p_{amb} = 1 bar, ϑ_{amb} = 20 °C)

Equation 34 $\vartheta_{air,out} = \vartheta_{air,in} + \frac{\dot{Q}_{transf,dem}}{c_{p,air} \times \dot{m}_{air}}$

where $\vartheta_{air,out}$ air temperature at outlet of air channels

$\vartheta_{air,in}$ air temperature at entrance of air channels (= ϑ_{amb} = 20 °C)

$\dot{Q}_{transf,dem}$ demanded heat flow, transferred from coolant to air flow in heat exchanger

$c_{p,air}$ heat capacity of air (= 1008 J/(kg·K))

Equation 35 $\rho_{air,out} = \frac{p_{amb}}{R_{s,air} \times (\vartheta_{air,out} + 273.2K)}$

where $\rho_{air,out}$ air density at air channels outlet

p_{amb} ambient pressure (= 1 bar), simplification: disregard of pressure loss over heat exchanger in range of 10 mbar

$R_{s,air}$ specific gas constant of air (= 287.21 J/(kg·K))

Equation 36 $\vartheta_{air,av} = \frac{\vartheta_{air,in} + \vartheta_{air,out}}{2}$

where $\vartheta_{air,av}$ average air flow temperature in air channels, important for effective temperature difference

Equation 37 $\dot{V}_{air,out} = \frac{\dot{m}_{air}}{\rho_{air,out}}$

where $\dot{V}_{air,out}$ volume flow of air at air channels outlet

Equation 38 $$v_{air.ch,av} = \frac{v_{air.ch,in} + \left(\frac{\dot{V}_{air,out}}{A_{cr,air.ch,tot}} \right)}{2}$$

where $v_{air.ch,av}$ average air flow velocity in air channels, important for all flow velocity-dependent factors like Reynolds number, tube loss factors ...

Equation 39 $$Re_{air} = \frac{v_{air.ch,av} \times d_{hy}}{\nu_{air}}$$ *; (von Böckh, 2011) p. 83 eq. 3.4*

where Re Reynolds number of air flow through air channels

ν_{air} kinematic viscosity of air (= $18.25 \cdot 10^{-6}$ m²/s)

Equation 40 $$Nu_{air,lam} = \sqrt[3]{3.66^3 + 0.644^3 \times Pr_{air} \times \sqrt{\left(Re_{air} \times \frac{d_{hy}}{L} \right)^3}}$$

(von Böckh, 2011) p. 88 eq. 3.17

where $Nu_{air,lam}$ Nusselt number of laminar air flow through air channels, 0 < Re < 2300

Pr_{air} Prandtl number of air (= 0.711)

Equation 41 $$\lambda = \frac{1}{\left(1.8 \times \log_{10}\left(Re_{air}\right) - 1.5\right)^2}$$ *; (von Böckh, 2011) p. 86 eq. 3.9*

where λ tube friction factor

Equation 42 $$f_1 = 1 + \sqrt{\left(\frac{d_{hy}}{L} \right)^3}$$ *(von Böckh, 2011) p. 87 eq. 3.10*

where f_1 factor for consideration of air channel length

Equation 43 $$f_2 = \left(\frac{\vartheta_{air,av}}{\vartheta_{water}} \right)^{0.45}$$ *; (von Böckh, 2011) p. 87 eq. 3.11*

where f_2 factor for consideration of direction of heat flow, simplification: wall temperature of heat exchanger equals water temperature

ϑ_{water} water temperature in heat exchanger (= 95 °C, assumed to be constant)

Equation 44 $$Nu_{air,turb} = \frac{\frac{x}{8} \times Re_{air} \times Pr_{air}}{1 + 12.7 \times \sqrt{\frac{x}{8}} \times \left(\sqrt{Pr_{air}^{2/3}} - 1 \right)} \times f_1 \times f_2$$ *; (von Böckh, 2011) p. 86 eq. 3.8*

where $Nu_{air,turb}$ Nusselt number of turbulent air flow through air channels, $10^4 < Re_{air} < 10^6$, $\frac{L}{d_{hy}} > 1$

Equation 45 $$\gamma = \frac{Re_{air} - 2300}{7700}$$ *; (von Böckh, 2011) p. 89 eq. 3.18*

where γ factor for consideration of share between laminar and turbulent flow

Equation 46 $$Nu_{air,trans} = (1 - \gamma) \times Nu_{air,lam,Re=2300} + \gamma \times Nu_{air,turb,Re=10^4}$$
(von Böckh, 2011) p. 89 eq. 3.18

where $Nu_{air,trans}$ Nusselt number of air flow in transition range, $2300 < Re_{air} < 10^4$

Equation 47 $$\alpha_{air} = \frac{Nu \times \lambda_{air}}{d_{hy}}$$ *; (von Böckh, 2011) p. 85 eq. 3.6*

where α_{air} heat transfer coefficient air channel walls to air

λ_{air} thermal conductivity of air (= 0.028 W/(m·K))

Equation 48 $$p_{fin} = \sqrt{\frac{\alpha_{air} \times C_{fin}}{\lambda_{fin} \times A_{cr,fin}}}$$ *; (von Böckh, 2011) p. 38 eq. 2.45*

where p_{fin} characteristic parameter of fin

λ_{fin} thermal conductivity of heat exchanger material (= 120 W/(m·K))

Equation 49 $$\eta_{fin} = \frac{\tanh(p_{fin} \times h_{fin})}{p_{fin} \times h_{fin}}$$ *; (von Böckh, 2011) p. 40 eq. 2.58*

where η_{fin} heat transfer efficiency of one cooling fin

Equation 50 $$k_{water} = \left(\frac{A_{o,water.ch}}{A_{i,water.ch}} \times \frac{1}{\alpha_{water}} \right)^{-1} = \left(\frac{w_{o,water,ch} + L}{w_{i,water,ch} + L_{i,water.ch}} \times \frac{1}{\alpha_{water}} \right)^{-1}$$
(von Böckh, 2011) p. 114 eq. 3.49

where k_{water} overall heat transfer coefficient: water to outer water channel surface

$w_{i,water.ch}$ inner width of water channel

$L_{i,water.ch}$ inner length of water channel

a_{water} heat transfer coefficient water to fin (= 11 kW/(m²·K))

Equation 51 $k_{fin} = \left(\frac{\lambda_{fin}}{l_{fin}} \right)^{-1}$ *; (von Böckh, 2011) p 19 eq. 2.7*

where k_{fin} overall heat transfer coefficient: outer water channel surface to outer fin surface

Equation 52 $k_{air} = \left(\frac{A_{o,water.ch}}{A_0 + A_{fin\,s} \cdot \eta_{fin}} \cdot \frac{1}{\alpha_{air}} \right)^{-1} = \left(\frac{(w_{o,water.ch} + L) \cdot h_{air.ch}}{(h_{fin} \cdot \eta_{fin} + h_{air.ch} - t_{fin}) \cdot L} \cdot \frac{1}{\alpha_{air}} \right)^{-1}$

(von Böckh, 2011) p. 114 eq. 3.49

where k_{air} overall heat transfer coefficient: air channel walls to air; referred to the outer surface of one water channel

Equation 53 $k_{water\text{-}air} = \left(\frac{1}{k_{water}} + \frac{1}{k_{fin}} + \frac{1}{k_{air}} \right)^{-1}$ *; (von Böckh, 2011) 2011 p. 237*

where $k_{water\text{-}air}$ overall heat transfer coefficient: water to air

Equation 54 $\dot{Q}_{transf,eff} = k_{water\text{-}air} \cdot A_{o,water.ch} \cdot (q_{water} - q_{air,av})$

where $\dot{Q}_{transf,eff}$ effectively transferred heat flow water to air flow

From 1 kW to $\dot{Q}_{transf,dem,max}$ the air flow velocity at air channels inlet ($v_{air,in}$) is interpolated in steps of 20 kW, where $\dot{Q}_{transf,eff}$ equals $\dot{Q}_{transf,dem}$. For example, for a typical tractor engine (V6, 12 litres, 370 kW_{mech}), the maximum waste heat to the coolant, which needs to be transferred to the air flow ($\dot{Q}_{transf,dem,max}$), is approx. 320 kW from 1600 to 1900 rpm. For these points of $v_{air,in}$ and $\dot{Q}_{transf,eff}$ the air volume flow at the heat exchanger outlet ($\dot{V}_{air,out}$) is also interpolated, which needs to be boosted by the fan. The result is the characteristic curve " 'transferred heat flow' over 'fan volume flow' " for this example heat exchanger, in stationary conditions. This calculation is done for coolant temperatures 80, 85, 90, 95, 100 and 105 °C, which creates the map shown in Figure 20.

7.2.3 Pressure loss of air flow through heat exchanger

Equation 55 $\Delta p_{loss} = \rho_{air,in} \times Y_{loss}$ *; (Sigloch, 2008) p. 132 eq. 4-5*

where Δp_{loss} pressure drop by flow losses in the heat exchanger

$\rho_{air,in}$ air density at heat exchanger entrance

Y_{loss} energy loss of air flow

Equation 56 $\zeta = -0.2287 \times \left(\frac{A_{cr,air.ch,tot}}{A_{cr,heatExch}} \right)^2 - 0.2603 \times \frac{A_{cr,air.ch,tot}}{A_{cr,heatExch}} + 0.4895$

(Sigloch, 2008) p. 159 fig. 4-25

where ζ drag coefficient for reduction of cross sectional area at air channel intake

$A_{cr,heatExch}$ cross sectional area of heat exchanger (= d_{fan}^2)

Equation 57 $Y_{loss,intake} = \zeta \times \frac{v_{air.ch,av}^2}{2}$ *; (Sigloch, 2008) p. 378 eq. 5-77*

where $Y_{loss,intake}$ energy loss due to reduction of cross sectional area at air channel intake

Equation 58 $\lambda_{frict,lam} = \frac{64}{Re_{air}}$ *; (Sigloch, 2008) p. 135 eq. 4-15*

where $\lambda_{frict,lam}$ tube friction number for laminar flow, $Re_{air} < 2300$

Equation 59 $\lambda_{frict,turb} = \frac{0.316}{\sqrt[4]{Re_{air}}}$ *; (Sigloch, 2008) p. 141 eq. 4-28 (Blasius)*

where $\lambda_{frict,turb}$ tube friction number for turbulent flow, $2300 < Re_{air} < 10\text{^}5$

Equation 60 $Y_{loss,tube} = \lambda_{frict} \times \frac{L}{d_{hy}} \times \frac{v_{air.ch,av}^2}{2}$ *; (Sigloch, 2008) p. 135 eq. 4-16*

(Hagen-Poiseuille)

where $Y_{loss,tube}$ energy loss due to wall friction of fluid in tube

λ_{frict} tube friction number

Equation 61 $\Delta p_{loss,tot} = \rho_{air,in} \times \left(Y_{loss,intake} + Y_{loss,tube} \right)$

where $\Delta p_{loss,tot}$ total pressure drop of air flow over heat exchanger

For the given points of air flow velocity at air channels inlet, effectively transferred heat flow, and air volume flow at heat exchanger outlet, the total pressure drop was calculated. The result is the characteristic curve "pressure drop over fan volume flow".

Equation 62 $L_{intake,lam} = 0.06 \times Re \times d_{hy}$ *; (Sigloch, 2008) p. 145 eq. 4-48 (Tietjens)*

where $L_{intake,lam}$ length of inlet path for flow in air channels, laminar flow

Equation 63 $L_{intake,turb} \gg 20 \times d_{hy}$ *; (Sigloch, 2008) p. 146*

where $L_{intake,turb}$ length of inlet path for flow in air channels, turbulent flow

The length of the inlet path was calculated only for control reasons. For turbulent conditions, it can reach nearly half of the air channel length. A high length of the inlet path increases the pressure drop, but for this example the effect was not considered.

7.3 Literature

ACEA CO2 declaration procedure HDV [White book]. - Brussels : Association des constructeurs européens d'automobiles (ACEA), 2013-12.

Al Alam A. et al. An Experimental Study on the Fuel Reduction Potential of Heavy Duty Vehicle Platooning [Conference] // 13th International IEEE Conference on Intelligent Transportation Systems (ITSC 2010). - Funchal : Institute of Electrical and Electronics Engineers (IEEE), New York, 2010-09. - pp. 306-311. - http://dx.doi.org/10.1109/ITSC.2010.5625054. - ISBN 9781424476572.

Almbauer R. et al. Motor- und Dampf-Kombiantrieb für Kfz [Report] = MuD : Final Report / Thermodynamik ; TU Graz, IVT. - Wien : Österreichische Forschungsförderungsgesellschaft mbH (FFG), 2013-11. - p. 40. - http://www2.ffg.at/verkehr/projekte.php?id=797. - FFG Projektnr.: 831082.

Almbauer R. et al. Thermische Rekuperation in Fahrzeugen [Report] = The-R-Components : Final Report / Thermodynamik ; TU Graz, IVT. - Wien : Österreichische Forschungsförderungsgesellschaft mbH (FFG), 2012-02. - p. 59. - http://www2.ffg.at/verkehr/projekte.php?id=686. - FFG Projektnr.: 824204.

Banzhaf M. Visco®-Lüfter und -Wasserpumpen zur Verbrauchssenkung im Nkw [technical press release]. - Stuttgart : MAHLE Thermomanagement (formerly Behr GmbH & Co. KG), 2010-05-12.

Biswas K. et al. High-performance bulk thermoelectrics with all-scale hierarchical architectures [Article] // Nature / ed. Campbell P.. - London : Nature Publishing, 2012-09. - Vol. 489. - pp. 414–418. - DOI: http://dx.doi.org/10.1038/nature11439. - ISSN 0028-0836.

Briggs I. Modelling waste heat recovery with a turbogenerator on a diesel engine [Conference] // Ricardo European User Conference. - Ludwigsburg : Ricardo plc, Shoreham-by-Sea, 2012-03. - http://www.ricardo.com/Documents/Downloads/Software%20Flyers/Conference%20Info/201

2%20EUC/EUC%20Presentation%20Paper%202012/QUB_WAVE.pdf , http://www4.dcu.ie/sites/default/files/conference_sbc/Ian%20Briggs_Queens.pdf.

Brito P. et al. Modelling of Thermoelectric Generator with Heat Pipe Assist for Range Extender Application [Conference] // 37th Annual Conference of the IEEE Industrial Electronics Society (IECON 2011). - Melbourne : Institute of Electrical and Electronics Engineers (IEEE), New York, 2011-11. - http://hdl.handle.net/1822/15748.

Cardano G. Artis Magnae sive de Regulis Algebraicis Liber I [Book]. - Nürnberg : Johann Petreius, 1545. - http://www.filosofia.unimi.it/cardano/testi/operaomnia/vol_4_s_4.pdf , http://www.mathematik.ch/anwendungenmath/Cardano/FormelCardano.php. - ISBN 9780486678115.

Dold R. Abgasenergierückgewinnung für schwere Fernverkehrsfahrzeuge [Conference] // 12. Internationale Nutzfahrzeugtagung. - Celle : VDI-Gesellschaft Fahrzeug- und Verkehrstechnik, Düsseldorf, 2013-06.

Espinosa E. Waste heat recovery [conference poster & exhibit] // Trucks/Off-Road powertrain. - Lyon : Société des ingénieurs de l'automobile (SIA), Suresnes, 2012-11.

Fontaras G. et al. An Experimental Methodology for Measuring of Aerodynamic Resistances of Heavy Duty Vehicles in the Framework of European CO2 Emissions Monitoring Scheme [Conference] // SAE 2014 World Congress & Exhibition. - Detroit, MI : SAE International, Warrendale, PA, 2014-04. - ISSN 0148-7191.

Hausberger S. et al. Emission Factors from the Model PHEM for the HBEFA Version 3 [Report]. - Graz : TU Graz, IVT, Fb Emissionen, 2009-12. - p. 76. - http://www.hbefa.net/e/documents/HBEFA_31_Docu_hot_emissionfactors_PC_LCV_HDV.pdf. - report no. I-20/2009 Haus-Em 33/08/679.

Hausberger S. et al. Reduction and Testing of Greenhouse Gas Emissions from Heavy Duty Vehicles - LOT 2 [Report] : Final Report / TU Graz, IVT, Fb Emissionen. - Brussels : EU Commission, Directorate General Climate Action, 2012-01. - p. 210. - http://ec.europa.eu/clima/policies/transport/vehicles/heavy/docs/hdv_2011_01_09_en.pdf. - contract no. 070307/2009/548300/SER/C3.

Hountalas D. et al. Potential for Improving HD Diesel Truck Engine Fuel Consumption Using Exhaust Heat Recovery Techniques [Book Section] // New Trends in Technologies / book auth. Er M.. - Rijeka : Sciyo, 2010. - http://www.intechopen.com/download/get/type/pdfs/id/12289. - ISBN 9789533072128.

LorenCook AF Tube Axial Fan [product catalogue]. - Springfield, MO : Loren Cook Company, 2004-09. - http://www.lorencook.com/PDFs/Catalogs/AF_Catalog.pdf.

Mamat A. et al. Design and development of a low pressure turbine for turbocompounding applications [Article] // International Journal of Gas Turbine, Propulsion and Power Systems (JGPP). - Tokyo : Gas turbine society of Japan (GTSJ), 2012-10. - 3 : Vol. 4. - http://www.gtsj.org/english/jgpp/v04n03tp01.pdf. - ISSN 1882-5079.

Martin H. Elektronisch geregelte elektromagnetische Visco-Lüfterkupplungen für Nutzfahrzeuge [Journal] / ed. Siebenpfeiffer W.. - Wiesbaden : Springer Fachmedien, 1993. - 5 : Vol. 95. - pp. 240-247. - ISSN 0001-2785.

Reif K. (ed.) Bosch Autoelektrik und Autoelektronik [Book]. - Wiesbaden : Vieweg+Teubner, 2010-12. - ISBN13 9783834812742.

Renhart W. et al. Recent NIMH-battery modeling supported by finite element thermal analysis [Conference] // 20th International Symposium on Power Electronics, Electrical Drives, Automation and Motion (SPEEDAM), Pisa. - Napoli : University Federico II of Naples, Dept. of Electrical Engineering, 2010-06. - http://dx.doi.org/10.1109/SPEEDAM.2010.5542280.

Seher D. et al. Waste Heat Recovery for Commercial Vehicles with a Rankine Process [Conference] // 21st Aachen Colloquium Automobile and Engine Technology 2012. - Aachen : RWTH Aachen, VKA & IKA, 2012. - http://www.aachen-colloquium.com/pdf/Vortr_Nachger/2012/E3.3_Seher_Bosch.pdf.

Sendyka B. et al. Recovery of exhaust gases energy by means of turbocompound [Conference] // Sixth International Symposium on Diagnostics and Modeling of Combustion in Internal Combustion Engines (COMODIA 2004). - Yokohama : Japan Society of Mechanical Engineers (JSME), Tokyo, 2004-08. - http://www.heat2power.net/competitors/turbocompoundbenchmark.pdf.

Sigloch H. Technische Fluidmechanik [Book]. - Berlin : Springer, 2008. - ISBN 9783540446330.

Six C. et al. Final report of the Research Program (VTP1) on an Emissions and CO2 Test Procedure for Heavy Duty Hybrids (HDH) [Report]. - Delft : Toegepast Natuurwetenschappelijk Onderzoek (TNO), Mobility, 2013-10. - https://www2.unece.org/wiki/download/attachments/4064802/TNO%202013%20R11430%20_Final%20report%20HDH%20project.pdf. - report no. TNO 2013 R11430.

Srinivasan M. et al. Advanced thermoelectric energy recovery system in light duty and heavy duty vehicles [Conference] // International Conference on Power Electronics and Drives Systems (PEDS). - Kuala Lumpur : Universiti Teknologi Malaysia, 2005-11. - Vol. 2. - pp. 977-982. - http://dx.dio.org/10.1109/PEDS.2005.1619829. - ISBN 9780780392960.

UNECE Working Party on Pollution and Energy (GRPE) - Heavy Duty Hybrids (HDH) [article on homepage]. - Genf : United Nations Economic Commission for Europe (UNECE), 2013-12. - https://www2.unece.org/wiki/pages/viewpage.action?pageId=2523163.

Voith Air compressors [article on homepage]. - Heidenheim : Voith GmbH, 2013-12. - http://voith.com/en/products-services/power-transmission/air-compressors-bus/air-compressors-9812.html.

von Böckh P. et al Wärmeübertragung [Book]. - Berlin : Springer, 2011. - ISBN 9783642159589.

Wagner W. Strömung und Druckverlust, 7th ed. [Book]. - Würzburg : Vogel, 2012. - ISBN 3834332739.

Zeitzen F. Volvo I-Torque [Article] // lastauto omnibus. - Stuttgart : EuroTransportMedia, 2012-09. - 10 : Vol. 86. - ISSN 0023-866X.